IChF
Institute of Physical Chemistry PAS

PhD Dissertation

Novel Systems for Ion-Transfer Studies

Marta Podrażka

IChF
Institute of Physical Chemistry PAS

PhD Dissertation

Novel systems for ion-transfer studies

Marta Adrianna Podrażka

Supervisor: dr hab. Martin Jönsson-Niedziółka, prof. IChF PAN

Auxiliary supervisor: dr inż. Emilia Witkowska Nery

This dissertation was prepared within
the International Doctoral Studies at the
Institute of Physical Chemistry of the Polish Academy of Sciences
Kasprzaka 44/52, 01-224 Warsaw

Warsaw, January 2020

Acknowledgments

First and foremost, I would like to thank my supervisors:

• dr hab. Martin Jönsson-Niedziółka for all the experience and knowledge I got being a part of your group, for giving me scientific freedom, for guidance, and dedicated time;

• dr inż Emilia Witkowska Nery, for great collaboration and all shared knowledge, thank you for showing me how amazing are paper-based devices and electronic tongues systems.

It has been a great pleasure working with you!

I am very grateful to my co-workers who were involved in the work described herein, especially to prof. Damien Arrigan and dr Terence Henares for sharing all their knowledge about liquid/liquid electrochemistry.

Warm thanks to the members of Charge Transfer Processes in Hydrodynamic Systems Group and other IPC PAS workers for their help and fruitful discussions. I especially thank Julia Maciejewska-Komorowska and my office roommates.

Chciałabym również podziękować moim rodzicom i bratu za nieustanne wsparcie i wiarę we mnie i moje możliwości. Dziękuję wam za wzbudzenie we mnie ciekawości świata, możliwość rozwijania pasji i za to, że zawsze jesteście przy mnie.

Dziękuję!

This work was supported by:

The National Science Centre

within the SONATA BIS Grant 2015/18/E/ST4/00319

List of publications

Publications related to the topic of the dissertation:

1. **M. Podrażka**, E. Witkowska Nery, A. Pacowska, D.W.M Arrigan, M. Jönsson-Niedziółka, *Paper-Based System for Ion Transfer Across the Liquid-Liquid Interface*, Analytical Chemistry, 90, 8727-8731, **2018**.

2. **M. Podrażka**, J. Maciejewska, W. Adamiak, E. Witkowska Nery, M. Jönsson-Niedziółka, *Facilitated cation transfer at a three-phase junction and its applicability for ionophore evaluation,* Electrochimica Acta, 307, 326-333, **2019**.

3. **M. Podrażka**, E. Witkowska Nery, T.G. Henares, M. Jönsson-Niedziółka**,** D.W.M. Arrigan, *Ion Transfer Voltammetry with an Electrochemical Pen*, Analytical Chemistry, 92, 24, 15997-16004, **2020**.

Other publications:

1. **M. Podrażka**, E. Bączyńska, M. Kundys, P.S. Jeleń, E. Witkowska-Nery, *Electronic tongue- A tool for all tastes?*, Biosensors, 8, 3, **2018**.

2. W. Mazurkiewicz, **M. Podrażka,** E. Jarosińska, K. Kappalakandy Valapil, M. Wiloch, M. Jönsson-Niedziółka, E. Witkowska Nery, *Paper-Based Electrochemical Sensors and How to Make Them (Work)*, ChemElectroChem, **2019**, DOI: 10.1002/celc.202000512.

Abstract

The goal of this thesis was to develop novel, low-cost systems for liquid/liquid electrochemistry that are easier to handle than presently used methods. Transfer of ions across the interface between two immiscible electrolyte solutions (ITIES) is a very interesting and powerful technique enabling direct electrochemical detection of various ionic species, even these non-electroactive. Unfortunately, traditional setups used for this kind of measurement require a lot of experience and present difficulties in practical handling, making ion-transfer voltammetry available only to a small number of scientists specialized in the field of liquid/liquid electrochemistry and keeping it confined to the laboratory. To solve these issues, simpler alternative versions of classic 3- and 4-electrode systems were developed and described herein.

Instead of a droplet-based 3-electrode approach, a system with paper as a liquid phase reservoir can be applied to investigate electrochemically driven anion-transfer. The unique absorptive properties of the cellulose matrix allow keeping both aqueous and organic phase soaked on a paper sheet. Moreover, the paper support helps increase the mechanical stability of the interface leading to better control of the three-phase junction line and higher reproducibility of the results. Proper performance of the system was confirmed through the observation of two effects typical for setups with three-phase junction, namely, the effect of anion concentration on the peak position and shift of the signal with increasing hydrophobic properties of the anion.

In the case of facilitated cation transfer as an alternative can serve a 3-electrode system with pencil lead as a working electrode. Successful experiments using three different ionophores prove that it can be an excellent tool for comparing ionophores' selectivities. In contrast to ion-selective electrodes, usually used for

that purpose, in the proposed system, the ionophore does not have to be immobilized in the membrane eliminating the influence of membrane components on the obtained results. Additionally, it was shown, for the first time, that fullerene C_{60} can be applied as a redox probe for electrochemically driven cation transfer.

The last setup described in this thesis simplifies ion-transfer measurements using polarizable ITIES. To create a system amenable for scientists from different fields and applicable for on-site analysis, the organic phase was gelled in the pen-like device while the aqueous phase was supported in a paper platform. This electrochemical pen system was applied for the transfer of model organic cations, facilitated cation transfer and stripping analysis of proteins. Moreover, it was shown that thanks to the presence of sodium ions in the cellulose matrix, ion-transfer experiments can be performed without the addition of any supporting electrolyte. Importantly adsorptive properties of cellulose fibers allow a sample to be analysed simply by spotting it on the platform or collecting it by swabbing. Furthermore, the electrochemical pen setup was combined with the paper-based flow system to chromatographically separate ions and proteins or protein mixtures then detected by ion-transfer technique. An alternative, entirely paper-based version of the organogel/paper system is also presented, in which the organic phase is gelled directly on the paper platform. Although the described results are very preliminary, they can serve as a basis for the future development of a flat, low-cost, paper-based system for ion transfer measurements using polarizable ITIES.

Streszczenie

Celem niniejszej pracy doktorskiej było opracowanie nowych, niskokosztowych i łatwych w obsłudze układów do pomiarów elektrochemicznych na granicy faz ciecz/ciecz. Przeniesienie jonów między dwoma niemieszającymi się roztworami elektrolitów (ang. *Interface between Two Immiscible Electrolyte Solutions, ITIES*) jest niezwykle ciekawym procesem, który umożliwia bezpośrednie wykrywanie różnych związków w formie jonowej, również tych które nie są elektroaktywne. Niestety, tradycyjne układy używane do tego rodzaju pomiarów wymagają dużego doświadczenia i stwarzają spore trudności w praktycznej obsłudze. Z tego względu badania procesów przeniesienia jonów prowadzone są tylko przez niewielką liczbę naukowców specjalizujących się w dziedzinie elektrochemii na granicy faz ciecz/ciecz i w związku z tym wykonywane są wyłącznie w odpowiednio wyposażonych laboratoriach. Aby rozwiązać powyższe problemy oraz umożliwić prowadzenie tego typu badań na większą skalę, opracowano i opisano w niniejszej pracy prostsze w konstrukcji oraz obsłudze, alternatywne wersje klasycznych systemów 3- i 4-elektrodowych.

Jako zamiennik dla układu 3-elektrodowego z elektrodą pracującą zmodyfikowaną kroplą organicznego rozpuszczalnika, do badania elektrochemicznie wymuszonego przeniesienia anionów można zastosować układ w którym papier służy jako rezerwuar fazy ciekłej. Unikalne właściwości adsorpcyjne matrycy celulozowej pozwalają na nasączenie papieru zarówną fazą wodną jak i rozpuszczalnikiem organicznym. Ponadto papierowa platforma pomaga zwiększyć stabilność mechaniczną granicy faz, prowadząc do lepszej kontroli linii trójfazowej (ang. *Three-phase junction*) a tym samym większej powtarzalności wyników. Prawidłowe działanie systemu zostało potwierdzone poprzez obserwację dwóch efektów typowych dla układów wykorzystujących elektrody trójfazowe (ang. *Three-Phase Electrode, TPE*) a mianowicie wpływu stężenia anionu

na położenie piku oraz przesunięcia sygnału wraz ze wzrostem właściwości hydrofobowych anionu.

W przypadku badania procesów ułatwionego przeniesienia kationów można zastosować układ 3-elektrodowy z grafitem ołówkowym jako elektrodą pracująca. Satysfakcjonujące wyniki pomiarów przeprowadzonych z użyciem trzech różnych jonoforów dowodzą, że przedstawiony układ jest doskonałym narzędziem do porównywania selektywności jonoforów. W przeciwieństwie do elektrod jonoselektywnych, zazwyczaj stosowanych w tym celu, w proponowanym układzie jonofor nie musi być unieruchomiony w membranie, co umożliwia wyeliminowanie wpływu inny składników membrany na uzyskiwane wyniki. Dodatkowo po raz pierwszy wykazano, że fulleren C_{60} może być stosowany jako próbnik redoks do badania elektrochemicznie wymuszonego przenoszenia kationów.

Ostatni układ opisany w tej rozprawie jest uproszczoną wersją standardowego układu do badania procesów przenoszenia jonów przez spolaryzowaną granicę faz ciecz/ciecz. Aby stworzyć łatwy w użyciu system, który mógłby być stosowany przez naukowców z różnych dziedzin, faza organiczna została zżelowana w urządzeniu przypominającym kształtem długopis, natomiast platforma papierowa została nasączona fazą wodną. Ten “elektrochemiczny długopis” został zastosowany do badania procesów przeniesienia modelowych kationów organicznych, ułatwionego przeniesienia kationów oraz zatężania białek metodą strippingu (ang. *stripping analysis*). Ponadto wykazano, że dzięki obecności jonów sodu w matrycy celulozowej pomiary przeniesienia jonów można wykonywać bez dodatku elektrolitu wspomagającego. Co ważne, dzięki adsorpcyjnym właściwościom włókien celulozowych ciekła próbka może być analizowana bezpośrednio po nakropleniu na papierową platformę lub nasączeniu nią papieru. Ponadto udowodniono, że “elektrochemiczny długopis” połączony z papierowymi systemem przepływowym umożliwia chromatograficzne rozdzielenie mieszaniny

jonów i białek lub mieszaniny dwóch białek, a następnie wykrycie poszczególnych składników poprzez pomiary przeniesienia jonów. Przedstawiono również alternatywną, w pełni papierową wersję systemu z granicą faz żel organiczny/papier, w którym faza organiczna została zżelowana bezpośrednio na platformie papierowej. Chociaż są to jedynie wyniki wstępne, mogą posłużyć jako podstawa do przyszłego rozwoju płaskiego, niskokosztowego, papierowego systemu do pomiarów procesów przeniesienia jonów przy użyciu spolaryzowanej granicy dwóch faz ciekłych.

List of abbreviations

AdDPSV	Adsorptive differential pulse stripping voltammetry
AdSV	Adsorptive stripping voltammetry
BLM	Black lipid membrane
BTPPA$^+$	Bis(triphenylphosphoranylidene) ammonium cation
BTPPACl	Bis(triphenylphosphoranylidene) ammonium chloride
BTPPATFPB	Bis(triphenylphosphoranylidene)ammonium tetrakis[3,5 bis(trifluoromethyl) phenyl] borate
BTPPATPBCl	Bis(triphenylphosphoranilydine) ammonium tetrakis(4-chlorophenylborate)
CA	Chronoamperometry
CE	Counter electrode
CV	Cyclic voltammetry
DB18C6	Dibenzo-18-crown-6 ether
DCB	1,2 - Dichlorobenzene
DCE	1,2 - Dichloroethane
DCH	1,2 - Dichlorohexane
DMFc	Decamethylferrocene
DPV	Differential pulse voltammetry
EMF	Electromotive force
ET	Electron transfer
FIT	Facilitated ion-transfer
GC	Glassy carbon
ISE	Ion-selective electrode
ITIES	Interface between two immiscible electrolyte solutions
IT	Ion-transfer
KTPClPB	Potassium tetrakis(4-chlorophenyl) borate

NPOE	2-Nitrophenyl octyl ether
NOP	N-Octyl-2-pyrrolidone
RE	Reference electrode
PCA	Principal component analysis
PVC	Polyvinyl chloride
SEM	Scanning electron microscopy
SSM	Separate solution method
SWV	Square wave voltammetry
TAA^+	Tetraalkylammonium cation
TBATB	Tetrabutylammonium tribromide
TCNQ	7,7,8,8-Tetracyanoquinodimethane
TEA^+	Tetraethylammoniun cation
TFE	Thin-film electrode
TFT	Trifluorotoluene
TMA^+	Tetramethylammonium cation
TPA^+	Tetrapropylammoniun cation
TPE	Three-phase electrode
WE	Working electrode

Contents

Introduction

Ion transfer processes across interfaces between two immiscible liquids are ubiquitous in nature as all living organisms are composed of cell membranes. Every species entering or leaving the cell has to cross the lipid/aqueous interface, and usually, ionic forms are involved. Transfer of ionic species across liquid phase boundary is also a basis for the extraction process, a well-known separation technique widely applied to purify organic synthesis products, in the production of eatable oils, or the petroleum industry. The same phenomenon is a working principle behind the ion-selective electrodes, present in almost every chemical laboratory in the form of pH-meters.

As can be seen, ion transfer is applied in many different fields of science however, due to differences in terminology, sometimes scientists are not aware that they use or study ion-transfer reactions. Moreover, the concept that the transfer of ions from one liquid phase to the other can be electrochemically influenced is not familiar to those who are not specialized in the field of liquid/liquid electrochemistry. As a matter of fact, electrochemistry at so-called soft interfaces is a relatively young and narrow branch of electrochemistry. Although it is dynamically developing for the last 20 years, still the knowledge and most important usage of the electrochemically controlled ion-transfer processes is not as widespread as it could be. It is especially surprising since electrochemistry at the liquid/liquid interface is a versatile sensing tool enabling fast and label-free detection of various charged species. Notably, on the contrary to classic electrochemical tools, it allows determining even non-electroactive analytes.

One of the reasons why it is still not a widely applied technique might be the fact that traditional setups used for performing such studies are not user-friendly and require considerable experience. Another issue is the problem with achieving

a mechanically stable phase boundary, which is a crucial factor for ion-transfer studies as it highly affects the reliability and reproducibility of the measurements.

In this work are presented a novel, low-cost, and easy to handle alternative versions of classic 3- and 4- electrode systems that help to overcome the mentioned issues. These setups provide a way to achieve a mechanically stable interface and are expected to make the ion-transfer measurements available for a wider group of users.

In the first chapter is described a paper-based alternative to the three-phase electrode (TPE) concept, applied for the investigation of electrochemically driven anion transfer. Traditionally 3-phase electrode configuration is realized by attaching the organic droplet to the electrode surface and then immersing it in the aqueous solution. Although it is claimed to be a very simple method, droplet-based TPE is not trivial to set up, and the organic droplet can easily detach. Instead, paper can be used as both aqueous and organic phase support to achieve a mechanically stable liquid/liquid interface in a very simple and reproducible manner.

The second chapter is devoted to another alternative approach to the TPE configuration. It includes results from the facilitated cation transfer experiments performed in the system with pencil lead as a working electrode. Utilization of a glass vial made from a Pasteur pipet together with a pencil graphite electrode passing through the phase boundary helps to stabilize the interface leading to better reproducibility than in the traditional droplet-based system.

The third chapter contains the description of the novel approach to ion-transfer measurements across the polarizable interface between two immiscible electrolyte solutions (ITIES). The combination of the gelled organic phase placed in

the glass tube and aqueous phase supported on the cellulose matrix led to the development of the electrochemical pen. This simple and portable device can be applied for the investigation of various types of ion-transfer reactions simply by spotting the sample directly onto the paper platform and pressing the pen against it.

The conclusions drawn from the presented herein results may hopefully bring the ion-transfer and liquid/liquid electrochemistry a step closer to point-of-care applications and, most importantly, make it a more user-friendly technique amenable for scientists from different fields.

1 Electrochemistry at liquid/liquid interface

1.1 Introduction

The history of electrochemistry at the liquid/liquid interface began in 1902 when Nernst and Riesenfeld observed the transfer of colored ions from water to phenol[1]. The experimental setup was composed of a U-shaped tube filled with the organic solvent enclosed from both sides by aqueous electrolyte solutions. Such liquid phase composition resembles the structure of biological membranes where the phospholipid layer is in contact with intra- and extracellular aqueous media. Thus results obtained by the authors were the first proof showing the possibility to study membrane transport using liquid/liquid electrochemistry. However, at that time, the concept of ion partitioning across the phase boundary for some reason did not attract much attention and almost 70 years had to pass before it gained back the interest of the scientific community.

The breakthrough came in the late 1960s when Gavach and co-workers reported the correlation between applied potential and measured current related to the transfer of charged species across the water/organic interface[2]. A few years later, Samec et al. [3] showed that apart from ionic currents also signals associated with the electron transfer reactions can be observed in biphasic systems. Almost at the same time, Koryta expanded the methodology and theory concerning ion-transfer processes, and since then acronym ITIES (Ion Transfer between Immiscible Electrolyte Solutions) became widely recognized[4]. These studies are treated as fundamentals of the modern liquid/liquid electrochemistry and triggered a rapid development of this field[5,6]. Since then, a variety of new experimental setups have been developed with a special focus on the miniaturization of the ITIES to overcome problems with uncompensated resistance faced by the initially proposed systems[7–9]. Moreover, a wide range of electrochemical methods, including stripping or AC voltammetry, has been applied to better

understand mechanisms of charge transfer reactions and enhance the sensitivity of the liquid/liquid electrochemistry as an analytical tool[6,10,11]. Additionally, ITIES was combined with other analytical techniques such as SECM[12–14] or spectroscopic methods[15–18] to bring more in-depth knowledge about the dynamics and the interfacial structure of the liquid phase boundary. The opportunity to measure both electronic and ionic currents makes liquid/liquid electrochemistry a very interesting alternative to classic approaches, applicable in various fields of chemistry, including extraction processes, catalysis, energy conversion, or sensing.

1.2 Structure of the interface

The development of a general theory describing the structure of the liquid/liquid interface is not a trivial task. The constant motion of the fluid matter makes the soft interface a very dynamic, continuously deforming structure difficult to thoroughly understand and define by mathematical models. The first attempt was made by Verwey and Niessen, who described the interface as a boundary between two oppositely charged phases analogously to the electrical double layer in Gouy-Chapman theory[19]. This model has later been modified by introducing a layer of oriented solvent molecules separating the "back-to-back" diffuse ion layers[20–23]. In the beginning, the interfacial region was claimed to be composed solely of pure solvent molecules however, numerous reports have shown that not all experimental data can be explained by this theory[22,24–27]. The interfacial capacitance turned out to be dependent on the concentration and type of the aqueous electrolyte leading to the conclusion that the compact inner layer cannot be ion-free[24]. Therefore, Girault and Schriffin postulated the presence of a mixed solvent boundary which can be penetrated by ions from each phase[24,25]. The existence of the overlapping aqueous and organic layers was corroborated by computer simulations with the lattice-gas model[28,29]. Further studies

employing different experimental approaches such as X-ray[30] and neutron reflectivity[31] supported with molecular dynamic simulations[32] resulted in a statement that liquid/liquid interface is molecularly sharp but roughened with capillary waves extending to approximately 1 nm (Figure 1.1). This model is currently considered as the most accurate representation of the interface structure[33].

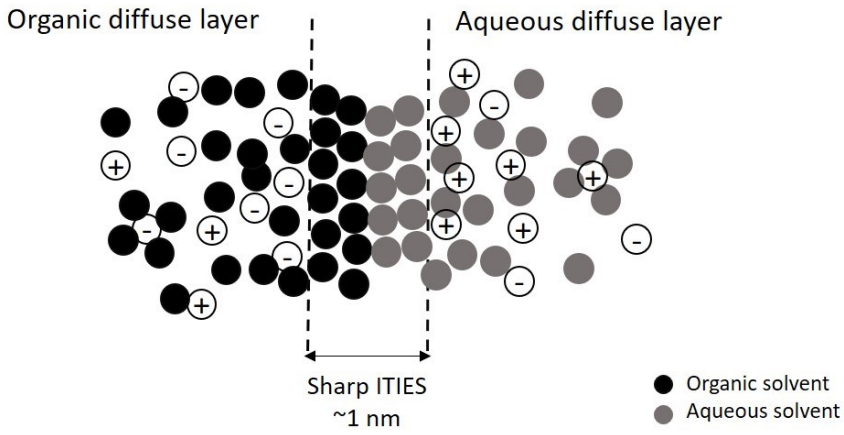

Figure 1.1 Schematic illustration of the liquid/liquid interface with a molecularly sharp interface.

Although probing of the interface with X-ray techniques helped to understand its structure, the obtained data was in disagreement with the predictions made by the Gouy-Chapman theory. The main reason behind this problem is the fact that the mentioned theory considers the liquids from a bulk point of view while their molecular-scale structure is omitted. Similar complications have been reported[22,27] before indicating a need for more precise mathematical formulas to properly estimate the ion-distribution in the vicinity of the charged interface. For that purpose, results from molecular mechanics simulations have been combined with mean-field theory leading to the development of Poisson-Boltzmann Potential of a Force (PB-PMF) model[34]. This approach, by accounting ion-solvent and ion-ion interactions, predicts the electron density at the ITIES, including both

sharp ion-densities and diffused density in the mixed solvent region[34–38]. Although more effective than the Gouy-Chapman model, PB-PMF fails when it comes to predicting ion-distribution at zero or negative polarization[39].

As demonstrated by non-linear optical spectroscopy measurements, molecules from both phases are oriented at the interface[40–42], and dependent on the dipole arrangement, they induce a potential difference estimated to be in the range of hundreds of millivolts[43–45]. This phenomenon can highly influence the predicted surface potential and capacitance, but it is not included in the mean-field approach. Recently Suarez-Herrera et al. showed that anion adsorption at the ITIES can significantly affect the capacitance as well as the ion-transfer process by impairing the water hydrogen bond network [46,47]. Therefore It is clear that we are still lacking comprehensive knowledge about the complexity of the liquid/liquid interface, and this impedes the development of universal mathematical models enabling the accurate simulation of ion-distributions at the ITIES.

1.3 A general theory of liquid/liquid electrochemistry

The characteristic feature of a boundary formed between two liquid phases is the presence of the liquid junction potential[48], $\Delta_O^W\phi$. It results from the charge distribution across the interface and is defined as a difference in Galvani potentials of aqueous (ϕ^W) and organic phase (ϕ^O) :

$$\Delta_O^W\phi = \phi^W - \phi^O \tag{1}$$

This parameter is a function of the chemical potential, which is the measure of the chemical affinity of a certain species in both solvents. Since ITIES is created by two liquids containing ionic species, their electrochemical potentials are equal under equilibrium conditions:

$$\mu_i^{0,W} + RTlna_i^W + z_iF\phi^W = \mu_i^{0,O} + RTlna_i^O + z_iF\phi^O \tag{2}$$

where $\mu_i^{0,W}$ and $\mu_i^{0,O}$ are standard chemical potentials of ion i with charge z_i in the aqueous and organic phase, respectively, while a_i^W and a_i^O are activities of this species in both phases.

Therefore, by combining the above formulas, the liquid junction potential can be expressed as a Nernst-like equation:

$$\Delta_O^W \phi = \Delta_O^W \phi_i^0 + \frac{RT}{z_i F} \ln \frac{a_i^O}{a_i^W} \tag{3}$$

in which $\Delta_O^W \phi_i^0$ stands for the standard transfer potential and can be linked with the Gibbs energy of transfer $\Delta G_i^{0,\ W \to O}$:

$$\Delta_O^W \phi_i^O = \frac{\Delta G_i^{0,\ W \to O}}{z_i F} \tag{4}$$

The standard transfer potential has a fixed value depending mainly on the hydrophobic properties of the ion transferred from the aqueous to the organic phase, and therefore the potential difference can be changed only by altering the activity ratio (a_i^O / a_i^W) of the common ion in the adjacent phases. This can be done either by modification of the chemical composition of both phases or by applying external voltage.

It is worth to note that contrary to the classical Nernst equation for solid electrodes, the formula derived for ion-transfer processes (3) does not involve any parameters related with the redox reaction, even though such can take place at the liquid/liquid interface.

1.4 Polarizable and non-polarizable interface

Liquid/liquid electrochemistry is based on the concept of utilizing the interface as a working electrode. Thus, similarly to classic solid electrodes, an ITIES can be described as polarizable or non-polarizable. The division is based on the way that $\Delta_O^W \phi$ is controlled in the system. The interface is considered as a non-polarizable

when its liquid junction potential is determined by the chemical composition of each phase. When an external voltage needs to be applied to change the $\Delta_O^W\phi$ interface is classified as polarizable.

The simplest way to create a non-polarizable interface is by dissolving the same electrolyte in the two liquids. Distribution of the ions between the phases leads to the polarization of the interface what can be quantitatively defined by including contributions of both anions and cations into the Nernst-like equation (3):

$$\Delta_O^W\phi = \Delta_O^W\phi_+^0 + \frac{RT}{F}ln\left(\frac{a_+^O}{a_+^W}\right) = \Delta_O^W\phi_-^0 - \frac{RT}{F}ln\left(\frac{a_-^O}{a_-^W}\right) \quad (5)$$

For dilute solutions, equation (5) can be expressed as follows:

$$\Delta_O^W\phi = \frac{1}{2}\left(\Delta_O^W\phi_+^0 + \Delta_O^W\phi_-^0\right) \quad (6)$$

In this case $\Delta_O^W\phi$ is called a distribution potential, and it depends solely on the standard transfer potentials of the anion ($\Delta_O^W\phi_-^0$) and the cation ($\Delta_O^W\phi_+^0$). Those parameters can be calculated according to equation (4).

Another method to obtain a non-polarizable interface is based on bringing in contact two immiscible electrolyte solutions that share a common ion, usually called a potential determining ion, since it enables control over the $\Delta_O^W\phi$. If it is a cation, liquid junction potential is given by:

$$\Delta_O^W\phi = \Delta_O^W\phi_+^0 + \frac{RT}{F}ln\left(\frac{a_+^O}{a_+^W}\right) \quad (7)$$

When the liquids share a common anion, liquid junction potential is described as follows:

$$\Delta_O^W\phi = \Delta_O^W\phi_-^0 - \frac{RT}{F}ln\left(\frac{a_-^O}{a_-^W}\right) \quad (8)$$

Independently on the chosen approach, the non-polarizable interface is characterized by a fixed value of the $\Delta_O^W \phi$, which is established once charge distribution between the phases reaches equilibrium (Figure 1.2).

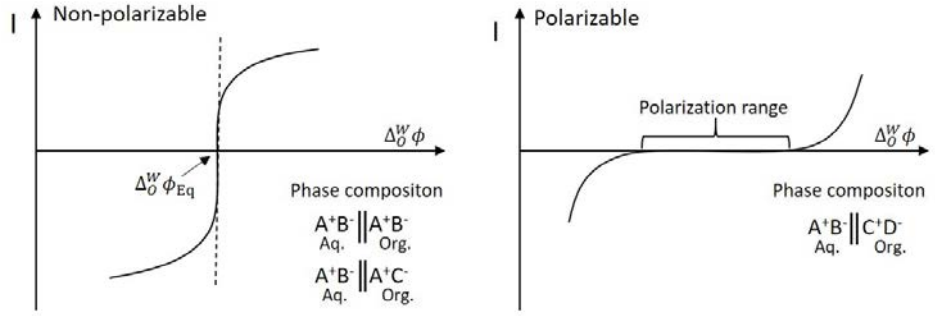

Figure 1.2 Schematic representation of a polarizable and non-polarizable interface. In the case of non-polarizable ITIES both liquid phases can contain the same ions A^+ B^- (top) with different concentrations or share a common ion (down), which in this scheme is represented as A^+. In the case of polarizable interface, the aqueous phase is composed of highly hydrophilic ions A^+ B^- and the organic phase contains highly hydrophobic ions C^+D^-.

On the contrary, the liquid junction potential of the ideally polarizable interface can be continuously altered by the external voltage because none of the liquids contains a common ion. This type of interface is observed in systems composed of ions that cannot spontaneously transfer across the phase boundary due to their infinitely high standard Gibbs energies of the transfer. It is achieved by choosing highly hydrophilic and highly hydrophobic salts as electrolytes for the aqueous and organic phase, respectively. However, ions with infinitely high transfer energies do not exist, and for that reason, the interface reveals ideal behavior only within a certain potential window (Figure 1.2).

1.5 Charge transfer reactions

1.5.1 Simple ion transfer

The flux of ions passing across the ITIES generates a current which can be measured by any technique available in the electrochemical toolbox. The lion's share of liquid/liquid experiments is performed using amperometric methods. However, the obtained response depends on whether the system is based on the non-polarizable or polarizable interface. In the former case, the application of an external potential even slightly higher than the equilibrium $\Delta_O^W\phi_{Eq}$ immediately induce ion transfer resulting in the detection of large current values, as shown in Figure 1.2. The direction of the ion transport is governed by the Nernst-like formula (Equation 7 and 8). Thus, the application of potentials more positive than $\Delta_O^W\phi$ causes movement of cations from the organic to the aqueous phase, while the application of potentials lower than $\Delta_O^W\phi$ leads to the opposite reaction so a transfer of the cation from the aqueous to the organic phase.

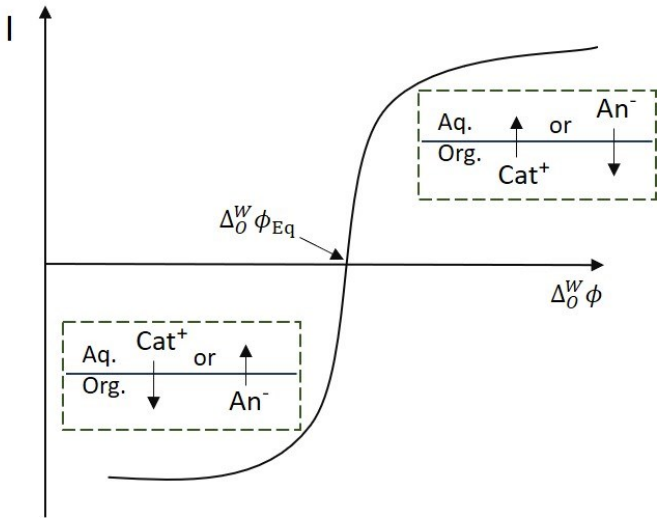

Figure 1.3 Schematic voltammogram for simple ion-transfer across a non-polarizable. Depending on the phase composition, cations or anions are transferred between the liquid phases.

The analogous effect can be observed when both liquid phases contain a common anion, although then transfer from the organic to the aqueous phase occurs upon application of potential more negative than $\Delta_O^W\phi$, while more positive potential results in the opposite transfer (Figure 1.3). Importantly, current changes are recorded only until the concentration of the common ion becomes equal on both sides of the interface. After that, current starts to be limited by the steady-state diffusion of ions from the bulk phase.

As mentioned before, the polarizable interface is characterized by a certain potential range within which no net current flow is recorded despite deviations from the equilibrium $\Delta_O^W\phi$ (Figure 1.4).

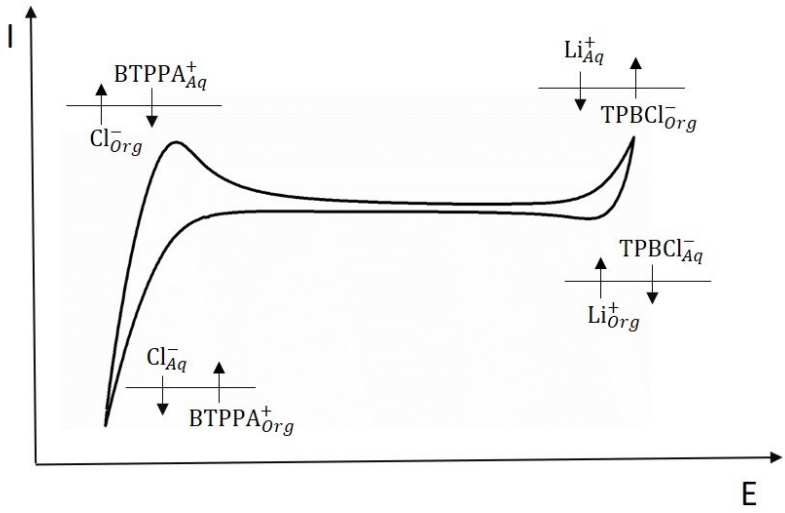

Figure 1.4 Schematic voltammogram for simple ion-transfer of background electrolyte ions in a system with the polarizable interface. The aqueous phase contains LiCl and organic phase highly hydrophobic salt BTPPATPBCl (bis(triphenylphosphoranilydine) ammonium tetrakis(4-chlorophenylborate)).

The width of the potential window is limited by the simple transfer of organic and aqueous electrolytes' components occurring when applied potential exceeds their Gibbs energy of transfer. It is stated that the positive side polarization region is restricted by the simultaneous transfer of hydrophilic cation and

hydrophobic anion while on the negative by the transport of the opposite pair, so hydrophilic anion and hydrophobic cation[49]. The influence of the background electrolytes and properties of organic solvent on the interface polarization will be discussed in detail in the chapter concerning measurements in the 4-electrode system.

Simple transfer of the electrolyte components, however, is not the most relevant when it comes to analytical applications. From the analytical point of view, the most interesting is the investigation of ions transferring at lower potentials than the background electrolyte. Detection of charged molecules by simple ion-transfer at polarizable ITIES can be realized as long as their transfer potentials fit within the polarization region. Simple ion-transfer can also be studied with potentiometric techniques however, this approach is limited only to systems composed of non-polarizable ITIES. The reason is that those measurements are based on variations in open circuit potential observed upon changes to the charge distribution at the interface.

1.5.2 Facilitated ion-transfer

Sometimes the transfer potential of the studied ion exceeds the boundary of the potential window preventing detection using simple ion transfer. One of the solutions for this problem is the addition of complexing agents (ionophores or ligands) to one of the phases to decrease the Gibbs transfer energy of the particular ion, leading to its facilitated transfer (FIT)[50]. To include the influence of the ion-ionophore interaction on the transfer process equation describing the liquid junction potential needs to be reformulated:

$$\Delta_O^W \phi = \Delta_O^W \phi_{ML}^0 + \frac{RT}{Z_M F} ln\left(\frac{a_{ML}^O}{a_M^W}\right) \quad (9)$$

where a_M^W refers to the activity of the ion transferred from the aqueous phase and a_{ML}^O to the activity of the complex ion-ionophore present in the organic phase. Apparent standard transfer potential $\Delta_O^W \phi_{ML}^0$ is given by:

$$\Delta_O^W \phi_{ML}^0 = \Delta_O^W \phi_M^0 - \frac{RT}{Z_M F} ln\left(K_a a_L^O\right) \quad (10)$$

where $\Delta_O^W \phi_M^0$ is the standard transfer potential of the ion and K_a is the association constant of the ion-ionophore complex.

The stronger is the interaction between the ionophore present in the organic phase and ion in the aqueous phase (the higher value of K_a), the bigger shift in the standard transfer potential of the ion is observed.

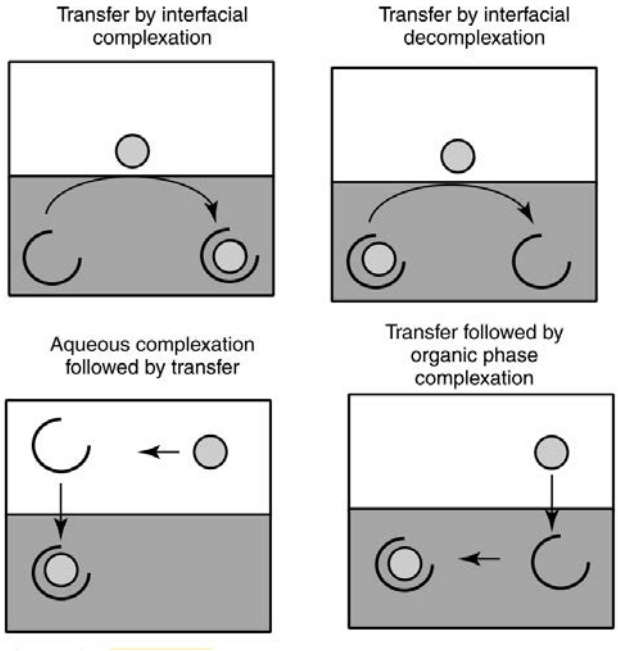

Figure 1.5 Scheme of four different mechanisms of facilitated ion-transfer at ITIES that might happen when a complexing agent is present in one of the liquid phases [50].

The mechanism of the process is not trivial and depends on the physicochemical properties of both ion and ligand as well as parameters related to the formed

complex such as association constant and stoichiometry. Based on the correlation between those parameters, four reaction mechanisms can be distinguished[50] (Figure 1.5).

The vast majority of liquid/liquid studies are focused on following the movement of aqueous ions across the ITIES and for that reason, ionophores are usually added to the organic phase. These molecules help not only to observe the IT process within the potential window but also enables to selectively enhance the transfer of chosen ions as happens in the case of ion-selective electrodes (ISE).

1.5.3 Ion-transfer driven by electrode reactions

Transfer of charged species across the ITIES can be triggered by a redox reaction taking place in one of the phases[49]. Let us consider the situation in which a redox probe present in the organic phase is oxidized. The initial equilibrium in charge distribution between both liquid phases becomes distorted by the excess of positive charge generated in the organic phase. To maintain electroneutrality, three types of processes can occur (Figure 1.6) depending on the phase composition.

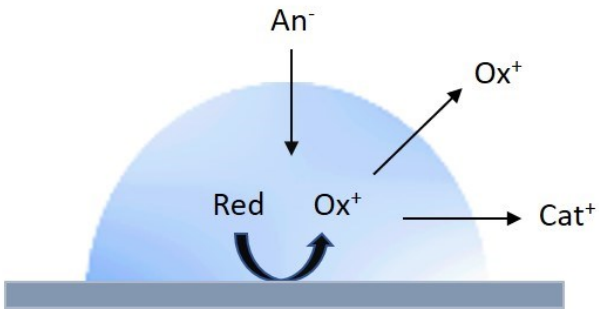

Figure 1.6 Possible ion-transfer reactions that may occur when a redox probe present in the organic phase becomes oxidized. To maintain charge-neutrality the oxidized form can be repelled from the organic phase or anions can be transferred from the aqueous to the organic phase. If the organic phase contains cations those can be ejected to the aqueous phase.

The most commonly studied process is the transfer of the oppositely charged species from the adjacent phase, which in the considered example means the transport of anions from the aqueous into the organic phase:

$$Red_{(org)} + An^-_{(aq)} \rightleftarrows Ox^+_{(org)} + An^-_{(org)} + e \quad (11)$$

The formal redox potential at which oxidation reaction occurs in such a system is determined by the Nernst-like equation[51]:

$$E_{Ox^+/Red} = E^0_{Ox^+/Red} + \Delta^W_O \phi^0_{An^-} - \frac{RT}{F} lnc_{An^-_{(org)}} + \frac{RT}{F} ln \frac{c^*_{Red}}{2} \quad (12)$$

where c^*_{Red} is the initial concentration of the oxidizable molecule in the organic phase and $\Delta^W_O \phi^0_{An^-}$ is the standard transfer potential of the aqueous anion.

When the organic phase contains supporting electrolyte then its cations can be expelled to the aqueous solution to balance the charge. The third possibility is the ejection of the oxidized redox probe from the organic phase. It is worth to stress that investigation of the two firstly mentioned processes requires choosing a redox probe which is sufficiently insoluble in water both in oxidized and reduced forms.

1.5.4 Electron transfer

Apart from different types of ion-transfer processes, liquid/liquid electrochemistry also offers the opportunity to study electron transfer reactions (ET). The main goal of most research work focused on electron transfer at ITIES is the determination of rate constants and transfer coefficients mostly by means of SECM[52–54] and spectroscopic techniques[55–57].

The necessary condition to perform such an experiment is the presence of an electron acceptor and an electron donor on the opposite sides of the interface. This requirement can be fulfilled by a variety of redox-active compounds,

including TCNQ or ferrocene derivatives soluble in organic solvents and $Fe(CN)_6^{4-}$ $Ru(CN)_6^{4-}$ or $Mo(CN)_8^{4-}$ suitable as an aqueous redox probe. Although electron transfer is a widely studied phenomenon, especially in classical electrochemistry, its mechanism at the ITIES is yet not clear. There is a lack of agreement about the dependence of the measured electron-transfer rate on the polarization potential as some authors claim there is a correlation[53,58] while others quite the opposite[59,60]. The mechanism responsible for the current generation during ET is also disputable however, there are two leading explanations: heterogeneous and homogenous mechanism. The first one is considered as the true interfacial electron transfer, while the other arises from the ion-transfer followed by the redox reaction in one of the phases[54,61,62] (Figure 1.7).

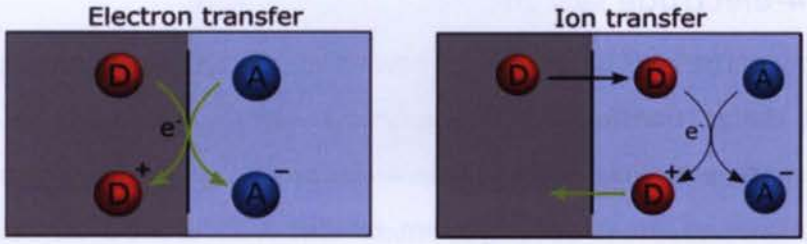

Figure 1.7 Schematic representation of electron and ion-transfer reactions occurring according to the heterogeneous (left) and homogenous (right) mechanism, respectively. Green arrows indicate the processes leading to the generation of an interfacial current[33].

The observed mechanism is highly dependent on the reagents used to create liquid/liquid interface, especially their solubility in the adjacent phase[62,63]. Therefore special attention must be paid when planning experiments based on electron transfer reaction to ensure correct interpretation of the obtained data.

1.6 Electrochemical systems for ion-transfer studies

Investigation of ion-transfer processes can be performed using a 4- or 3-electrode approach. The polarizable interface present in the 4-electrode configuration is suitable for simple and facilitated ion-transfer studies as well as for measurements of electron-transfer reactions. On the contrary 3-electrode configuration allows examination also of ion-transfer driven by redox reactions and it can be realized in two ways: by using a three-phase electrode (TPE) or thin-film electrode (TFE).

Both systems have advantages and disadvantages and the choice of the appropriate one should be made based on the research goal and individual needs.

1.6.1 4-electrode system

The acronym ITIES has become well known since the pioneering work of Koryta showing charge transfer across a polarized water/nitrobenzene interface[4]. Those experiments were performed in 4-electrode glass cells, which until now is considered as the standard system for liquid/liquid electrochemistry[4,64]. It consists of two pairs of a counter (Pt) and reference electrodes (Ag/AgCl) placed in each phase (Figure 1.8). The interface is polarized by the external voltage applied between the platinum electrodes, while reference electrodes enable control over the potential of the whole cell. The latter mentioned is introduced into the setup by Luggin capillaries. The aqueous reference is simply immersed into the capillary filled with an electrolyte solution containing chloride anions. Proper performance of the organic Ag/AgCl electrode is ensured by the so-called reference solution which is added on top of the organic solvent. It is composed of the cationic part of the non-aqueous salt dissolved in the aqueous electrolyte. To make it clearer, if we consider one of the most widely used combinations of electrolytes, that is BTPPATPBCl as an organic electrolyte and LiCl as the aqueous, then the reference solution is made from BTPPACl dissolved in LiCl. In this

way, the potential difference at the interface between the organic phase and aqueous reference solution has a fixed value defined by the equilibrium distribution of the common cation ($BTPPA^+$). Therefore this interface can be considered as a non-polarizable.

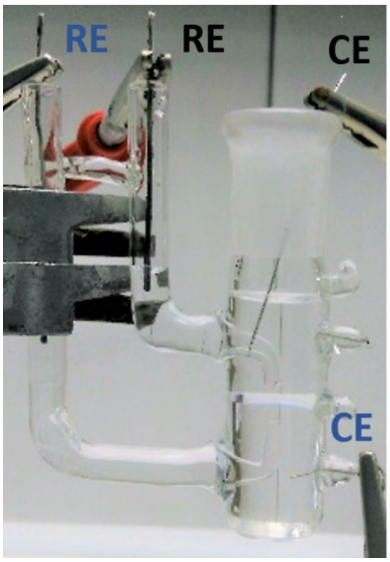

Figure 1.8 Picture of the classic four-electrode glass cell for measurements of the ion-transfer across polarizable ITIES. A pair of a counter (CE) and reference (RE) electrodes is placed in both aqueous and organic phase.

Since this configuration is based on the polarizable interface, ion transfer processes can be observed as long as transfer potentials of the analytes fall within the polarization region. The model reaction employed to verify the proper performance of the studied system is the transfer of quaternary ammonium cations (e.g, TMA^+, TEA^+, TPA^+) presented in Figure 1.9.

The width of the potential window is restricted by the background electrolyte transfer so, to maximize it, the organic phase has to contain highly hydrophobic ions, whereas the aqueous phase highly hydrophilic species[49]. The aqueous electrolyte is usually composed of small inorganic ions characterized by a highly localized charge, among which LiCl is the standard choice. In general, the choice

of organic salt is the limiting factor because there are not many electrolytes soluble in organic solvents and at the same time being hydrophobic enough to not escape to the aqueous phase. High molecular weight lipophilic ammonium salts e.g, TBATB, BTPPATFPB, or BTPPATPBCl satisfy these conditions and therefore are used for the majority of the experiments performed in the 4-electrode setup[6,49].

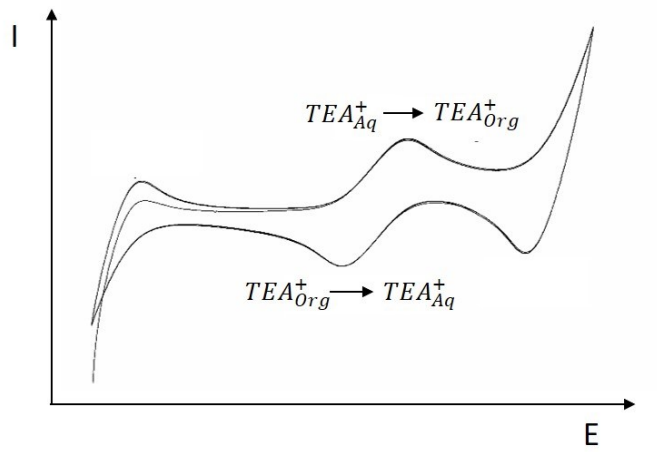

Figure 1.9 Cyclic voltammogram of reversible transfer of a model cation TEA^+ across the polarizable ITIES.

Appropriate selection of the organic solvent is also a very important factor as it has to be not only immiscible with water but also possess relatively high polarity to dissolve the organic electrolyte and enable interface polarization. Solvents such as DCE (dichloroethane), DCH (dichlorohexane), or nitrobenzene are preferable due to low solvation energies of the aqueous ions leading to wide polarization windows when brought in contact with the aqueous solution[46]. Recently it was shown by Kasuno and co-workers that solvents with low dielectric constants, namely chloroform, toluene, and benzene, can also provide experimentally useful polarization ranges however, only with BTPPATFPB as a supporting electrolyte[65,66]. The problematic issue related to all mentioned solvents is their

toxicity and for that reason, less harmful solvents, including TFT (trifluorotoluene)[67], 5-nonanone[68], or solvent mixtures[69] have been tested as an alternative for creating polarizable ITIES.

The main drawback of the 4-electrode system is the high impact of the IR-drop effect related to the inherent resistivity of the organic phase[70]. Since it cannot be fully compensated, it leads to problems with the separation of the faradaic current from the double-layer charging and significantly limits the sensitivity of the analytical response. To overcome this issue, liquid/liquid electrochemistry followed an analogous path as solid-state electrodes and ITIES became miniaturized starting from the pioneering work of Taylor and Girault published in 1986[70].

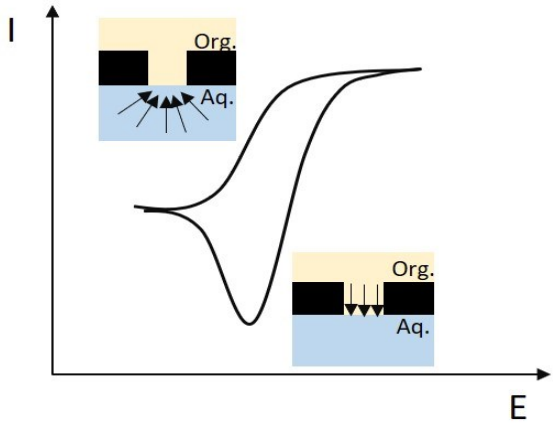

Figure 1.10 Illustration of the typical voltammogram obtained for the ion-transfer process at microITIES. The difference in the diffusion profiles between the aqueous and organic phase is reflected in the voltammogram. Transfer from the aqueous to the organic phase is limited by the steady-state current while the reverse process is controlled by linear diffusion resulting in a peak-shape response.

Apart from minimizing the Ohmic drop, a decrease of the interface area brings many other advantages such as increased stability of the interface and enhanced rate of mass transport, which is directly responsible for reaching lower detection limits[9]. Moreover, the magnitude of the current generated during the transfer

of ions across micro- or nanoITIES allows reducing the number of electrodes from four to two. This means that Ag/AgCl, present in each phase, can serve both as a reference and counter electrode. 2-electrode configuration can be realized by creating either a single micro-interface or an array of micro-sized pores however, regardless of the chosen approach, the registered voltammetric response will often have an asymmetric shape due to asymmetry in diffusion zones between both phases[8] (Figure 1.10).

1.6.2 Three-phase electrode

Difficulties in finding suitable organic electrolytes and, related to that, a limited number of solvents possible to use in the 4-electrode system led to the development of an alternative approach to charge-transfer studies based on classical 3-electrode configuration. The three-phase electrode is a concept in which both liquid phases are in contact with the electrode surface, forming a so-called three-phase junction. Typically it is realized by attaching a droplet of the organic solvent containing a redox probe to the electrode surface and immersing it into the aqueous electrolyte solution where reference and counter electrodes are placed[71] (Figure 1.11). Another way to obtain TPE is by modifying the electrode with a microdroplet array[72] or by placing a metal wire through the liquid/liquid boundary[73].

The three-phase junction is a unique feature of the TPE since it enables performing ion-transfer experiments without a supporting electrolyte in the organic phase. An electric double layer formed along the three-phase boundary provides a potential drop that allows the start of the redox reaction even though the organic phase is initially non-conductive. The excessive charge generated by the electrochemical oxidation or reduction is immediately compensated by the transfer of a counter ion from the aqueous phase. In this way, the conductivity of the organic droplet increases with time and electrochemical reaction

progresses from the edge to the droplet interior[74,75]. Not needing to use organic electrolyte eliminates the problem encountered by the 4-electrode system and opens a way to use non-polar solvents such as octanol[76,77], 2-nitrophenyloctyl ether[78], or alkanes[72,79,80]. On the other hand, the number of solvents to choose is limited to those enabling creation of stable and well-defined droplets because the mechanical instability of the unsupported interface affects the reproducibility of the measurements.

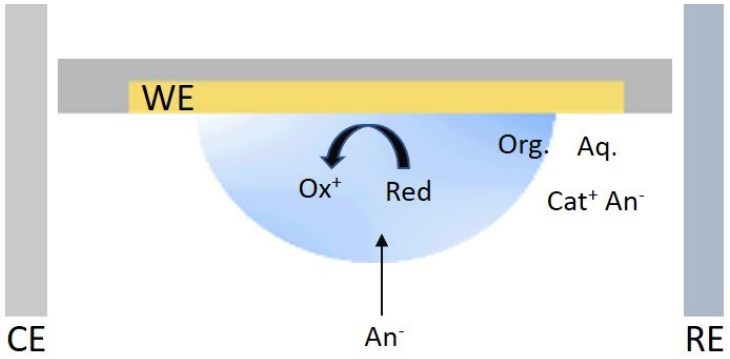

Figure 1.11 Schematic representation of the droplet-based TPE system. A droplet of the organic solvent is deposited on the surface of the working electrode (WE) and immersed into the aqueous solution in which reference (REF) and counter (CE) electrodes are placed.

Since the TPE configuration is based on ion-transfer driven by an electrochemical reaction, the measured redox potential can be correlated with the standard transfer potential as described by equation 9 concerning the case of anion transfer. Of course, an analogous relation is found for the cation transfer, which occurs when the redox probe undergoes electroreduction[51]. In general, the more hydrophobic the ion is, the higher potential needs to be applied to force its transport to the organic solvent. In practice, it is observed as a shift of the redox potential to more positive values with increased hydrophobicity of the cation (more positive $\Delta_O^W \phi_{Cat^+}^0$) or to more negative when highly hydrophobic anions (more negative $\Delta_O^W \phi_{An^-}^0$) are studied. Therefore the TPE can serve as a tool to

access the hydrophobic properties of ions as well as to determine their Gibbs energy of transfer thorough the correlation with the standard transfer potential[51,71]. The latter can be calculated only if the standard redox potential of the redox probe is known.

Although it is usually not clearly stated, the interface obtained using the TPE configuration should be considered as polarizable since charge distribution across the phase boundary appears only upon electrode reaction triggered by the applied external voltage. Ion partitioning cannot happen spontaneously because the liquid phases do not share any common ion. Moreover, the term ITIES is not strictly applicable since supporting electrolyte is present only on one side of the interface.

1.6.3 Thin-film electrode

The thin-film electrode is another version of the 3-electrode system available for ion-transfer experiments. The difference in comparison to the TPE comes from the fact that in TFE the whole electrode surface is covered by the organic solvent (Figure 1.12). This means that the three-phase junction cannot be formed thus, the organic phase has to contain supporting electrolyte. It might seem like this concept reflects the idea already known from the 4-electrode system where two electrolyte solutions come in contact, however in this case, the interface can be either polarizable or non-polarizable depending on the phase composition. When thin organic film and aqueous phase contain the same cation or anion, the potential difference between those liquids is controlled by the partitioning of the common ion, so the external voltage does not have to be applied[81–84]. On the contrary, the external voltage is necessary to control the liquid junction potential in thin-film electrode with a polarizable interface since in such a system, both phases have a different chemical composition and do not contain any common ions[59,85–88].

Since in TFE the electrode surface is completely covered by the organic phase, there is no limitations in terms of solvents, which can be used as long as they create an immiscible interface with water. A wide range of organic solvent including benzonitrile[81,83,86,87], nitrobenzene[59,82,84,88], benzyl cyanide[86], or 2-nitrophenyloctyl ether[85] has been applied for measurements with TFE.

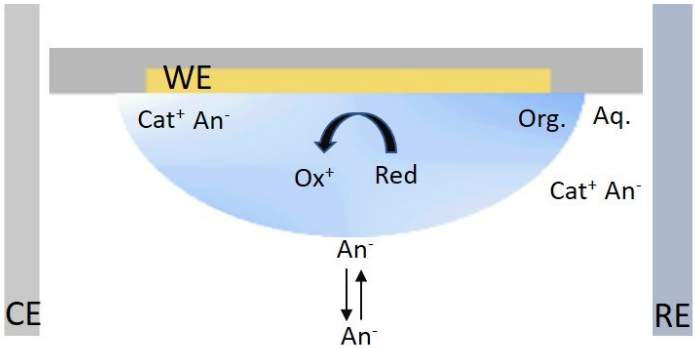

Figure 1.12 Schematic representation of the thin-film electrode. Working electrode (WE) completely covered by the organic phase is immersed into an aqueous solution in which counter (CE) and reference (RE) electrodes are placed.

Depending on the composition of the organic phase, TFE can be applied for the investigation of facilitated or electrochemically driven ion transfer. The first mentioned reaction is the basis for the detection mechanism in ion-selective electrodes, probably the most well-known commercial application of ion-transfer. ISEs are made for selective determination of inorganic ions mostly by means of potentiometric methods, although voltammetric ISEs have been developed as well[89].

When the organic film contains a redox probe, its oxidation/reduction upon applied potential extorts transfer of aqueous anions/cations due to the disturbance in organic phase electroneutrality. Similarly, as in the case of TPE, measured redox potential can be used to calculate standard transfer potentials of ions and their Gibbs energies of the transfer. Moreover, as was shown by Mirceski and

co-workers TFE enables kinetic studies of both electron and ion transfer processes as well as provides information about the rate-limiting step[90].

1.7 Applications of liquid/liquid electrochemistry

Electrochemistry at the liquid/liquid interface is a very versatile sensing tool since it enables fast and label-free detection of various charged species. Of course, the most straightforward application of this technique is ion detection, which can be now realized by commercially available products, namely ion-selective electrodes. ISEs are based on facilitated ion transfer, and thus selectivity of the measurement can be controlled by choosing suitable ionophore present in the organic phase[89,91,92]. The concentration of the analyte is determined by its correlation with the measured open circuit potential or deduced from changes in the measured ionic currents. The sensitivity of the latter approach can be enhanced by using stripping voltammetry, leading to remarkable subnanomolar detection limits[93–95].

In contrast to classical electrochemistry, analytes do not have to be redox-active to be detected by means of ion-transfer, which is a significant advantage in terms of biosensing applications. The majority of biologically important molecules do not exhibit redox activity. However, they can be present in their ionic forms at some specific pH range, which makes them perfect analytes for liquid/liquid electrochemistry. Investigation of biological compounds is mostly performed in 4- or 2-electrode systems with miniaturized polarizable interfaces[8,9]. Detection of proteins at the ITIES is a leading topic of research done in the field and has led to the development of various strategies enabling the detection of proteins at a nanomolar level as well as analysis of complex samples such as biomolecule mixtures[96–100]. Another important aspect is the investigation of the electrochemical behavior of proteins at the ITIES, providing information about the mechanism of protein adsorption at the liquid/liquid interface and

conformational changes related to this process[101–105]. Other compounds widely studied using systems based on ion-transfer are neurotransmitters[106,107] and drugs[108–111]. In pharmacological studies, ITIES serves as a tool to assess drugs' bioavailability by determining parameters such as partition coefficients and membrane permeability[112]. It can also be used to examine the interaction between active substances and other drug compounds[113,114]. The above-mentioned studies are performed using water/organic interfaces that mimic one half of a biologic membrane. Thus, to get more precise information about the molecular transport, biologists went a step further and constructed experimental setups resembling the whole cell structure. The two most interesting systems are so-called black lipid membranes (BLM) [115–120] and the Ussing chamber[118,121,122]. The former is composed of a thin phospholipid layer entrapped between two aqueous electrolytes, while in the latter, the phospholipid membrane is exchanged for the piece of tissue. In both systems, the organic membrane is polarized by the application of an external voltage between standard Ag/AgCl electrodes placed in each aqueous compartment. Experiments performed using BLMs provide information about the functioning of ion channels as well as enable bioaffinity studies with receptors or enzymes. The Ussing chamber is a unique method to investigate the movement of ions actively transported by epithelial cells due to the elimination of osmotic and hydrostatic gradients. In fact, the article describing sodium transfer in frog skin using the Ussing chamber was published more than 10 years before the polarizable interface proposed by Gavach became a popular topic in the electrochemical community[121]. Since all living organisms consist of liquid/liquid interfaces, electrochemistry at the ITIES is widely used in biology to study molecular transport and mechanism of functioning of ion channels[123–127].

Another field of application of liquid/liquid electrochemistry is the electrosynthesis of polymers and nanomaterials directly at the phase boundary[128,129].

Depending on the properties of the deposited material, the decorated interface can be utilized to catalyze electron transfer reactions or to enhance the efficiency of ion separation processes[130–132]. The interfacial generation of mesoporous silica materials triggered by the transfer of surfactant ions present in the organic phase is one of the most widely used methods to obtain polarizable liquid/liquid interface with sieving properties[133–135]. The tunable porous structure of the silica enables the separation of various species based on their charge and size. Modification of the soft interface does not necessarily have to be electrochemically induced, it can occur spontaneously if amphiphilic molecules are present in one of the phases. The most well-known molecules composed of both hydrophilic and hydrophobic groups are surfactants, which can easily assemble at the liquid/liquid interface leading to the drop in the interfacial tension. As was shown by Kakiuchi, adsorption of the ionic surfactants reaches the maximum when the value of the liquid junction potential is close to the value of the standard transfer potential of the surfactant ion[136,137]. In some cases, affinity of the molecules to the organic or aqueous phase can be controlled by the pH adjustment. One of the examples is the self-assembly of water-soluble porphyrins, which function as light harvesters in systems made for interfacial photoinduced electron transfer studies[138].

Further examples of applications of liquid/liquid electrochemistry in various fields of chemistry can be found in a recent review article in which I was responsible for the part concerning analytical chemistry.

1.8 References

[1] W. Nernst, E. H. Riesenfeld, *Ann. Phys.* **1902**, *313*, 600–608.

[2] C. Gavache, T. Mlodnicka, J. Guastalla, *Comptes rendus Hebd. des séances l'Académie des Sci. Série C, Sci. Chim.* **1968**, *266*.

[3] Z. Samec, V. Mareček, J. Weber, *J. Electroanal. Chem.* **1979**, *96*, 245–247.

[4] J. Koryta, *Electrochim. Acta* **1979**, *24*, 293–300.

[5] F. Reymond, D. Fermín, H. J. Lee, H. H. Girault, *Electrochim. Acta* **2000**, *45*, 2647–2662.
[6] Z. Samec, *Pure Appl. Chem.* **2004**, *76*, 2147–2180.
[7] E. Alvarez De Eulate, L. Serls, D. W. M. Arrigan, *Anal. Bioanal. Chem.* **2013**, *405*, 3801–3806.
[8] S. Liu, Q. Li, Y. Shao, *Chem. Soc. Rev.* **2011**, *40*, 2236–2253.
[9] M. D. Scanlon, D. W. M. Arrigan, *Electroanalysis* **2011**, *23*, 1023–1028.
[10] A. Izadyar, *Electroanalysis* **2018**, *30*, 2210–2221.
[11] G. Herzog, *Analyst* **2015**, *140*, 3888–3896.
[12] Y. Shao, M. V. Mirkin, *J. Phys. Chem. B* **1998**, *102*, 9915–9921.
[13] Y. Shao, M. V. Mirkin, *J. Electroanal. Chem.* **1997**, *439*, 137–143.
[14] Y. Wang, K. Kececi, M. V. Mirkin, *Chem. Sci.* **2013**, *4*, 3606–3616.
[15] Y. Gründer, J. F. W. Mosselmans, S. L. M. Schroeder, R. A. W. Dryfe, *J. Phys. Chem. C* **2013**, *117*, 5765–5773.
[16] R. P. Sperline, H. Freiser, *Langmuir* **1990**, *6*, 344–347.
[17] J. Lambert, R. Hergenröder, D. Suter, V. Deckert, *Angew. Chemie - Int. Ed.* **2009**, *48*, 6343–6345.
[18] A. Martínez, A. Colina, R. A. W. Dryfe, V. Ruiz, *Electrochim. Acta* **2009**, *54*, 5071–5076.
[19] E. J. W. Verwey, K. F. Niessen, **1939**, 435–446.
[20] C. Gavach, P. Seta, B. D'epenoux, *J. Electroanal. Chem.* **1977**, *83*, 225–235.
[21] M. Gros, S. Gromb, C. Gavach, *J. Electroanal. Chem.* **1978**, *89*, 29–36.
[22] Z. Samec, V. Marecek, D. Homolka, *J. Electroanal. Chem.* **1985**, *187*, 31–51.
[23] T. kakiuchi, M. Senda, *Bull. Chem. Soc. Jpn.* **1983**, *56*, 1322–1326.
[24] H. H. J. Girault, D. J. Schiffrin, *J. Electroanal. Chem.* **1984**, *170*, 127–141.
[25] D. J. S. Girault, H. H., *J. Electroanal. Chem.* **1983**, *150*, 43–49.
[26] Z. Samec, V. Mareček, K. Holub, S. Račinský, P. Hájková, *J. Electroanal. Chem.* **1987**, *225*, 65–78.
[27] C. M. Pereira, A. Martins, M. Rocha, C. J. Silva, F. Silva, *J. Chem. Soc. Faraday Trans.* **1994**, *90*, 143–148.
[28] C. M. Pereira, W. Schmickler, F. Silva, M. J. Sousa, *J. Electroanal. Chem.* **1997**, *436*, 9–15.
[29] T. Huber, O. Pecina, W. Schmickler, *J. Electroanal. Chem.* **1999**, *467*, 203–206.

[30] G. Luo, S. Malkova, S. V. Pingali, D. G. Schultz, B. Lin, M. Meron, T. J. Graber, J. Gebhardt, P. Vanysek, M. L. Schlossman, *Faraday Discuss.* **2005**, *129*, 23–34.

[31] J. Strutwolf, A. L. Barker, M. Gonsalves, D. J. Caruana, P. R. Unwin, D. E. Williams, J. R. P. Webster, *J. Electroanal. Chem.* **2000**, *483*, 163–173.

[32] D. Michael, I. Benjamin, *J. Electroanal. Chem.* **1998**, *450*, 335–345.

[33] G. C. Gschwend, A. Olaya, P. Peljo, H. H. Girault, *Curr. Opin. Electrochem.* **2020**, *19*, 137–143.

[34] G. Luo, S. Malkova, J. Yoon, D. G. Schultz, B. Lin, M. Meron, I. Benjamin, P. Vanýsek, M. L. Schlossman, *Science (80-.).* **2006**, *311*, 216–218.

[35] N. Laanait, J. Yoon, B. Hou, P. Vanysek, M. Meron, B. Lin, G. Luo, I. Benjamin, M. L. Schlossman, *J. Chem. Phys.* **2010**, *132*, DOI 10.1063/1.3428395.

[36] N. Laanait, M. Mihaylov, B. Hou, H. Yu, P. Vanýsek, M. Meron, B. Lin, I. Benjamin, M. L. Schlossman, *Proc. Natl. Acad. Sci. U. S. A.* **2012**, *109*, 20326–20331.

[37] B. Hou, N. Laanait, H. Yu, W. Bu, J. Yoon, B. Lin, M. Meron, G. Luo, P. Vanysek, M. L. Schlossman, *J. Phys. Chem. B* **2013**, *117*, 5365–5378.

[38] B. Hou, W. Bu, G. Luo, P. Vanýsek, M. L. Schlossman, *J. Electrochem. Soc.* **2015**, *162*, H890–H897.

[39] N. Laanait, *Ion Correlations at Electrified Soft Matter Interfaces*, **2013**.

[40] M. De Serio, H. Mohapatra, R. Zenobi, V. Deckert, *Chem. Phys. Lett.* **2006**, *417*, 452–456.

[41] F. G. Moore, G. L. Richmond, *Acc. Chem. Res.* **2008**, *41*, 739–748.

[42] L. F. Scatena, M. G. Brown, G. L. Richmond, *Science (80-.).* **2001**, *292*, 908–912.

[43] S. M. Kathmann, I. F. W. Kuo, C. J. Mundy, G. K. Schenter, *J. Phys. Chem. B* **2011**, *115*, 4369–4377.

[44] S. M. Kathmann, I. F. W. Kuo, C. J. Mundy, *J. Am. Chem. Soc.* **2008**, *130*, 16556–16561.

[45] L. Wang, *Annu. Rev. Biochem.* **2012**, *81*, 615–635.

[46] M. F. Suárez-Herrera, M. D. Scanlon, *Electrochim. Acta* **2019**, *328*, 1–9.

[47] M. F. Suárez-Herrera, P. A. Cazade, D. Thompson, M. D. Scanlon, *Electrochem. commun.* **2019**, *109*, 106564.

[48] A. G. Volkov, D. M. Deamer, *Liquid-Liquid Interfaces : Theory and Methods*, CRC, Boca Raton, **1996**.
[49] P. Vanysek, L. Basaez Ramirez, *J. Chil. Chem. Soc.* **2008**, *53*, DOI 10.4067/S0717-97072008000200002.
[50] P. Peljo, H. H. Girault, in *Encycl. Anal. Chem.*, John Wiley & Sons, Ltd, Chichester, UK, **2012**.
[51] F. Scholz, R. Gulaboski, *ChemPhysChem* **2005**, *6*, 16–28.
[52] T. Solomon, A. J. Bard, *J. Phys. Chem.* **1995**, *99*, 17487–17489.
[53] M. Tsionsky, A. J. Bard, M. V. Mirkin, *J. Phys. Chem.* **1996**, *100*, 17881–17888.
[54] C. Wei, A. J. Bard, M. V. Mirkin, *J. Phys. Chem.* **1995**, *99*, 16033–16042.
[55] R. A. W. Dryfe, Z. Ding, R. G. Wellington, P. F. Brevet, A. M. Kuznetzov, H. H. Girault, *J. Phys. Chem. A* **1997**, *101*, 0–5.
[56] D. J. Fermín, Z. Ding, H. D. Duong, P. F. Brevet, H. H. Girault, *Chem. Commun.* **1998**, 1125–1126.
[57] Z. Ding, P. F. Brevet, H. H. Girault, *Chem. Commun.* **1997**, 2059–2060.
[58] M. Tsionsky, A. J. Bard, M. V. Mirkin, *J. Am. Chem. Soc.* **1997**, *119*, 10785–10792.
[59] C. Shi, F. C. Anson, *J. Phys. Chem. B* **1999**, *103*, 6283–6289.
[60] B. Liu, M. V. Mirkin, *J. Am. Chem. Soc.* **1999**, *121*, 8352–8355.
[61] P. Peljo, E. Smirnov, H. H. Girault, *J. Electroanal. Chem.* **2016**, *779*, 187–198.
[62] H. Hotta, S. Ichikawa, T. Sugihara, T. Osakai, *J. Phys. Chem. B* **2003**, *107*, 9717–9725.
[63] T. Osakai, S. Ichikawa, H. Hotta, H. Nagatani, *Anal. Sci.* **2004**, *20*, 1567–1573.
[64] T. . G. Gavach, C.; Mlodnick, *Comptes rendus Hebd. Des Seances L Acad. Des Sci. Ser. C* **1968**, *266*.
[65] M. Kasuno, Y. Matsuyama, M. Iijima, *ChemElectroChem* **2016**, *3*, 694–697.
[66] M. Kasuno, K. Wakabayashi, Y. Matsuyama, R. Yamamura, *Electrochim. Acta* **2020**, 136069.
[67] A. J. Olaya, P. Ge, H. H. Girault, *Electrochem. commun.* **2012**, *19*, 101–104.
[68] P. S. Toth, R. A. W. Dryfe, *Analyst* **2015**, *140*, 1947–1954.
[69] N. E. A. Cousens, A. R. Kucernak, *Electrochem. commun.* **2011**, *13*, 1539–1541.

[70] G. Taylor, H. H. J. Girault, *J. Electroanal. Chem.* **1986**, *208*, 179–183.
[71] F. Scholz, Š. Komorsky-Lovrić, M. Lovrić, *Electrochem. commun.* **2000**, *2*, 112–118.
[72] D. Rayner, N. Fietkau, I. Streeter, F. Marken, B. R. Buckley, P. C. Bulman Page, J. Del Campo, R. Mas, F. X. Muñoz, R. G. Compton, *J. Phys. Chem. C* **2007**, *111*, 9992–10002.
[73] E. Bak, M. Donten, Z. Stojek, *J. Electroanal. Chem.* **2007**, *600*, 45–53.
[74] M. Donten, Z. Stojek, F. Scholz, *Electrochem. commun.* **2002**, *4*, 324–329.
[75] Š. Komorsky-Lovrić, V. Mirčeski, C. Kabbe, F. Scholz, *J. Electroanal. Chem.* **2004**, *566*, 371–377.
[76] G. Bouchard, A. Galland, P. A. Carrupt, R. Gulaboski, V. Mirčeski, F. Scholz, H. H. Girault, *Phys. Chem. Chem. Phys.* **2003**, *5*, 3748–3751.
[77] R. Gulaboski, V. Mirčeski, F. Scholz, *Electrochem. commun.* **2002**, *4*, 277–283.
[78] R. Gulaboski, A. Galland, G. Bouchard, K. Caban, A. Kretschmer, P.A. Carrupt, Z. Stojek, H. H. Girault, F. Scholz, *J. Phys. Chem. B* **2004**, *108*, 4565–4572.
[79] M. Opallo, J. Kukulka-Walkiewicz, M. Saczek-Maj, *J. Sol-Gel Sci. Technol.* **2003**, *26*, 1045–1048.
[80] M. Saczek-Maj, M. Opallo, *Electroanalysis* **2002**, *14*, 1060–1066.
[81] C. Shi, F. C. Anson, *Anal. Chem.* **1998**, *70*, 3114–3118.
[82] F. Quentel, V. Mirčeski, M. L'Her, *Anal. Chem.* **2005**, *77*, 1940–1949.
[83] C. Shi, F. C. Anson, *J. Phys. Chem. B* **2001**, *105*, 8963–8969.
[84] C. Shi, F. C. Anson, *J. Phys. Chem. B* **2001**, *105*, 1047–1049.
[85] F. Quentel, V. Mirčeski, C. Elleouet, M. L'Her, *J. Phys. Chem. C* **2008**, *112*, 15553–15561.
[86] H. O. Shafer, T. L. Derback, C. A. Koval, *J. Phys. Chem. B* **2000**, *104*, 1025–1032.
[87] T. D. Chung, F. C. Anson, *J. Electroanal. Chem.* **2001**, *508*, 115–122.
[88] R. Gulaboski, V. Mirćeski, C. M. Pereira, M. N. D. S. Cordeiro, A. F. Silva, F. Quentel, M. L'Her, M. Lovrić, *Langmuir* **2006**, *22*, 3404–3412.
[89] E. Bakker, *Ion-Selective Electrodes*, Elsevier Inc., **2018**.
[90] V. Mirčeski, F. Quentel, M. L'Her, A. Pondaven, *Electrochem. commun.* **2005**, *7*, 1122–1128.
[91] J. Zhang, A. R. Harris, R. W. Cattrall, A. M. Bond, **2010**, *82*, 1624–1633.

[92] Z. Jarolímová, J. Bosson, G. M. Labrador, J. Lacour, E. Bakker, *Electroanalysis* **2018**, *30*, 1378–1385.
[93] B. Kabagambe, A. Izadyar, S. Amemiya, *Anal. Chem.* **2012**, *84*, 7979–7986.
[94] B. Kabagambe, M. B. Garada, R. Ishimatsu, S. Amemiya, *Anal. Chem.* **2014**, *86*, 7939–7946.
[95] A. Izadyar, F. Al-Amoody, D. R. Arachchige, *J. Electroanal. Chem.* **2016**, *782*, 43–49.
[96] S. O'Sullivan, E. Alvarez De Eulate, Y. H. Yuen, E. Helmerhorst, D. W. M. Arrigan, *Analyst* **2013**, *138*, 6192–6196.
[97] D. W. M. Arrigan, *Anal. Lett.* **2008**, *41*, 3233–3252.
[98] D. W. M. Arrigan, **2013**, 167–188.
[99] D. W. M. Arrigan, M. J. Hackett, R. L. Mancera, *Curr. Opin. Electrochem.* **2018**, *12*, 27–32.
[100] E. Alvarez De Eulate, S. O'Sullivan, S. Fletcher, P. Newsholme, D. W. M. Arrigan, *Chem. - An Asian J.* **2013**, *8*, 2096–2101.
[101] G. Herzog, V. Kam, D. W. M. Arrigan, *Electrochim. Acta* **2008**, *53*, 7204–7209.
[102] H. Sakae, Y. Toda, T. Yokoyama, *Electrochem. commun.* **2018**, *90*, 83–86.
[103] M. D. Scanlon, E. Jennings, D. W. M. Arrigan, *Phys. Chem. Chem. Phys.* **2009**, *11*, 2272–2280.
[104] S. O'Sullivan, D. W. M. Arrigan, *Electrochim. Acta* **2012**, *77*, 71–76.
[105] G. Herzog, W. Moujahid, J. Strutwolf, D. W. M. Arrigan, *Analyst* **2009**, *134*, 1608–1613.
[106] M. L. Colombo, J. V. Sweedler, M. Shen, *Anal. Chem.* **2015**, *87*, 5095–5100.
[107] N. T. Iwai, M. Kramaric, D. Crabbe, Y. Wei, R. Chen, M. Shen, *Anal. Chem.* **2018**, *90*, 3067–3072.
[108] S. Jeshycka, H. Y. Han, H. J. Lee, *Electrochim. Acta* **2017**, *245*, 211–218.
[109] M. Sairi, D. W. M. Arrigan, *Talanta* **2015**, *132*, 205–214.
[110] A. Izadyar, D. R. Arachchige, H. Cornwell, J. C. Hershberger, *Sensors Actuators, B Chem.* **2016**, *223*, 226–233.
[111] X. Huang, L. Xie, X. Lin, B. Su, *Anal. Chem.* **2017**, *89*, 945–951.
[112] M. Velický, A. N. J. Rodgers, R. A. W. Dryfe, K. Tam, *ADMET DMPK* **2014**, *2*, 143–156.
[113] M. A. Deryabina, S. H. Hansen, J. Østergaard, H. Jensen, *J. Phys. Chem. B* **2009**, *113*, 7263–7269.
[114] H. Sakae, H. Nagatani, H. Imura, *Electrochim. Acta* **2016**, *191*, 631–639.

[115] Z. F. Su, J. J. Leitch, J. Lipkowski, *Curr. Opin. Electrochem.* **2018**, *12*, 60–72.
[116] O. Shirai, Y. Yoshida, S. Kihara, *Anal. Bioanal. Chem.* **2006**, *386*, 494–505.
[117] R. S. Ries, H. Choi, R. Blunck, F. Bezanilla, J. R. Heath, *J. Phys. Chem. B* **2004**, *108*, 16040–16049.
[118] J. Yeste, X. Illa, M. Alvarez, R. Villa, *J. Biol. Eng.* **2018**, *12*, 1–19.
[119] O. Shirai, Y. Yoshida, S. Kihara, T. Ohnuki, A. Uehara, H. Yamana, *J. Electroanal. Chem.* **2006**, *595*, 53–59.
[120] S. Ozaki, S. Aoki, T. Hibi, K. Kano, O. Shirai, *Electrochem. commun.* **2008**, *10*, 1509–1512.
[121] H. H. USSING, K. ZERAHN, *Acta Physiol. Scand.* **1951**, *23*, 110–127.
[122] L. L. Clarke, *Am. J. Physiol. - Gastrointest. Liver Physiol.* **2009**, *296*, 1151–1166.
[123] A. P. Davis, D. N. Sheppard, B. D. Smith, *Chem. Soc. Rev.* **2007**, *36*, 348–357.
[124] J. T. Davis, O. Okunola, R. Quesada, *Chem. Soc. Rev.* **2010**, *39*, 3843–3862.
[125] J. R. Vieregg, T. D. Tang, *Curr. Opin. Colloid Interface Sci.* **2016**, *26*, 50–57.
[126] L. J. S. Vallejo, J. M. Ovejero, R. A. Fern, S. A. Dassie, *Int. J. Electrochem.* **2012**, *2012*, DOI 10.1155/2012/462197.
[127] C. Wood, C. Williams, G. J. Waldron, *Drug Discov. Today* **2004**, *9*, 434–441.
[128] L. Poltorak, A. Gamero-Quijano, G. Herzog, A. Walcarius, *Appl. Mater. Today* **2017**, *9*, 533–550.
[129] R. A. W. Dryfe, *Phys. Chem. Chem. Phys.* **2006**, *8*, 1869–1883.
[130] V. J. Cunnane, U. Evans, *Chem. Commun.* **1998**, 2163–2164.
[131] A. N. J. Rodgers, S. G. Booth, R. A. W. Dryfe, *Electrochem. commun.* **2014**, *47*, 17–20.
[132] P. Peljo, M. D. Scanlon, A. J. Olaya, L. Rivier, E. Smirnov, H. H. Girault, *J. Phys. Chem. Lett.* **2017**, *8*, 3564–3575.
[133] V. Mareček, H. Jänchenová, *J. Electroanal. Chem.* **2003**, *558*, 119–123.
[134] L. Poltorak, K. Morakchi, G. Herzog, A. Walcarius, *Electrochim. Acta* **2015**, *179*, 9–15.
[135] L. Poltorak, G. Herzog, A. Walcarius, *Electrochem. commun.* **2013**, *37*, 76–79.
[136] T. Kakiuchi, *J. Electroanal. Chem.* **2002**, *536*, 63–69.
[137] T. Kakiuchi, *J. Electroanal. Chem.* **2001**, *496*, 137–142.
[138] A. F. Molina-Osorio, D. Cheung, C. O'Dwyer, A. A. Stewart, M. Dossot, G. Herzog, M. D. Scanlon, *J. Phys. Chem. C* **2020**, *124*, 6929–6937.

2 Paper-based system for anion transfer studies

2.1 Introduction

Electrochemically driven anion transfer is one of the most widely studied processes in the three-phase electrode systems. As explained in the previous chapter, to investigate the transport of anions from the aqueous to the organic phase, the latter one has to contain a redox probe that can undergo a reversible oxidation reaction. Moreover, it has to be lipophilic, both in the neutral and charged form, to not be expelled from the organic phase during the measurement since that would affect the liquid junction potential and the recorded current related to the anion transfer. Decamethylferrocene (DMFc) fulfils all those requirements, and for that reason, it is usually the first choice for the experiments performed in the TPE systems[1–6]. Results presented in this chapter were obtained using decamethylferrocene as the redox probe.

The standard way of creating a three-phase junction is by modifying the electrode surface with a droplet of an organic solvent[7]. Although it is claimed to be a very simple method, droplet-based TPE is not trivial to set up and requires some experience because the organic droplet can easily detach from the electrode surface during the immersion into the aqueous solution. Mechanical instability of the liquid/liquid interface is the biggest drawback of this approach since the lack of control over the length of the three-phase junction leads to the poor reproducibility of the measured ionic currents. It also limits the number of solvents that can be used to those, enabling creation of reasonably stable droplets. This issue can be overcome by combining liquid/liquid electrochemistry with microfluidic flow systems[8]. The well-defined width of the microchannels through which aqueous and organic solutions flow helps to precisely determine and control the contact area between immiscible solvents and electrode embedded into the device. Such an approach increases the stability of the interface but

at the same time confines ion-transfer studies to specialized laboratories equipped with cleanroom facilities necessary for the preparation of the microfluidic systems.

Therefore there is a need to develop systems enabling the creation of a mechanically stable phase boundary and at the same time being easy to set up and available for a wide range of users. Paper seems to be a perfect candidate for that purpose – it is cheap, easy to use or modify, and able to adsorb both aqueous and organic solvents. The unique properties of the paper structure are well-known for centuries[9] and have been incisively explored for applications in the field of analytical sensors[10,11]. The ability of cellulose structure to transport fluids solely by means of capillary forces, remarkable absorbency, and abundance are the main factors responsible for the growing interest in paper as a sensor substrate. A variety of paper-based devices, including spot-tests, lateral flow assays, or microfluidic systems (μPADs, microfluidic paper-based devices) have been developed over the past decade[12–20]. A colorimetric bioassay with a multichannel paper platform presented by Whitesides group is considered by many researchers as the first modern paper-based analytical device[21]. They patterned paper using photolithography to create well-defined hydrophilic channels restricted by hydrophobic walls allowing for spacial control of fluids and simultaneous detection of glucose and proteins in artificial urine. The first electrochemical paper-based sensor was introduced by Henry's group to detect glucose, lactate, and uric acid in biological samples[22]. The screen-printing technique described by authors is, until now, one of the most commonly used methods to integrate conductive materials in the cellulose matrix. Technical aspects related to the preparation of paper-based systems can be found in many excellent reviews[10,14,23,24].

Although widely used in analytical chemistry, paper did not attract as much attention in the field of liquid/liquid electrochemistry. Applications of cellulose

matrix in ITIES studies are scarcely explored and limited to paper-based ISEs[25–29]. The pioneering work in this field was done by Novell et al., who developed a potentiometric sensor with carbon modified paper as a platform[27] and used it for lithium detection in blood samples[26]. This work was followed by other reports of potentiometric ion-sensing systems using functionalized paper as a support. It is, however, surprising that other ion-transfer systems were not developed using paper since its adsorptive properties make the cellulose matrix an ideal support for biphasic studies. Therefore in my research, I used paper to create an easy to handle and low-cost alternative to standard droplet-based TPE configuration. In this system, paper acts as a reservoir of both the aqueous and organic phases, helping to stabilize and better control the liquid/liquid interface. The three-phase junction is formed along a gold mesh (working electrode) placed between two pieces of paper – one soaked with organic and the other with an aqueous solution (Figure 2.1).

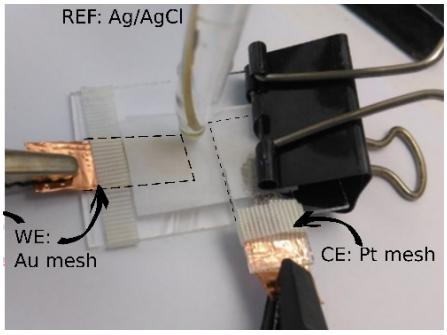

Figure 2.1 Picture of the paper-based three-phase electrode system. The counter (Pt) and working (Au) electrodes are attached to the separate glass slides using insulating tape to prevent their displacement during the experiment. The gold grid is placed between two pieces of paper (1.5 cm × 2.5 cm) soaked in NOP (bottom one) and aqueous electrolyte solution (top one). The reference and counter electrodes are in direct contact with the aqueous solution kept in the top piece of paper.

I used the paper-based TPE system to investigate the transfer of seven different anions (X^-) from the aqueous to the organic phase triggered by the oxidation of DMFc dissolved in NOP:

$$DMFc_{NOP} + X_W^- \rightarrow DMFc_{NOP}^+ + X_{NOP}^- + e^-$$

Moreover, I also performed experiments showing that simultaneous double transfer of anions depends on the concentration ratio between the redox probe and anions of interest. To the best of my knowledge, it is the first paper-based system made for ion-transfer studies using a 3-phase electrode configuration.

Results presented in this chapter were published as a research article in Analytical Chemistry:

M. Podrażka, E. Witkowska Nery, A. Pacowska, D. W. M. Arrigan, M. Jönsson-Niedziółka, *Paper-Based System for Ion Transfer Across the Liquid-Liquid Interface*, Anal. Chem. 2018, 90, 8727−8731.

Computer simulations in COMSOL were performed by dr hab. Martin Jönsson-Niedziółka and PCA analysis of water samples was done by dr Emilia Witkowska Nery.

2.2 Materials and Methods

2.2.1 Chemicals and Materials

Decamethylferrocene (DMFc) (97%, Sigma-Aldrich); N-octyl-2-pyrrolidone (NOP) (98%, Santa Cruz Biotechnology); inorganic salts of analytical grade, KPF_6 (99%, ABCR), $KClO_4$ (pure p.a. International Enzymes Limited), NaSCN (pure p.a., Fluka), KNO_3 (99%, POCh), KBr (pure p.a., POCh), KCl (>99.99%, Sigma-Aldrich), NaF (pure p.a., POCh), and K_2SO_4 (pure p.a., ChemPur) were used as received. Water was filtered and demineralized with ELIX system (Milipore). Whatman no. 1 cellulose chromatography paper was purchased from Sigma-Aldrich.

2.2.2 Electrochemical Measurements

Cyclic voltammetry (CV) and differential pulse voltammetry (DPV) were performed with an Autolab potentiostat (Metrohm Autolab B.V., The Netherlands) controlled by the NOVA software (version 2.1.2). Parameters for DPV were as follows: step potential 0.005 V, modulation amplitude 0.025 V, modulation time 0.05 s, interval time 0.5 s, and scan rate 0.01 V/s. All measurements were performed in a three-electrode system with a silver−silver chloride electrode (Ag|AgCl|saturated KCl) as a reference electrode, platinum mesh (Goodfellow) as a counter electrode, and gold mesh (Goodfellow) as a working electrode. All measurements were carried out at room temperature.

2.3 Results and discussion

2.3.1 Effect of anion hydrophobicity

Since the paper-based system had never been used before to study electrochemically driven ion-transfer, first, I had to verify if it works similarly to the traditional droplet-based approach. One of the typical effects observed in the classic TPE systems is the dependence between the measured voltammetric response and the lipophilic properties of the transported ions. The general rule is that the more hydrophilic the ion is, the more positive is the value of its standard transfer potential from the aqueous to the organic phase. In the case of anions, which I used in the experiments the $\Delta_O^W \phi^0$ increases in the following order:

$$PF_6^- < ClO_4^- < SCN^- < NO_3^- < Br^- < Cl^- \approx F^-$$

As explained in the chapter 1.5.3 of the literature part, a Nernst-like equation describes the formal potential of the redox reaction coupled to the anion transfer process observed in the TPE systems (Equation 12). For the reversible oxidation of DMFc dissolved in NOP, it can be written in the following form:

$$E_{DMFc^+/DMF} = E^0_{DMFc^+/DMFc} + \Delta^W_{NOP}\phi^0_{An^-} - \frac{RT}{F} ln c_{An^-_{(org)}} + \frac{RT}{F} ln \frac{c^*_{DMFc}}{2} \qquad (1)$$

Based on the above formula, one can see that the measured peak potential ($E_{DMFc^+/DMFc}$) should shift to more positive values with increasing hydrophilic properties of the transferred anion (more positive $\Delta^W_{NOP}\phi^0_{An^-}$). This effect is observed on the DPV plots, which I measured in the paper-based system (Figure 2.2A)

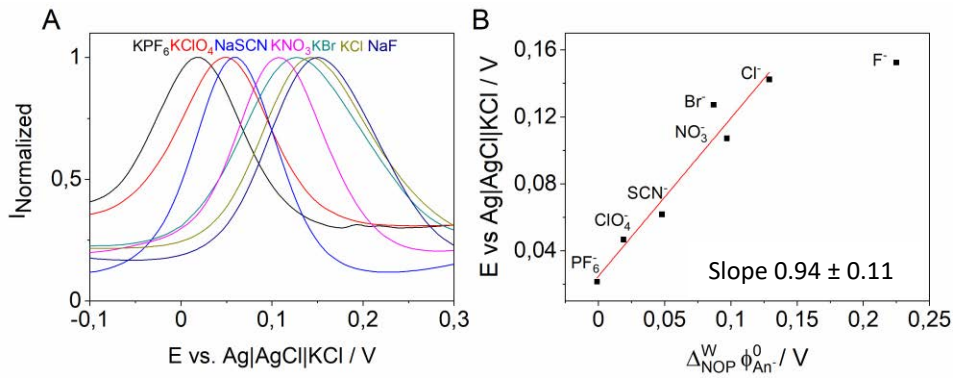

Figure 2.2 DPV plots measured for seven different anions transferring from aqueous to the organic phase (A) and the correlation between the peak potential and standard transfer potential of all studied anions (B). The concentration of anions was 0.1 M and DMFc 0.01 M.

Equation (1) also leads to the conclusion that the peak potential is a linear function of the standard transfer potential of the anion. To verify if this correlation is valid for the paper-based system, I plotted the dependence of E_p taken from DPV plots on $\Delta^W_{NOP}\phi^0_{An^-}$ determined by the L'Her method[3] (Figure 2.2B). The slope of the obtained plot is very close to 1 (0.94±0.11), confirming that the paper device is based on the same working principle as the droplet-based system. It is noteworthy that the transfer potential of fluoride ion does not follow the linear trend which is related to its highly hydrophilic nature and will be explained in the next chapter.

2.3.2 Effect of anion concentration

Another effect observed in the classic droplet-based systems is the linear correlation between the peak potential and the anion concentration. For one-electrode redox reactions such as oxidation of DMFc the slope of this dependence should be 59 mV per decade (Equation 1). The electrochemical response related to the transfer of PF_6^- across the paper-supported interface is consistent with this model (Figure 2.3A). However, results obtained for the transfer of the highly hydrophilic Cl^- do not exhibit any concentration dependence (Figure 2.3B).

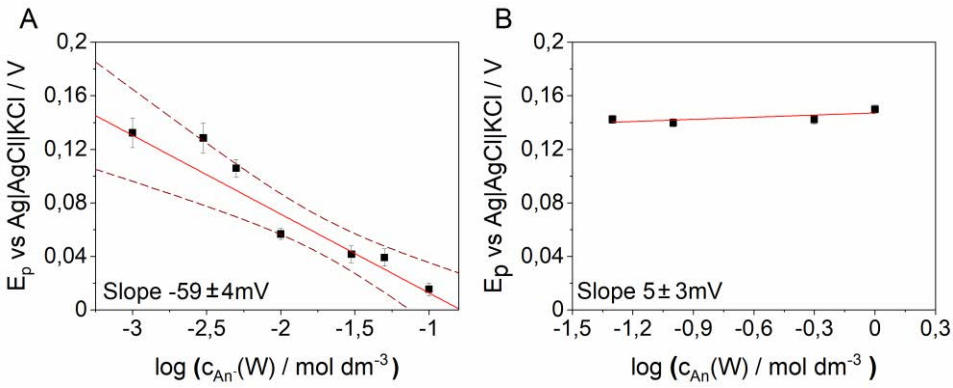

Figure 2.3 Correlation between peak potential and logarithm of the concentration of (A) KPF_6 and (B) KCl in the aqueous phase. The dashed lines represent 95% confidence limits.

The reason is the very high value of the Cl^- standard transfer potential resulting in the expulsion of $DMFc^+$ from the organic phase:

$$DMFc_{NOP} \rightarrow DMFc_W^+ + e^-$$

In this case, the formal redox potential is given by the modified Nernst-like equation, which does not contain any terms related to the concentration of the anion[5]:

$$E_{DMFc^+/DMF} = E^0_{DMFc^+/DMFc} - \Delta^W_{NOP}\phi^0_{DMFc^+} + \frac{RT}{F} ln \frac{c_{DMFc^+}(W)}{c_{DMFc}(NOP)} \qquad (2)$$

where $\Delta^{W}_{NOP}\phi^{0}_{DMFc^+}$ is the standard transfer potential of $DMFc^+$ from NOP to water, $c_{DMFc^+}(W)$ is the concentration of $DMFc^+$ in the aqueous phase and $c_{DMFc}(NOP)$ is the initial concentration of DMFc in the organic phase.

Lack of concentration dependence in the presence of highly hydrophilic anions like Cl^- or F^- is a well-known effect described for other systems where ion-transfer was driven by the electrooxidation of DMFc[30]. Observation of this effect in the paper-based configuration proves that it can be used as an alternative to the traditional droplet-based setup.

2.3.3 Mixture of anions

The vast majority of literature reports concerning electrochemically driven ion-transfer is focused on single anion or cation transport. However, the simultaneous determination of two or more anions at the same time is very interesting from an applicational point of view. It would open the way to use a three-phase ion-transfer as a tool for the detection of pollutants (e.g., NO_3^-) in water samples. Therefore, to verify the possibility of double anion transfer, I performed experiments using mixtures containing 100 mM, 10 mM or 1 mM $KClO_4$ and KNO_3. I chose those anions due to the significant difference in their transfer potentials and the fact that they are often present in tap or mineral water. Since the main objective of the measurement was to investigate the simultaneous transfer of ClO_4^- and NO_3^- I expected to see on DPV plots two peaks with potential values similar to transfer potentials of these ions. Surprisingly, for 100 mM and 10 mM mixtures, the measured current reached a maximum only once at the potential corresponding to ClO_4^- (Figure 2.4A). A double-peak shaped response appeared only for the 1 mM mixture; however, both signals were shifted to more positive potentials than those observed for single anion transfer (Figure 2.4A).

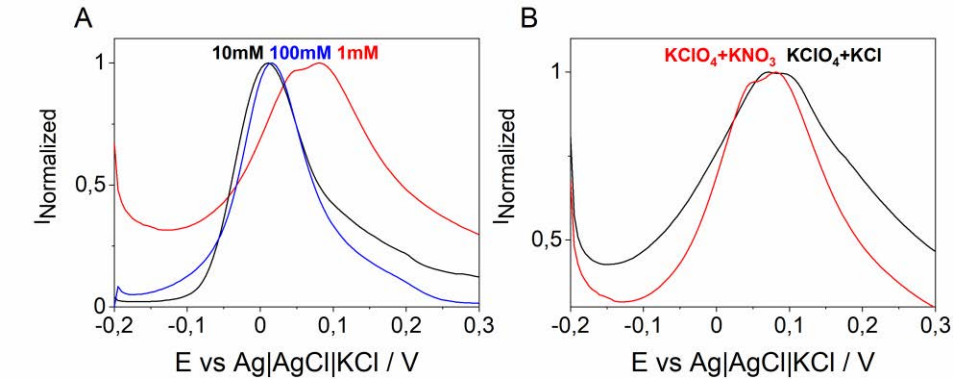

Figure 2.4 DPV curves measured for the mixture of $KClO_4$ and KNO_3 of different concentrations (A) and 1 mM mixture composed of $KClO_4$, KNO_3, and $KClO_4$, KCl (B). DMFc (10 mM) dissolved in NOP was used as the organic phase in both experiments.

Since, in all experiments, the concentration of DMFc was constant (10 mM), differences in the observed electrochemical responses have to be related to the concentration ratio between the redox probe and the anions of interest. This phenomenon can be explained based on the mechanism of the electrochemically driven anion transfer. Anions are crossing the phase boundary only until the positive charge generated by oxidation of DMF is balanced. When, in the aqueous phase two different anions are present, in concentrations higher than the redox probe, the first one to transfer already neutralizes the whole charge of the organic phase. It means that there is simply no more redox probe at the interface, which could oxidase to trigger the transfer of the second anion. Due to stronger hydrophobic properties, transport of ClO_4^- is thermodynamically favorable over NO_3^-. Therefore, signals registered for 100 mM and 10 mM mixtures correspond to the transfer potential of ClO_4^-. However, when the concentration of the redox probe exceeds the concentration of anions, the double transfer can be observed as in the case of the 1 mM mixture. Two peaks are also observed on DPV plot for 1 mM mixture of ClO_4^- and Cl^- confirming the importance

of proper concentration ratio for the success of simultaneous double anion transfer (Figure 2.4B).

This explanation is also supported by the computer simulation performed in COMSOL. A simple model of the heterogeneous reaction was used to simulate the transfer of two anions (An1 and An2) of different concentrations across the interface between two liquids in 2D. The transfer potentials of An1 and An2 were set for 0 V and 0.2 V, respectively. In such a model, the rate of the forward reaction, k_f is given by:

$$k_f = k_0\left[DMFc_{org}\right]\left[X_{aq}^{-}\right] \quad (3)$$

where k_0 has a Butler-Volmer exponential potential dependence, $\left[DMFc_{org}\right]$ is the concentration of the redox probe $\left[X_{aq}^{-}\right]$ is the concentration of anion at the organic and aqueous sides of the interface, respectively.

Although the utilized model does not include details captured by more advanced simulations[31,32], it clearly shows that simultaneous transfer of An1 and An2 can be observed only when their concentrations are lower than the concentration of DMFc (Figure 2.5).

In the case of the high concentration of both species, only one peak is present on the simulated linear sweep voltammogram. Similar results were described by Zanotto et al. ion-transfer in a thin film electrode[33]. Importantly, for very low anion concentrations Equation 1 might not be valid anymore, as it is strictly dependent on the value of the logarithm of the concentration ratio between the ion and the redox probe[34]. This should be taken into account when considering the limits of the ion-transfer detection in TPE configuration.

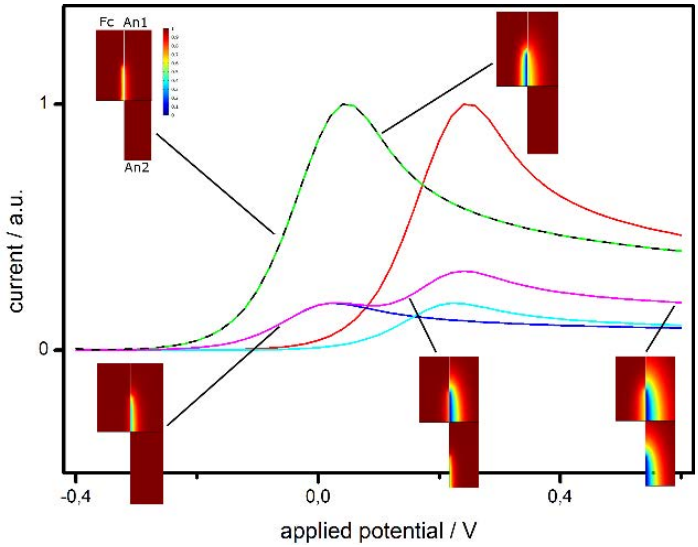

Figure 2.5 Simulation of linear sweep voltammograms for systems in which the aqueous phase contains two anions (An1 and An2). The curves show the results of different initial concentrations of An1 and An2, $c_{0,An1}$ and $c_{0,An2}$: black curve shows the response when only An1 is present in the aqueous phase an its concentration is equal to the concetration of the redox probe, $c_{0,An1} = c_{0,DMFc}$, $c_{0,An2} = 0$; red is the opposite case so only An2 present in the aqueous phase, $c_{0,An2} = c_{0,DMFc}$, $c_{0,An1} = 0$; green curve shows the results for concentrations of both cations equal to the the concentration of the redox probe, $c_{0,An1} = c_{0,An2} = c_{0,DMFc}$; blue curve is the case when the concetration of the An1 is 10 times lower than the concentration of the redox probe, $c_{0,An1} = 0.1 \times c_{0,DMFc}$, $c_{0,An2} = 0$; teal is the opposite case so when the An2 is present at 10 times lower concentration level than DMFc $c_{0,An2} = 0.1 \times c_{0,DMFc}$, $c_{0,An1} = 0$; magenta curve shows results when both cations in the aqueous phase have lower concentrations than the redox probe $c_{0,An1} = c_{0,An2} = 0.1 \times c_{0,DMFc}$. The insets show the concentrations of the redox probe in the organic solution (on the left), and the anions (An1 and An2 shown separately) in the aqueous solution (on the right), at different points during the scan. The map for An2 has been displaced vertically for clarity.

Experimental and theoretical results prove that double-anion transfer is possible, however, only under certain conditions. For that reason, the determination of specific anions in water samples might be challenging to achieve. However, I decided to verify if the discrimination of water samples of different overall ionic compositions could be done using the three-phase ion-transfer technique.

For that purpose, I performed several measurements with real samples, including tap water obtained from two places in Warsaw and two in Radom (Poland), a rainwater sample, water from a lake, and mineral water both bottled and directly from the spring (Figure 2.6A). Although analysis of DPV plots does not allow for the straightforward classification of samples, using Principal Component Analysis (PCA, mean-centered data, 3 factors) it is possible to distinguish clusters of potable and contaminated samples (Figure 2.6B). To further confirm the applicability of the paper-based system for such analysis, future studies should focus on optimization of the redox probe concentration and expanding the measurements to the higher number of water samples, including analysis of their chemical composition.

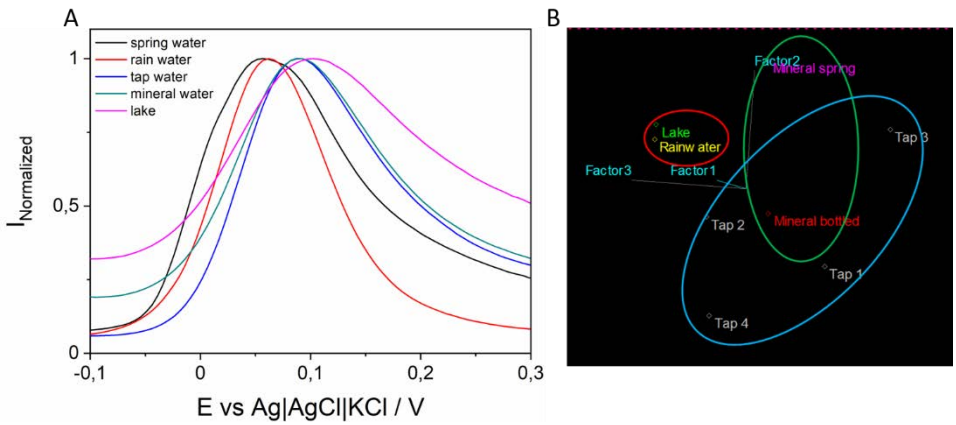

Figure 2.6 DPV measurements of real samples: rainwater, tap, lake, mineral bottled and spring water (A). PCA scores plot showing clustering of potable and contaminated samples (B).

Presented results show that the electrochemically driven ion-transfer can be, in principle, applied for water discrimination however, it would require much more time and effort to optimize it and make it competitive with other detection methods. Due to the limited amount of time for PhD research, further

optimization of the system for the qualification of water samples was not possible within this project.

2.4 Conclusions

The results described here show that a simple paper-based system can be successfully applied for the investigation of electrochemically driven ion-transfer. Observation of the two effects typical for setups with TPE, namely, the effect of anion concentration on the peak position and shift of the signal with increasing hydrophobic properties of the anion, confirm it can serve as an alternative for traditional droplet-based configuration. Moreover, experiments and computer simulations made for anion mixtures prove that the simultaneous transfer of two anions is possible under certain conditions. When planning such an analysis, one should remember that the concentration of anions has to be at least a few times lower than the concentration of the redox probe. Of course, to thoroughly explain the mechanism of double-ion transfer, more detailed analysis is needed; however, the presented results help to understand the basis of this phenomenon.

Thanks to the adsorptive properties, the paper is an excellent substrate for systems with ion-transfer detection. It serves not only as an efficient reservoir of liquid phases but also helps to increase the mechanical stability of the interface leading to better control of the three-phase junction line and higher reproducibility of the results. Another advantage is the fact that the paper-based device is much easier to set up than the droplet configuration and enables experiments with a wide range of organic solvents.

2.5 References

[1] F. Scholz, *Annu. Reports Prog. Chem. - Sect. C* **2006**, *102*, 43–70.

[2] Š. Komorsky-Lovrić, M. Lovrić, F. Scholz, *J. Electroanal. Chem.* **2001**, *508*, 129–137.

[3] D. Kaluza, W. Adamiak, M. Opallo, M. Jonsson-Niedziolka, *Electrochim. Acta* **2014**, *132*, 158–164.
[4] F. Scholz, R. Gulaboski, *ChemPhysChem* **2005**, *6*, 16–28.
[5] F. Scholz, Š. Komorsky-Lovrić, M. Lovrić, *Electrochem. commun.* **2000**, *2*, 112–118.
[6] M. Donten, Z. Stojek, F. Scholz, *Electrochem. commun.* **2002**, *4*, 324–329.
[7] R. Gulaboski, V. Mirceski, S. Komorsky-lovric, M. Lovric, **2020**.
[8] D. Kaluza, W. Adamiak, T. Kalwarczyk, K. Sozanski, M. Opallo, M. Jönsson-Niedziolka, *Langmuir* **2013**, *29*, 16034–16039.
[9] P. the Elder, **n.d.**
[10] W. Mazurkiewicz, M. Podrażka, E. Jarosińska, K. Kappalakandy Valapil, M. Wiloch, M. Jönsson-Niedziółka, E. K. Witkowska Nery, *ChemElectroChem* **2020**, DOI 10.1002/celc.202000512.
[11] E. W. Nery, L. T. Kubota, *Anal. Bioanal. Chem.* **2013**, *405*, 7573–7595.
[12] A. W. Martinez, S. T. Phillips, G. M. Whitesides, E. Carrilho, *Anal. Chem.* **2010**, *82*, 3–10.
[13] Y. Yang, E. Noviana, M. P. Nguyen, B. J. Geiss, D. S. Dandy, C. S. Henry, *Anal. Chem.* **2017**, *89*, 71–91.
[14] W. J. Paschoalino, S. Kogikoski, J. T. C. Barragan, J. F. Giarola, L. Cantelli, T. M. Rabelo, T. M. Pessanha, L. T. Kubota, *ChemElectroChem* **2019**, *6*, 10–30.
[15] L. L. Shen, G. R. Zhang, B. J. M. Etzold, *ChemElectroChem* **2020**, *7*, 10–30.
[16] J. Adkins, K. Boehle, C. Henry, *Electrophoresis* **2015**, *36*, 1811–1824.
[17] H. Liu, R. M. Crooks, *J. Am. Chem. Soc.* **2011**, *133*, 17564–17566.
[18] J. D. Newman, A. P. F. Turner, *Biosens. Bioelectron.* **2005**, *20*, 2435–2453.
[19] N. S. Oliver, C. Toumazou, A. E. G. Cass, D. G. Johnston, *Diabet. Med.* **2009**, *26*, 197–210.
[20] and G. M. W. Andres W. Martinez, Scott T. Phillips, Manish J. Butte, *Angew. Chemie - Int. Ed.* **2013**, *46*, 1318–1320.
[21] A. W. Martinez, S. T. Phillips, M. J. Butte, G. M. Whitesides, *Angew. Chemie - Int. Ed.* **2007**, *46*, 1318–1320.
[22] W. Dungchai, O. Chailapakul, C. S. Henry, *Anal. Chem.* **2009**, *81*, 5821–6.
[23] J. Houghtaling, T. Liang, G. Thiessen, E. Fu, **2013**.
[24] E. Noviana, C. P. McCord, K. M. Clark, I. Jang, C. S. Henry, *Lab Chip* **2020**, *20*, 9–34.

[25] J. Hu, A. Stein, P. Bühlmann, *Angew. Chemie - Int. Ed.* **2016**, *55*, 7544–7547.
[26] M. Novell, T. Guinovart, P. Blondeau, F. X. Rius, F. J. Andrade, *Lab Chip* **2014**, *14*, 1308–14.
[27] M. Novell, M. Parrilla, G. a. Crespo, F. X. Rius, F. J. Andrade, *Anal. Chem.* **2012**, *84*, 4695–4702.
[28] N. Ruecha, O. Chailapakul, K. Suzuki, D. Citterio, *Anal. Chem.* **2017**, *89*, 10608–10616.
[29] J. Ding, T. Cherubini, D. Yuan, E. Bakker, *Sensors Actuators, B Chem.* **2019**, *280*, 69–76.
[30] W. Adamiak, M. Opallo, *J. Electroanal. Chem.* **2010**, *643*, 82–88.
[31] Š. Komorsky-Lovrić, M. Lovrić, *Cent. Eur. J. Chem.* **2005**, *3*, 216–229.
[32] J. C. Myland, K. B. Oldham, *J. Electroanal. Chem.* **2002**, *530*, 1–9.
[33] F. M. Zanotto, R. A. Fernández, S. A. Dassie, *J. Electroanal. Chem.* **2017**, *784*, 25–32.
[34] Š. Komorsky-Lovrić, M. Lovrić, F. Scholz, *Collect. Czechoslov. Chem. Commun.* **2001**, *66*, 434–444.

3 Pencil-based system for ionophore evaluation

3.1 Introduction

Ionophores are often used in liquid/liquid electrochemistry to facilitate the transfer of ions and therefore enhance the discrimination capabilities of the analysis. These are lipophilic molecules able to decrease the transfer energy of charged species based on host-guest interaction[1]. The stronger this interaction is, the higher is the ionophore's selectivity towards the specific ion. In the literature plenty of examples of different ionophores can be found. Some of them are neutral, like hexyl trifluoroacetyl benzoate for carbonate detection or antibiotic valinomycin selective to potassium ions, and others are charged like metal porphyrins often applied for nitrate determination[2].

Selective ion discrimination is one of the main factors responsible for the commercial success of Ion Selective Electrodes. The vast majority of them consist of ionophore-doped polymeric membranes representing the organic side of the liquid/liquid interface. Ions of interest are transported across the phase boundary according to one of the four possible mechanisms (Chapter 1.5.2 Literature part) and detected by voltammetric or potentiometric methods. Depending on the needs, different types of ionophores can be incorporated into the membrane, making ISEs a versatile tool for inorganic ions detection[3–5]. Some authors claim that observations made by Moore and Pressman served as an inspiration to develop ionophore based thin-film sensors[1]. They noticed that valinomycin causes a release of H^+ from the mitochondria and simultaneous transfer of K^+ inside the cell[6]. However, the first polymeric membrane ISE described in the scientific publication used ammonium-selective receptors called monactin and nonactin[7].

Later studies showed that neutral ion-carriers allow discriminating monovalent cations at selectivity levels similar to those exhibited by biological systems[8–10]. Among them, valinomycin became one of the most well-known due to its remarkable selectivity towards K^{+}, enabling detection of these ions in biological samples like blood or urine[11]. Although very effective, valinomycin also has some drawbacks, including low hydrophobicity and limited solubility in the polymeric membranes[12]. Synthetic ionophores such as bis-crown ethers are often used as an alternative since they provide a satisfactory compromise between reasonably good selectivity, high lipophilicity, and low cost[13].

Applications of ionophores, however, are not restricted to discrimination of inorganic ions. Crown ethers, as well as calixarenes, can also be applied for the detection of amines in cationic form and amino acids[2]. Selective recognition of more complex organic molecules requires the synthesis of dedicated ionophores. An interesting example is an adenine-selective host molecule with five-six-five-membered heteroaromatic rings able to bind adenine nucleobases[14].

To verify whether a newly synthesized ionophore possess better selectivity than the existing ones or to evaluate what kind of molecules it can bind complexing equilibrium constant has to be determined. Traditionally, it was measured using calorimetric, potentiometric, or spectroscopic methods[15]; however, new approaches have been developed during the last decades. One of them, called sandwich technique allows the determination of complex formation constant in a variety of polymeric environments by measuring the potential of a double-layer sandwich membrane in which only one segment contains ionophore[16]. A different approach proposed by Amemiya and co-workers is based on the voltammetric characterization of a thin ionophore-doped membrane[17]. Voltammograms obtained in such experiments are not affected by the diffusional effect what

helps to simplify the theoretical modeling needed for estimation of complex stoichiometry and formation constant.

All of those methods, however, require immobilization of the ionophore in the polymeric membrane, which components such as plasticizers or ionic additives might influence the overall performance of the ionophore. Different research groups have shown that the equilibrium constant of complex formation highly depends on the type of organic solvent used for membrane preparation[1,4,17]. Finding the proper composition of a polymeric membrane is, in fact, one of the most troublesome features of ISE. The influence of the concentration of each constituent on the electrochemical response has to be verified separately what makes the optimization process very arduous and time-consuming.

Alternatively, the selectivity of new ionophores can be evaluated using setups with polarizable ITIES. Facilitated cation transfer across the aqueous/nitrobenzene interface was already studied in 1979 by Koryta in the traditional 4-electrode glass cell[18]. This approach not only allows to determine ion-to-ligand stoichiometry but also enables calculation of Gibbs energies of transfer[19,20]. Moreover, a modified version of the system equipped with a pair of working electrodes can be a very convenient tool for selective and sensitive detection of inorganic ions[21][22], even in biological samples[23]. The main difference between the mentioned setup and ISE is a very simple composition of the gelled organic phase, which does not require optimization for every single ionophore.

Another option to study facilitated ion-transfer is by using a three-phase electrode configuration. As already shown in chapter 2, TPE is most often applied for studies of direct anion transfer, while cation and facilitated transfer are rather scarcely explored. The main reason is the lack of proper redox probes, which would be sufficiently hydrophobic both in the oxidized and reduced form. In the literature, there are only a few examples of electrochemically driven cation

transfer in which iron(III) tetraphenyl porphyrin chloride[24], lutetium bis(tetra-tert-butylphthalocyaninato)[25] or 7,7',8,8'-tetracyanoquinodimethane[26] were used as redox probes. Unfortunately, all of them have some substantial drawbacks. The reduced form of 7,7',8,8'-tetracyanoquinodimethane is not hydrophobic enough to stay in the organic phase[27], while the reduction of porphyrin derivatives is often accompanied by the expulsion of anion present in the organic phase what significantly complicates the analysis of obtained results.

Fullerene C_{60} can be potentially an ideal candidate for that purpose as it can undergo multiple reductions, and each of the reduced forms is characterized by very low solubility in water. Previously, this molecule was used for the investigation of direct anion transfer in thin-film configuration[28] and kinetic studies of electron transfer processes with the scanning electron microscope[29]. However, to the best of my knowledge, no reports are describing its application for facilitated cation transfer studies.

Therefore in my research, I decided to use fullerene C_{60} to study assisted transfer of both inorganic and organic ions in a setup inspired by the cylindrical TPE electrode (Figure 3.1) proposed by Stojek and co-workers[30]. Utilization of a glass vial made from a Pasteur pipet together with pencil graphite electrode passing through the phase boundary helps to stabilize the interface leading to better reproducibility than in the traditional droplet-based system.

To show the applicability of this system for ionophore evaluation, I performed experiments with three commonly used potassium ionophores: valinomycin, ionophore III, and DB18C6 and calculated their selectivity coefficients. Additionally, I used the previously described paper-based setup to verify if it too can be applied for the investigation of the facilitated transfer of sodium and potassium ions.

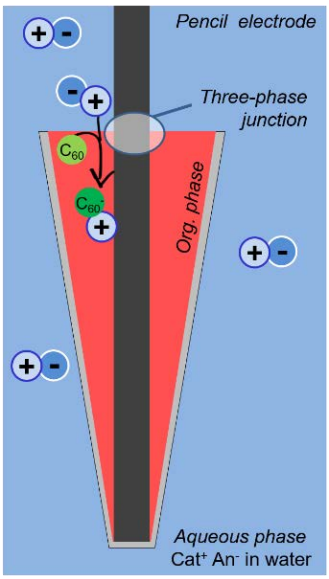

Figure 3.1 Scheme of the pencil-based TPE system. The three-phase junction is formed at the boundary between the organic phase (red color) placed in the glass vial, graphite electrode, and aqueous phase (blue color).

Results presented in this chapter were published as a research article in Electrochimica Acta:

M. Podrażka, J. Maciejewska, W. Adamiak, E. Witkowska Nery, M. Jönsson-Niedziółka, *Facilitated cation transfer at a three-phase junction and its applicability for ionophore evaluation*, Electrochimica Acta 307 (2019) 326-333.

Selectivity coefficients presented in subchapter 1.3.3 were calculated by dr inż Emilia Witkowska Nery and experiments were performed in collaboration with Julia Maciejewska-Komorowska.

3.2 Materials and methods

3.2.1 Chemicals and materials

Fullerene C_{60} (99,9%, Sigma-Aldrich), 1,2-dichlorobenzene (DCB) (99%, Sigma-Aldrich), inorganic and organic salts of analytical grade: KNO_3 (99%, POCh), KCl (>99.99%, Sigma-Aldrich), NaCl (pure p.a., POCh), $NaNO_3$ (pure p.a., Chem-Pur), LiCl (99%, Sigma-Aldrich), NH_4NO_3 (pure p.a., Chempur), $MgCl_2$ (99%, Sigma-

Aldrich), $CaCl_2$ (99%, POCh), $AlCl_3$ (≥98%, ROTH), Tetramethylammonium chloride (TMA) (≥99%, Fluka), Tetraethylammonium, chloride (TEA) (≥99%, Fluka), Tetrapropylammonium chloride (TPA) (≥98%, Sigma-Aldrich) were used as received. The ionophores dibenzo-18-crown 6 (DB18C6) (≥98%) and valinomycin were purchased from Sigma-Aldrich, while 2-Dodecyl-2-methyl-1,3-propanediyl bis[N-[5'-nitro(benzo-15-crown-5)-4'-yl]carbamate] (Potassium ionophore III, BME-44) was obtained from Fluka. Water was filtered and demineralized with ELIX system (Milipore). HB graphite pencil leads of 0.7 mm diameter and 16 mm length were purchased from Pentel.

3.2.2 Electrochemical measurements

Cyclic voltammetry (CV) and square wave voltammetry (SWV) were performed with an Autolab potentiostat (Metrohm Autolab B.V., Netherlands) controlled by the NOVA software (version 2.1.2). Parameters for SWV were as follows: step potential -0.005 V, modulation amplitude 0.025 V, frequency 25 Hz. All measurements were performed in a three-electrode system with a silver-silver chloride reference electrode (Ag|AgCl|saturated KCl) and a platinum wire as a counter electrode. Neither the organic nor the aqueous solution was degassed before measurements.

3.2.3 Electrochemical setups

Droplet-modified electrode

A glassy carbon (GC) electrode with a diameter of 1.5 mm was polished with 1, 0.3, and 0.05 µm Al_2O_3 slurry, then rinsed with demineralized water and sonicated in ethanol. Next, a 2 µL droplet of the organic phase was deposited on the electrode surface. The droplet-modified electrode was immersed into the various aqueous electrolyte solutions, in which the reference and counter electrodes were also positioned (Figure 3.2A).

Pencil graphite electrode

As an alternative to the droplet-based system, I used a device in which the organic solution is placed in a small glass vial made from a Pasteur pipette with a pencil lead as a working electrode. First, the pencil lead was inserted into one end of the glass pipette, and then the end of the pipette was melted off using a Bunsen burner to prevent leakage of the organic solution during measurements. Electrical contact was made at the end of the pencil lead using copper tape. This glass vial was filled with the organic solvent and immersed in a beaker with the aqueous electrolyte to create an interface between the two immiscible liquids (Figure 3.2B).

Paper-based system

A paper-based three-electrode setup (Figure 3.2C) was constructed in the same way as the system previously described for the study of anion transfer. In the case of facilitated cation transfer measurements, one of the papers was soaked with DCB solution containing 1 mM fullerene C_{60} and 10 mM DB18C6 and the other with the aqueous solution of the studied electrolyte.

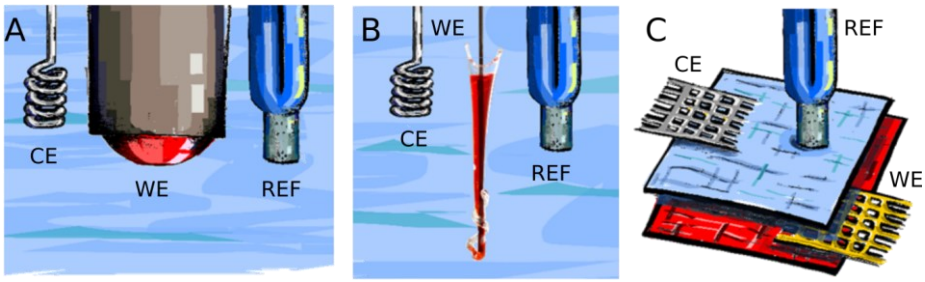

Figure 3.2 Schematic representation of the measurement setups: Droplet-modified electrode (A), Pencil graphite electrode (B), Paper-based setup (C); Organic and aqueous phases are marked in red and blue, respectively.

3.3 Results and discussion

3.3.1 Facilitated transfer of inorganic cations

Since fullerene C_{60} has never been used before for assisted ion-transfer, first, I checked its electrochemical behavior at the aqueous/dichlorobenzene interface using a traditional droplet-based system. The primary purpose of the experiment was to verify whether the reduced form of fullerene does not escape to the aqueous phase during the measurement.

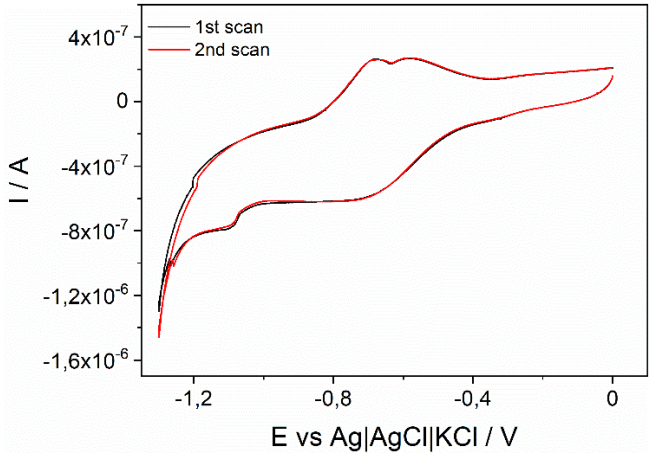

Figure 3.3 Cyclic voltammograms recorded on GC electrode modified with a droplet containing 1 mM fullerene C_{60} and 10 mM DB18C6 immersed in 0.1 M KNO_3, scan rate 50 mV/s. Experiments were performed in the droplet setup.

Stable current value and lack of peak shift on the two consecutive cyclic voltammograms confirm that C_{60}^- is not expelled from the DCB droplet (Figure 3.3). Importantly, the presence of the ionophore is crucial for the success of the experiment since, in its absence, no peaks were observed on SWV voltammograms. It can be assumed that the ion-transfer reaction happening at the phase boundary follows the equation:

$$C_{60(DCB)} + Cat_W^+ + e \rightarrow C_{60(DCB)}^- + Cat_{DCB}^+$$

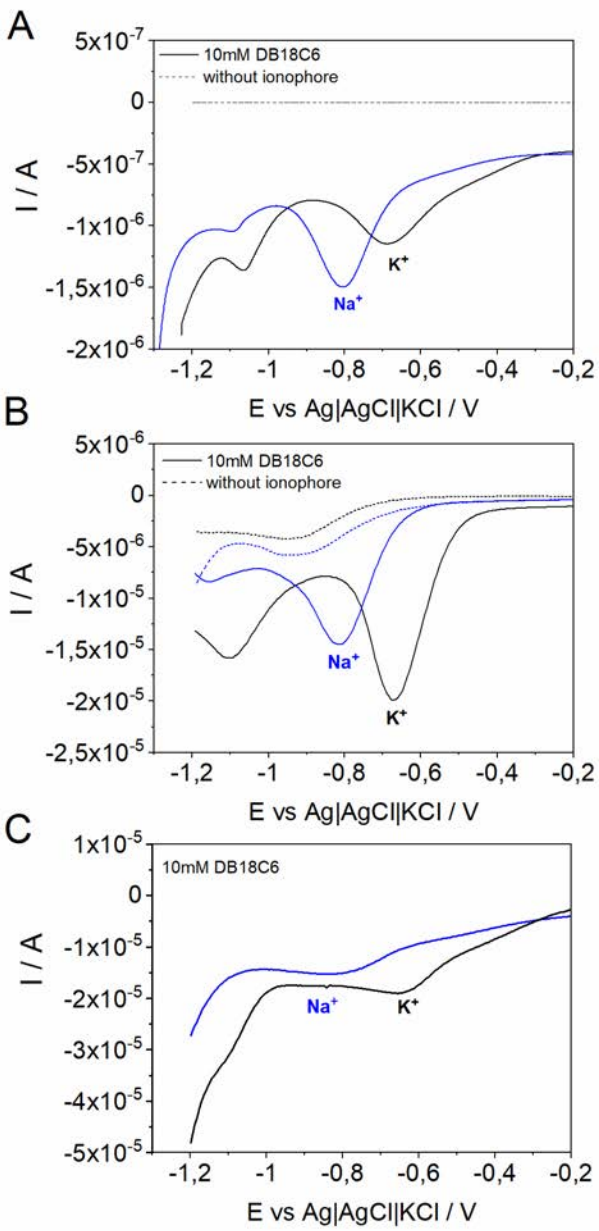

Figure 3.4 SWV curves measured for transfer of K^+ and Na^+ in droplet-based electrode system (A), glass cell with a pencil graphite electrode (B), and paper-based system (C). In all setups, the aqueous phase contained 0.1 M KNO_3 or 0.1 M $NaNO_3$. The solid lines represent results obtained when the organic phase contained 1 mM fullerene C_{60} and 10 mM DB18C6. The dashed lines are blank experiments without the ionophore.

Analysis of SWV plots leads to the conclusion that the potential at which fullerene undergoes the first reduction depends on the type of the cation (Figure 3.4A). A significant potential difference between K^+ (-0.7 V) and Na^+ (-0.8 V) transfer allows for straightforward discrimination of both ions. The second reduction is also visible however, the peaks are much less pronounced and appear almost at the same potential for both cations. Therefore I analyzed only changes of the signal related to the reduction of C_{60} to C_{60}^- in all further experiments described in this chapter.

This system was an object of further studies performed by colleagues from the research group. Experiments done under stringent deoxygenation suggest that peaks visible in the absence of the ionophore (Figure 3.4B, dashed line) might come from oxygen and not, as previously suspected, direct ion-transfer. Oxygen-free conditions cannot be achieved through standard purging of the measurement system with argon in case of the droplet but can be achieved in the glass cell, although after more than 1 hour of degassing.

It is noteworthy that the peak shift is influenced solely by the nature of the cation since SWVs registered for sodium and potassium salts with different anions did not show any substantial differences (Figure 3.5).

I performed analogous measurements of assisted sodium and potassium transfer in the glass cell with pencil graphite as a working electrode (Figure 3.4B). Results are almost identical, in terms of transfer potential values, with those obtained before. The most visible difference is the shape of the peak related to the K^+ transfer. It is sharper, better-defined, and characterized by one order magnitude higher peak current compared to the droplet-based system. The explanation for such a result can be the increased mechanical stability of the interface providing a well-defined three-phase boundary, which is crucial for ion-transfer studies in TPE configuration. The higher current can also be caused by the bigger diffusion

zone to the three-phase junction. In the droplet, which is relatively flat, the diffusion occurs only in a thin wedge, whereas in the pencil-based setup, the bulky organic phase leads to a much larger diffusion zone.

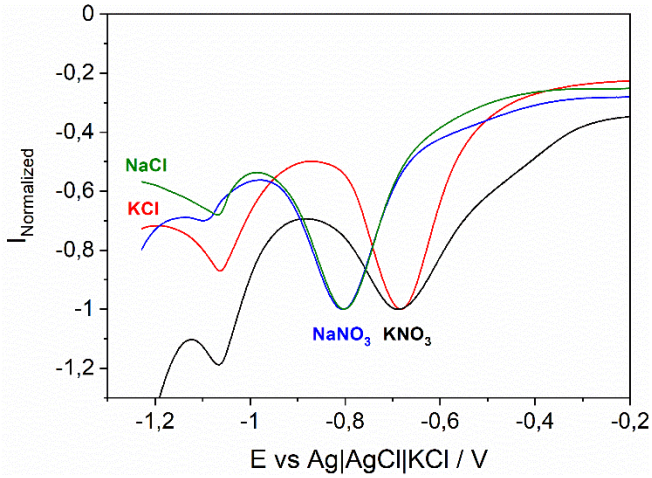

Figure 3.5 Comparison of SWV plots obtained for aqueous phase containing 0.1 M potassium or sodium salts with two different anions (NO_3^- or Cl^-). Organic phase contained 1 mM fullerene C_{60} and 10 mM DB18C6 dissolved in DCB. Experiments performed in the pencil-based system.

Setup with paper acting as a liquid phase reservoir, described in chapter 2, was also utilized in this study. Although very beneficial as an alternative approach for the investigation of anion-transfer, in the case of facilitated cation-transfer reactions, the results are less satisfactory. The peaks of both sodium and potassium transfer are broad and not well developed (Figure 3.4C), which affects the sensitivity of the analysis. The low quality of the electrochemical signal might be related to the problems with ion-ionophore interactions caused by the dense paper structure. To bind with the ion, the ionophore has to be present in the close vicinity of the liquid/liquid interface. However, the fibrous cellulose matrix can possibly decrease ionophore's diffusion and therefore hinder the assisted cation-transfer process resulting in broadening of the measured signal.

3.3.2 Effect of ionophore concentration

The concentration of the ionophore used in the previous experiments can be considered as relatively high, especially when taking into account the fact that commercially available ionophores are quite expensive. At the same time, novel compounds are often synthesized in very small amounts, so the tool enabling their characterization should use as little of the sample as possible. For that reason, I repeated the experiment using a ten times lower concentration of DB18C6.

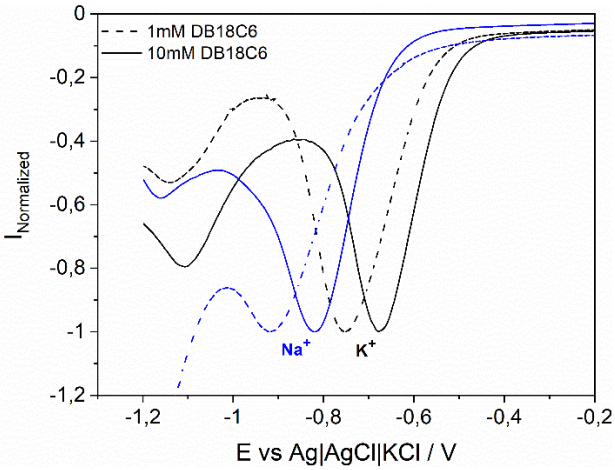

Figure 3.6 SWV curves measured for A. transfer of Na^+ and K^+ in the presence of 1 mM and 10 mM DB18C6 in the organic phase.

The impact of this change is visible on the SWV plots as a shift of the peak potentials to more negative values (Figure 3.6). Since the main role of the ionophore is to lower the Gibbs energy of transfer, the decrease in its concentration diminishes the transfer process, which was visualized by the lower current obtained with 1mM ionophore concentration. In the case of voltammetric experiments were cation transfer is strictly related to the reduction of the redox probe, it results in a more negative value of the peak potential.

3.3.3 Determination of K^+ ionophores selectivities

The primary goal of the project was to verify if the simple, disposable pencil-based device could be used for the evaluation of ionophores' selectivities as an alternative to ISE. Basic experiments performed with K^+ and Na^+ proved that this setup works according to the same principles as the classic droplet-modified TPE. The next step was to compare the influence of different ionophores on the electrochemical signal related to the simultaneous reduction of C_{60} and the transfer of cations. Thus, besides already used DB18C6, I chose two other potassium selective ion-carriers: valinomycin and potassium ionophore III (Figure 3.7). Moreover, measurements were done with a wider range of monovalent cations, including K^+, Na^+, Li^+, and NH_4^+, to thoroughly test the analytical performance of the proposed system.

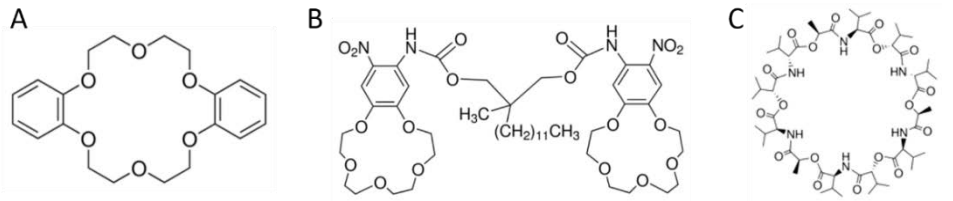

Figure 3.7 Structure of studied ionophores: Dibenzo-18-crown 6 (DB18C6) (A), Potassium Ionophore III (B), Valinomycin (C).

As can be seen in Figure 3.8 all cations can be easily distinguished based on their transfer potentials. Regardless of the ionophore type, peaks on the SWV plots always appear in the same order, governed by the hydrophilic properties and radius of the cation. The latter one is strictly correlated with the size matching effect, so the ability of the ion to fit into the ionophore's cavity. In the case of DB18C6, theoretical calculations confirmed its strong binding affinity towards potassium cations[31] what explains why K^+ is transferred at the least negative potential (Figure 3.8B).

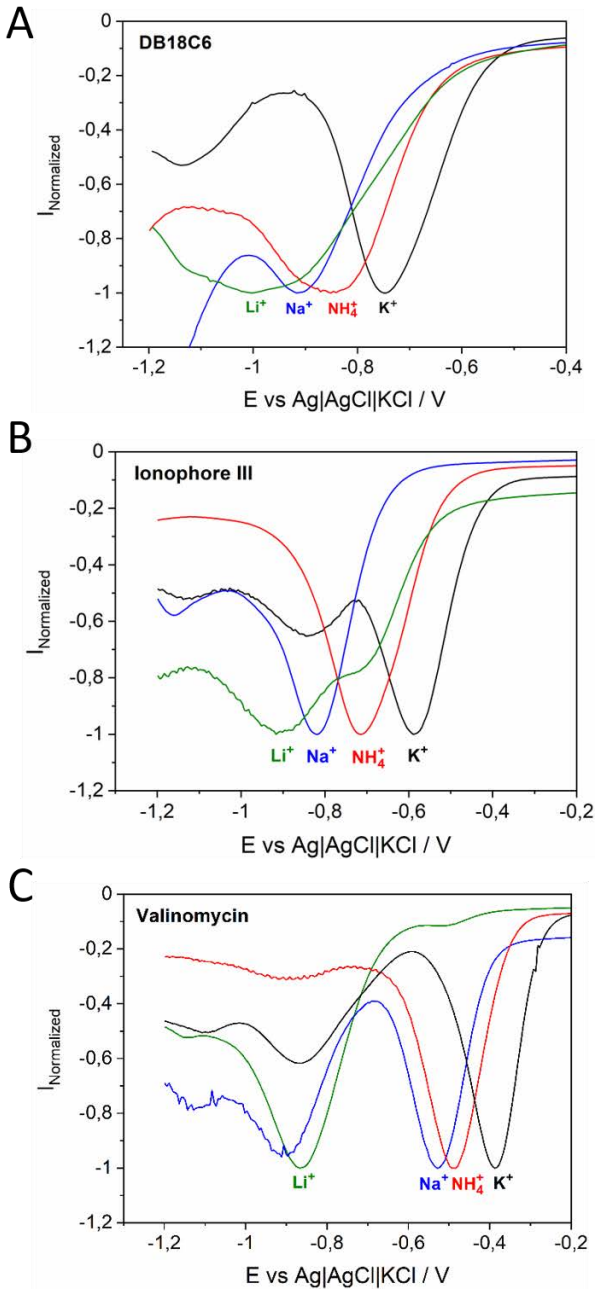

Figure 3.8 SWV plots measured for transfer of different single charged cations in the presence of 1 mM DB18C6 (A) Ionophore III (B) and valinomycin (C) in the organic phase. Experiments were performed in the pencil-based system.

When the metal cation gets smaller or larger than the $K^{+,}$ the binding selectivity decreases, and facilitated transfer becomes less effective. The radii of other studied cations decrease as follows $NH_4^+ > Na^+ > Li^+$, reflecting the order in which peaks appear on the SWV plot (Figure 3.8A). It is not surprising that the same trend is visible for ionophore III (Figure 3.8B) and valinomycin (Figure 3.8C) since both of them are as well selective towards potassium.

Similarly to anion transfer, measured peak potential should be a linear function of the transfer potential of the cation $\Delta^W_{DCB}\phi^0_{Cat^+}$according to the Nernst-like equation[32]:

$$E_p = E^0_{C_{60}/C_{60}^-} + \Delta^W_{DCB}\phi^0_{Cat^+} + \frac{RT}{F} ln c_{Cat^+_{(aq)}} + \frac{RT}{F} ln \frac{2}{c_{C_{60}}} \quad (1)$$

where $E^0_{C_{60}/C_{60}^-}$ is the standard redox potential of C_{60}/C_{60}^- couple, $c_{Cat^+_{(aq)}}$ is the concentration of the cation in the aqueous phase, and $c_{C_{60}}$is the concentration of fullerene in the organic phase. Since the field of facilitated cation transfer at the three-phase junction is scarcely explored, there is no literature data on $\Delta^W_{DCB}\phi^0_{Cat^+}$. For that reason, linear dependence between E_p and $\Delta^W_{DCB}\phi^0_{Cat^+}$ cannot be verified.

Apart from monovalent cations also double charged ions like Ca^{2+} and Mg^{2+} can be discriminated using the ion-transfer technique (Figure 3.9). The most suitable for that purpose are DB18C6, and ionophore III, providing sharp and well-separated peaks allowing to distinguish analyzed species. It is noteworthy that observed peaks are shifted to more negative potentials in comparison to Na^+ transfer even though the radii of ions are similar. This can be explained by other effects than size matching, such as electrostatic interaction between the cation and the cavity, conformation of the ionophore and type of solvation patterns[33]. Moreover, in this case, the stoichiometry of the ion-transfer process is more

complicated since divalent ions compensate for the single charge reduction of fullerene.

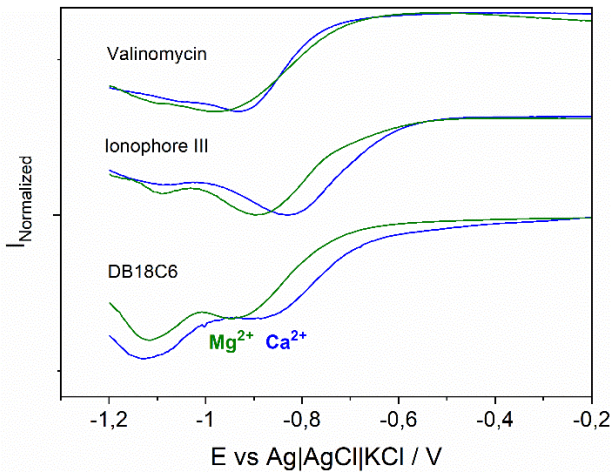

Figure 3.9 Comparison between SWV plots obtained for the transfer of Ca^{2+} and Mg^{2+} facilitated by 1 mM valinomycin, ionophore III or DB18C6. Experiments were performed in the pencil-based system.

Valinomycin, although very useful in supporting the transfer of single charged ions, does not work well as a carrier of Ca^{2+} and Mg^{2+}. Signals for both cations are broad and overlap thus, it is very difficult to separate one from the other.

To compare the performance of ionophores in a more quantitative way, selectivity coefficients were calculated based on the separate solution method (SSM)[34]:

$$logK_{I,J}^{vol}\,\frac{z_i F\left(\Delta_W^m\phi_J-\Delta_W^m\phi_I\right)}{2.303RT} \qquad (2)$$

where, $\Delta_W^m\phi_J$ and $\Delta_W^m\phi_I$ are the corresponding phase boundary potentials for the interfering (J) and primary (I) ion, respectively, z_i is the charge of the primary ion, F is the Faraday constant, R the gas constant, and T the temperature. Since the phase boundary potential was not measured during the ion-transfer experiments, instead of it, the reduction potential of fullerene was used for the calculations. All values were calculated against the peak potential obtained for

potassium. In general, the higher the value of $log\ K_{K,J}^{vol}$ the more selective is the ionophore towards a particular cation.

The obtained results are compared in Table 1, with the selectivity coefficients determined for traditional ion-selective electrodes using the same SSM method. High discrepancies between the literature data taken from different publications on $log\ K_{K,J}^{vol}$ are most probably caused by the influence of the membrane composition on the ionophore's performance.

Table 1 Values of the peak potential and selectivity coefficients for facilitated and non-facilitated transfer of inorganic cations. Peak potential (Ep) vs Ag/AgCl.

	Valinomycin			**Ionophore III**			**DB18C6**		
	Ep	$log\ K_{K,J}^{vol}$	$log\ K_{K,J}^{pot}$ [35,36]	Ep	$log\ K_{K,J}^{vol}$	$log\ K_{K,J}^{pot}$ [37,38]	Ep	$log\ K_{K,J}^{vol}$	$log\ K_{K,J}^{pot}$ [39,40]
K^+	-0.39	0	0	-0.59	0	0	-0.75	0	0
Na^+	-0.53	-2.38	-2.6:-4.0	-0.82	-3.92	-3.0: -3.3	-0.92	-2.81	-0.5:-2.7
NH_4^+	-0.48	-1.61	-1.3:-1.9	-0.72	-2.13	-2.0: -2.1	-0.85	-1.71	-0.6: -4.1
Li^+	-0.87	-8.08	-3.1:-4.0	-0.92	-5.53	-3.4: -3.8	-1.00	-4.26	-3.9
Mg^{2+}	-0.97	-9.87	-3.0:-6.3	-0.90	-5.19	-3.8: -5.0	-0.94	-3.16	-2.5: -3.1
Ca^{2+}	-0.93	-9.19	-2.9:-5.9	-0.83	-4.09	-4.0: -4.5	-0.91	-2.64	-2.6: -3.7

As can be seen, valinomycin facilitates the transfer of monovalent cations most effectively, providing the lowest peak potentials. However, in the case of Na^+ and NH_4^+ ionophore III presents slightly better selectivity. It is also most suitable for the detection of calcium and magnesium ions. Although potassium ionophore III is not a very well-known ion-carrier, it should be considered as an interesting alternative to valinomycin due to higher lipophilicity and higher binding affinity towards some of the cations. Crown ether DB18C6 is the least selective among the studied ionophores, but the competitive price makes it a perfect choice for low-cost systems such as the device described herein or for conducting preliminary tests to verify the performance of setups based on facilitated cation transfer reaction.

It should be remembered that the values of $log\ K_{K,J}^{vol}$ calculated based on ion-transfer voltammetry cannot be compared directly with those obtained using ISEs because of the previously mentioned issues with the organic phase composition. In the proposed pencil-based system, the ionophore is just dissolved in DCB, while in ISE, it is immobilized in the polymeric membrane containing various other components leading to significantly different values of selectivity coefficients. However, the overall trend indicating a decrease of ionophores' selectivity towards alkali metal cations in the following order valinomycin > potassium ionophore III > DB18C6 correlates very well with the literature data.

3.3.4 Concentration dependence

One of the characteristic features of TPE approach is the linear correlation between the peak potential and ion concentration with the slope 59 mV per decade for a one-electron redox reaction (see Equation 1). A similar effect is observed in potentiometric ISEs, where the measured electromotive force (EMF) changes linearly with the logarithm of a single charged ion concentration[41].

To verify if the pencil-based system responds in the same manner as classic TPE setup, concentration dependence for K^+ transfer was investigated in the presence of valinomycin, ionophore III and DB18C6. The choice of potassium was dictated by the fact that all studied ionophores exhibit the highest selectivity towards this cation.

As can be seen in Figure 3.10, linear dependence between E_p and $logc_{K^+}$ was obtained for all ion-carriers but only in the case of ionophore III the slope is close to the Nernstian value (Figure 3.10). A possible explanation for such results could be the fact that Equation 1 was derived for the non-facilitated cation transfer and therefore does not take into account the influence of the ionophore concentration or ion-ionophore interactions on the transfer process. However, even if

the term related to the association energy between ion and ionophore would be included, it should affect just the peak position but not the slope[4]. Another issue is that a high concentration of cations in the organic phase due to the facilitated transfer and the partitioning of ions due to the limited but non-vanishing solubility of water in DCB can influence the conductivity of the organic phase. Unfortunately, I still do not know what is the exact reason for the observed non-Nerstian slopes. In my opinion, these results imply a different stoichiometry of the ion-ionophore complex than the expected 1:1 for valinomycin and DB18C6[42–45]. There might be an interaction between the ionophore and fullerene molecules or fullerene anions, leading to distortion of the stoichiometry. Nevertheless, to thoroughly understand and explain the origin of this phenomenon, more extensive studies would be needed. However, I decided to focus on the development of the paper-based setup, and therefore, this project was not continued.

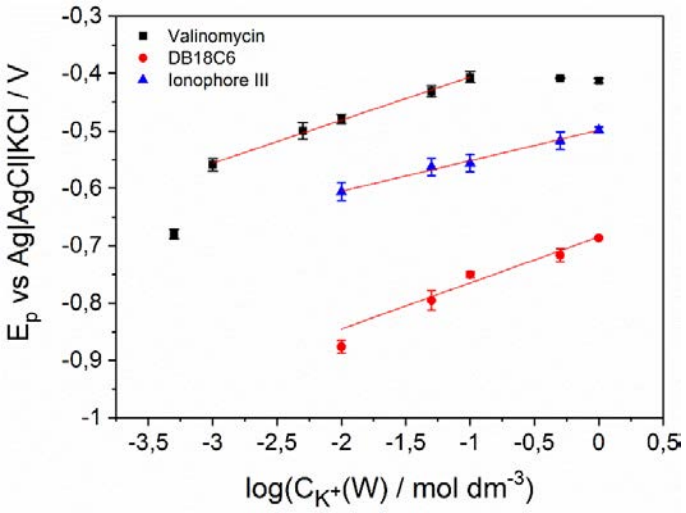

Figure 3.10 Correlation between peak potential and concentration of K^+ in the presence of 1 mM valinomycin (black squares), ionophore III (blue triangles) or DB18C6 (red circles). The slope of the fitted line and R^2 value are 74 ± 5 mV and R^2 = 0.99, 53 ± 2 mV and R^2 = 0.995, 80 ± 10 mV and R^2 = 0.94 for valinomycin, ionophore III and DB18C6.

Results of the concentration dependence measurements again confirm the outstanding selectivity of valinomycin. On the contrary, to ionophore III and DB18C6, it allowed for the detection of K^+ in a wide range of concentrations up to 0.5 mM. The detection limit for the two other ionophores could be improved by adjusting the concentration ratio between the redox probe and potassium cation, as was shown in the case of anion transfer (see Chapter 2). However, because of the poor solubility of the fullerene C_{60} in DCB I was not able to optimize the proper phase composition.

3.3.5 Transfer of organic cations

Detection of inorganic cations is the leading application of ion-selective electrodes and facilitated cation transfer in general. On the other hand, investigation of the transfer of organic species is equally interesting since it gives access to the identification of biologically important molecules like proteins. Therefore I performed experiments to check how the presence of the ionophore will influence the transfer of quaternary ammonium ions: TMA^+, TEA^+, and TPA^+. These molecules are often used as model cations in liquid/liquid electrochemistry.

Lipophilicity of the studied cations increases with the length of the aliphatic chain, thus it is not surprising that measured peak potentials increase in the following order $TMA^+ > TEA^+ > TPA^+$ (Figure 3.11). Moreover, as shown by Dubois et al., a large diffuse charge of longer-chained quaternary ammonium cations interact with the reduced C_{60} and stabilize its charge[46]. As a consequence, C_{60}^- serves as an ionophore and facilitates the transfer of these molecules. The longer the aliphatic chain is, the more pronounced this effect is. For that reason, the presence of the additional ionophore practically does not change the peak position of TEA^+ and TPA^+ transfer. Interaction between C_{60}^- and relatively small TMA cation is much weaker, and therefore, the peak potential of its transfer shifts when DB18C6, ionophore III or valinomycin are dissolved in the organic phase.

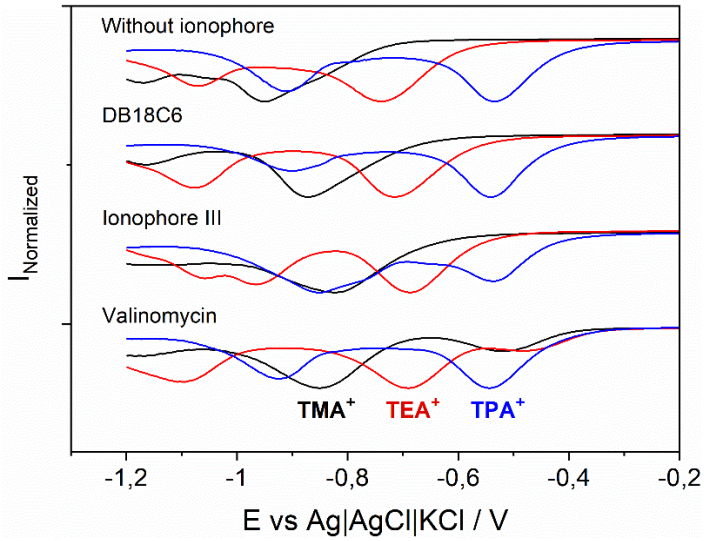

Figure 3.11 Comparison of SWV plots obtained for the transfer of organic salts without deliberately added ionophore and in the presence of 1 mM DB18C6, ionophore III, or valinomycin in the organic phase. The concentration of all organic salts was 0.1 M.

Non-facilitated transfer of various tetraalkylammonium ions (TAA^+) across the aqueous/DCB interface was studied by Hundhammer and co-workers[47]. They observed a shift in transfer potential of around 150 mV from TPA^+ to TEA^+ and from TEA^+ to TMA^+, while in Figure 3.11, one can see a shift of about 200 mV (196 mV and 217 mV, respectively). One of the reasons explaining this discrepancy is the difference in systems used for the investigation of TAA^+ transfer. As pointed out by the authors, the association between the transferred ion and the ions already available in the organic solution influences the value of the transfer potential. Experiments described in the cited article were done using thin-film electrode in which the organic phase contains partially dissolved electrolyte – compounds absent in the TPE pencil-based setup. Moreover, already mentioned strong interaction between the fullerene anion and TAA cations certainly affects the value of $\Delta_{DCB}^{W}\phi$. It is also highly possible that there is an additional

electrostatic interaction between the diffuse charge of the quaternary ammonium cation and ionophore molecule, further complicating the transfer mechanism. Therefore, a direct comparison of the literature data and results obtained in the pencil-based system is problematic and might not be reliable.

Facilitated transfer of organic cations is, without any doubt, much more complicated than the transfer of inorganic species. Since different types of interactions are involved in the overall process, interpretation of the measured signal is not trivial and requires a detailed analysis of the transfer reaction. To fully understand this mechanism, a more in-depth investigation would be needed, however, it was beyond the focus of this study.

3.4 Conclusions

The presented results confirm that a simple system with pencil lead as a working electrode can be an excellent alternative to the classic droplet-based setup. It is easy to handle and provides a mechanically stable and reproducible three-phase junction. The successful investigation of the electrochemically driven transfer of six different cations across the water/DCB interface proves that fullerene C_{60} is a perfect redox probe for such studies.

Facilitated cation transfer was studied using three potassium selective ionophores: valinomycin, ionophore III, and DB18C6. Thanks to the addition of the ionophore, alkali metal cations can be easily distinguished based on the measured peak potentials. Selectivity coefficients calculated using the data from ion-transfer voltammetry are consistent with the literature reports. Valinomycin was identified as the most effective ion-carrier since it significantly decreases the transfer potential of all studied monovalent cations. However, the less well-known ionophore III exhibits better selectivity towards sodium and ammonium ions and, therefore, could be an interesting replacement for valinomycin in some applications.

Successful experiments performed using pencil-based and paper-based setups show that voltammetric ion-transfer devices are a convenient alternative to ion-selective electrodes for the purpose of comparing ionophores. Although some aspects related to the transfer mechanism are yet unexplained, these three-phase systems allow to directly and reliably compare the selectivity of ionophores in a fast and reproducible manner. On the contrary to ISEs, the ionophore does not have to be immobilized in the membrane eliminating the influence of membrane components on the obtained results. Moreover, these are useful tools to assess the effect of ionophore on both the selectivity and Gibbs energy of transfer.

3.5 References

[1] P. Bühlmann, L. D. Chen, in *Supramol. Chem.*, John Wiley & Sons, Ltd, Chichester, UK, **2012**, pp. 562–567.

[2] P. Buhlmann, E. Pretsch, E. Bakker, **1998**, *2665*, DOI https://doi.org/10.1021/cr970113+.

[3] Z. Jarolímová, J. Bosson, G. M. Labrador, J. Lacour, E. Bakker, *Electroanalysis* **2018**, *30*, 1378–1385.

[4] J. Zhang, A. R. Harris, R. W. Cattrall, A. M. Bond, **2010**, *82*, 1624–1633.

[5] F. Kivlehan, W. J. Mace, H. A. Moynihan, D. W. M. Arrigan, *Anal. Chim. Acta* **2007**, *585*, 154–160.

[6] C. Moore, B. C. Pressman, *Biochem. Biophys. Res. Commun.* **1964**, *15*, 562–567.

[7] L. A. R. Pioda, H. A. Wachter, R. E. Dohner, W. Simon, *Helv. Chim. Acta* **1967**, *50*, 1373–1376.

[8] P. Oggenfuss, W. E. Morf, U. Oesch, D. Ammann, E. Pretsch, W. Simon, *Anal. Chim. Acta* **1986**, *180*, 299–311.

[9] E. Bakker, P. Bühlmann, E. Pretsch, *Chem. Rev.* **1997**, *97*, 3083–3132.

[10] M. S. Frant, *J. Chem. Educ.* **1997**, *74*, 159.

[11] E. Bakker, *J. Electrochem. Soc.* **1996**, *143*, L83.

[12] O. Dinten, U. E. Spichiger, N. Chaniotakis, P. Gehrig, B. Rusterholz, W. E. Morf, W. Simon, *Anal. Chem.* **1991**, *63*, 596–603.

[13] K. Kimura, H. Tamura, T. Shono, *J. Chem. Soc. Chem. Commun.* **1983**, 492–493.
[14] Y. Hisamatsu, K. Hasada, F. Amano, Y. Tsubota, Y. Wasada-Tsutsui, N. Shirai, S. I. Ikeda, K. Odashima, *Chem. - A Eur. J.* **2006**, *12*, 7733–7741.
[15] H. K. Frensdorff, *J. Am. Chem. Soc.* **1971**, *93*, 4684–4688.
[16] Y. Mi, E. Bakker, *Anal. Chem.* **1999**, *71*, 5279–5287.
[17] P. J. Greenawalt, M. B. Garada, S. Amemiya, **2015**, DOI 10.1021/acs.analchem.5b02355.
[18] J. Koryta, *Electrochim. Acta* **1979**, *24*, 293–300.
[19] F. Reymond, P. A. Carrupt, H. H. Girault, *J. Electroanal. Chem.* **1998**, *449*, 49–65.
[20] A. Sabela, J. Koryta, O. Valent, *J. Electroanal. Chem.* **1986**, *204*, 267–272.
[21] Y. Yuan, Y. Shao, *J. Phys. Chem. B* **2002**, *106*, 7809–7814.
[22] H. Bingol, E. G. Akgemci, M. Ersoz, T. Atalay, *Electroanalysis* **2007**, *19*, 1327–1333.
[23] F. S. Diba, H. J. Lee, *J. Electroanal. Chem.* **2016**, *769*, 5–10.
[24] F. Scholz, R. Gulaboski, K. Caban, *Electrochem. commun.* **2003**, *5*, 929–934.
[25] F. Quentel, V. Mirčeski, M. L'Her, *J. Phys. Chem. B* **2005**, *109*, 1262–1267.
[26] S. Wu, B. Su, *J. Electroanal. Chem.* **2011**, *656*, 237–242.
[27] R. S. Vishwanath, E. Witkowska Nery, M. Jönsson-Niedziółka, *J. Electroanal. Chem.* **2019**, *854*, DOI 10.1016/j.jelechem.2019.113558.
[28] W. Adamiak, G. Shul, M. Opallo, *Electrochem. commun.* **2009**, *11*, 149–152.
[29] J. Zhang, P. R. Unwin, *J. Chem. Soc. Perkin Trans. 2* **2001**, 1608–1612.
[30] E. Bak, M. Donten, Z. Stojek, *Electrochem. commun.* **2005**, *7*, 483–489.
[31] C. M. Choi, J. Heo, N. J. Kim, *Chem. Cent. J.* **2012**, *6*, 1–8.
[32] F. Scholz, R. Gulaboski, *ChemPhysChem* **2005**, *6*, 16–28.
[33] B. Su, S. Zhang, Y. Yuan, J. Guo, L. Gan, Y. Shao, *Anal. Chem.* **2002**, *74*, 373–378.
[34] S. Amemiya, *Anal. Chem.* **2016**, *88*, 8893–8901.
[35] E. Witkowska Nery, E. Jastrzebska, K. Zukowski, W. Wróblewski, M. Chudy, P. Ciosek, *Biosens. Bioelectron.* **2014**, *51*, 55–61.
[36] P. C. Hauser, D. W. L. Chiang, G. A. Wright, *Anal. Chim. Acta* **1995**, *302*, 241–248.

[37] E. Lindner, K. Tóth, J. Jeney, M. Horváth, E. Pungor, I. Bitter, B. Ágai, L. Töke, *Mikrochim. Acta* **1990**, *100*, 157–168.
[38] J. Tarcali, G. Nagy, K. Tóth, E. Pungor, G. Juhász, T. Kukorelli, *Anal. Chim. Acta* **1985**, *178*, 231–237.
[39] M. M. Zareh, M. A. Akl, A. K. Gohneim, M. H. Abd El-Aziz, *Turkish J. Chem.* **2007**, *31*, 449–456.
[40] K. Taheri, T. Afsari, *Anal. Bioanal. Electrochem.* **2014**, *6*, 475–484.
[41] E. Bakker, P. Bühlmann, E. Pretsch, *Talanta* **2004**, *62*, 843–860.
[42] Z. Samec, P. Papoff, *Anal. Chem.* **1990**, *62*, 1010–1015.
[43] N. Nishi, H. Murakami, S. Imakura, T. Kakiuchi, *Anal. Chem.* **2006**, *78*, 5805–5812.
[44] H.-K. Wipf, W. Simon, *Biochem. Biophys. Res. Commun.* **1969**, *34*, 707–711.
[45] W. Simon, E. Pretsch, D. Ammann, W. E. Morf, M. Güggi, R. Bissig, M. Kessler, *Recent Developments in the Field of Ion Selective Electrodes*, International Union Of Pure And Applied Chemistry, **1975**.
[46] D. Dubois, G. Moninot, W. Kutner, M. T. Jones, K. M. Kadish, *J. Phys. Chem.* **1992**, *96*, 7137–7145.
[47] B. Hundhammer, C. Müller, T. Solomon, H. Alemu, H. Hassen, *J. Electroanal. Chem.* **1991**, *319*, 125–135.

4 Electrochemical pen - organogel and paper-based system

4.1 Introduction

Systems described in the previous two chapters provide an alternative and a low-cost way of creating a mechanically stable polarizable liquid/liquid interface. However, the three-phase junction on which they are based cannot be treated as an interface between two immiscible electrolyte solutions as the electrolyte is present only in one phase. Traditionally studies of electrochemistry at ITIES are performed in a macroscopic glass cell with counter and reference electrodes at either side of the liquid-liquid interface. Since the pioneering experiments performed by Koryta in 1979[1], the 4-electrode setup has become a well-known standard commonly associated with the acronym ITIES.

Although it is a convenient tool for basic research, like studies of various charge transfer reactions or electroanalytical behavior of proteins at soft interfaces[2–4], its application for analytical purposes is somewhat limited. The main reason is very poor sensitivity of this system caused by mechanical instability of the interface and linear diffusion control of the transfer process. To overcome these issues, various ways of interface modification accompanied by a suitable electrochemical technique have been developed[5,6]. All existing strategies of ITIES modification can be divided into three main categories.

The first and most intuitive approach is based on the self-assembly of amphiphilic molecules. Phospholipids, which spontaneously organize into monolayers at the aqueous/organic interface, can serve as an example. Such systems are often used as a biomembrane model to study specific biological interactions[7–10].

Another option is the application of an external voltage to trigger the interfacial deposition of species dissolved in one of the liquid phases. Various routes of electrochemically induced modifications of the liquid/liquid interface have been

thoroughly discussed in the excellent review by Półtorak et al.[11]. One of the very recent and interesting examples is the electrochemically controlled co-deposition of silica and proteins at the aqueous/1,2-DCE interface[12]. This approach allows immobilization of biological compounds in the silica membrane, protecting them from the denaturation effect of organic solvent and at the same time maintaining their activity.

The third way is the ex-situ modification, usually realized by introducing a microporous membrane between the two liquids. It can be a simple PET foil with needle-punched holes[13,14], or a more sophisticated silicon membrane with laser drilled microarrays[15]. Also, other materials such as polyimide[16][17], polyester (called Melinex)[18][19], or even cellulose[20] have been tested as membranes for μITIES. However, the latter was found not suitable for this purpose because it swells after contact with the aqueous solution. In general, the limited interface area helps minimize the IR-drop and enhance diffusional mass transport, resulting in even 1000 times higher sensitivity than macroscopic ITIES[21]. Moreover, it allows to simplify the electrochemical cell and reduce the number of electrodes from 4 to 2 (one Ag/AgCl in each phase). The same effect can be achieved with micro- or nanopipets. Girault and Taylor were the first who miniaturized the liquid/liquid interface using glass micropipets as a support[22]. Since then, μITIES has been applied for various analytical purposes[23] as well as for kinetic studies[24–26]. As an alternative, fused silica capillaries can be used, as was shown by Rudnicki et al., who applied such system for analytical screening of fluoroquinone antibiotics[27].

Further development in this field led to the implementation of nanopipets providing even higher sensitivity and enabling detection of drugs[28] and neurotransmitters[29,30]. Qualitative and quantitative analysis of the latter is highly demanded in biomedical research since they play a critical role in brain functions.

The main advantage of nanoITIES sensors is the direct and selective determination of different neurotransmitters, including those non redox-active, even in the presence of other organic compounds[30].

Another advantage of interface miniaturization is the improvement of its mechanical stability. This property of the liquid/liquid interface can also be increased by gellification of one of the phases. It can be achieved by adding gelatin or agarose to the aqueous solution or PVC to the organic solvent. The latter approach, combined with membrane-supported µITIES is widely applied for the detection of proteins. Arrigan's group developed an adsorptive stripping voltammetry protocol enabling the accumulation of the proteins at the interface resulting in nanomolar detection limits[31–33]. Application of the adsorption potential is also a helpful trick for selective pre-concentration of the protein when it is present in the mixture of other biomolecules[34]. Detection strategy based on potential-dependent adsorption was also applied for the determination of ionized drugs such as ractopamine[35] or the β-blocker propranolol[36] at micromolar concentration levels.

Despite the variety of possible ways to miniaturize the liquid/liquid interface and enhance the analytical performance of ion-transfer measurements, there is a lack of simple, low-cost systems that could be used in non-specialized laboratories or applied for point-of-care sensing. Recently Półtorak et al. showed that 3D-printed polyamid-based cells could be a very promising and low-cost alternative to traditional glass cells used for ITIES systems with 4-electrode configuration[37].

To create a system amenable for scientists from different fields and applicable for on-site analysis, I decided to again use paper as aqueous phase support and combine it with the gelled organic phase. It led to the development of the so-called electrochemical pen (Figure 4.1) in which organogel is kept in a glass

tube sealed at one end with a porous plastic membrane. This pen is then pressed against the paper containing the aqueous phase to form the ITIES. As a membrane limiting the interface area, I used Melinex film with a mechanically drilled macro-sized orifice or a laser-drilled µpore array. The performance of the setup was verified through the investigation of direct and facilitated ion-transfer. The absorption properties of cellulose fibers make the sample preparation very easy since the analyte can be spotted directly on the paper platform or collected by swabbing. Additionally, thanks to the presence of ions in the paper structure, measurements can be performed without the addition of any supporting electrolyte. Moreover, the electrochemical pen can be combined with paper-based flow systems to chromatographically separate ions and proteins or protein mixtures, which can be then detected by means of ion-transfer.

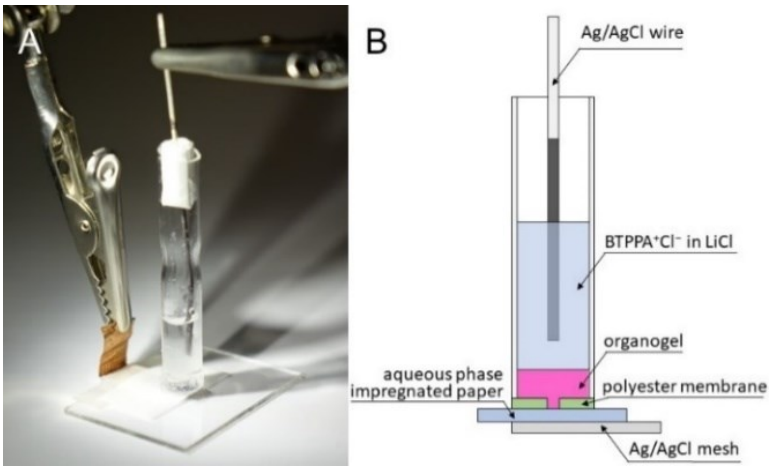

Figure 4.1 Design of the electrochemical pen: picture of the assembled setup (A), schematic representation of the system (B).

The simplicity of the device, small sample volumes needed for the analysis, and reproducible current response make the electrochemical pen an easy to handle system bringing the ion-transfer technique a step closer towards point-of-care applications.

Additionally, the chapter includes results from the experiments in an alternative fully paper-based system. In this approach, the organic phase was gelled directly on the paper sheet and put in contact with paper soaked with the aqueous solution. The interface area was again limited by the Melinex membrane, but of a bigger size than the one used for the electrochemical pen setup. The performance of the system was tested by investigating the transfer of model quaternary ammonium cations. However, it has to be stressed that these are preliminary results showing only the possibility of using such a system for ion-transfer studies, but it is not its optimized version.

The results presented in this chapter were partially published as a research article in Analytical Chemistry: M. Podrażka, E. Witkowska Nery, T.G. Henares, M. Jönsson-Niedziółka, D. W. M. Arrigan, *Ion transfer voltammetry with an electrochemical pen, 92, 24, 15997–16004, 2020.* The project was done in collaboration with prof. Damien Arrigan and dr Terence Henares from Curtin University, Perth, Australia. I performed the initial experiments with the electrochemical pen setup in prof. Arrigan's group during an internship within the „Mobility of Young Researchers of IPC PAS" program. Laser-drilled Melinex membranes and wax-printed paper channels were prepared by dr inż. Emilia Witkowska Nery.SEM images of the µpore membranes were done by dr hab. Martin Jönsson-Niedziółka. Atomic emission spectroscopy analysis was performed by dr Stanisław Kuś (Warsaw University of Technology).

4.2 Materials and methods

4.2.1 Chemicals and materials

NaCl (pure p.a., POCh), LiCl (99%, Sigma-Aldrich) Tetraethylammonium chloride (TEA) (≥99%, Fluka), Tetrapropylammonium chloride (TPA) (≥98%, Sigma-Aldrich), dibenzo-18-crown 6 (DB18C6) (≥98%, Sigma Aldrich), $FeCl_3$ (pure p.a, Chempur), $FeCl_3$ (pure p.a, Chempur), dichlorobenzene (DCE) (pure p.a,

Chempur), 2-Nitrophenyl octyl ether (NPOE) (99%, Sigma-Aldrich) were used as received. Water was filtered and demineralized with ELIX system (Milipore). Aqueous stock solutions of lysozyme (from hen-egg white) and BSA (bovine serum albumin) were prepared in 10 mM HCl and stored at +4°C. The electrolyte salt of the organic phase, bis(triphenylphosphoranylidene) ammonium tetrakis (4-chlorophenylborate) ($BTPPA^+TPBCl^-$), was prepared by metathesis of bis(triphenylphosphoranlidene) ammonium chloride ($BTPPA^+Cl^-$) and potassium tetrakis (4-chlorophenyl)borate (K^+TPBCl^-), following the procedure described by Girault's group[38]. Both components for this salt were purchased from Sigma Aldrich. The organic phase was gelled using 10 mM $BTPPA^+TPBCl^-$ in DCE and low molecular polyvinyl chloride (PVC)[39]. Organogel based on NPOE was prepared in an analogous way. The only difference was the fact that the mixture containing NPOE, PVC, and $BTPPA^+TPBCl^-$ was heated up to 80°C while the mixture with DCE as a solvent up to 60°C. In the case of facilitated cation transfer experiments, the organogel additionally contained 1 mM DB18C6.

Whatman no. 1 cellulose chromatography paper was purchased from Sigma-Aldrich. Polyester film (Melinex) of 127 µm thickness was purchased from Mulford Plastics (Balcatta, Western Australia).

4.2.2 Electrochemical setup

Cyclic voltammetry (CV) and differential pulse voltammetry (DPV) were performed with an Autolab potentiostat (Metrohm Autolab B.V., The Netherlands) controlled by the NOVA software (version 2.1.2). If not otherwise mentioned, CV measurements were performed with 10 mV/s scan rate. Parameters for DPV were as follows: step potential 0.005 V, modulation amplitude 0.025 V, modulation time 0.05 s, interval time 0.5 s, and scan rate 0.01 V/s. For all measurements, a two-electrode electrochemical cell was employed. Schemes of all electrochemical cell utilized in the research are listed in Table 2. The interface was polarized by applying a potential difference between two Ag/AgCl electrodes. The Ag/AgCl

wire was placed in a reference solution on the top of the organogel and the Ag/AgCl mesh (1 cm x 0.5 cm) underneath the paper aqueous with the aqueous phase (1.5 cm x 2.5 cm). The AgCl was created by immersing the Ag mesh/wire in a saturated solution of $FeCl_3$ overnight. Copper tape was attached to one end of the Ag/AgCl mesh to provide electrical contact. To define the interface area a Melinex membrane with a mechanically drilled 1 mm diameter orifice was attached to the end of the glass tube by a silicone sealant (Selleys®). The organogel solution was then introduced into the glass tube and left for around 15 min to set. Once ready, a reference solution (saturated $BTPPA^+Cl^-$ in 10 mM LiCl) was added on the top of the gel. The electrochemical pen prepared this way was pressed against the paper soaked with an aqueous solution containing the analyte of interest.

Table 2 Scheme of the electrochemical cells used for the measurements.

Cell I:	Ag|AgCl	Saturated BTPPACl in 10 mM LiCl	10 mM BTPPATPBCl in gelled 1,2-DCE	1 µM TPA^+ in 10 mM LiCl	Ag|AgCl
Cell II:	Ag|AgCl	Saturated BTPPACl in 10 mM LiCl	10 mM BTPPATPBCl, 1 mM DB18C6 in gelled 1,2-DCE	X mM Na^+ in 10 mM LiCl	Ag|AgCl
Cell III:	Ag|AgCl	Saturated BTPPACl in 10 mM LiCl	10 mM BTPPATPBCl in gelled 1,2-DCE	x mM Lysozyme in 10 mM HCl	Ag|AgCl
Cell IV:	Ag|AgCl	Saturated BTPPACl in 10 mM LiCl	10 mM BTPPATPBCl, 1 mM DB18C6 in gelled 1,2-DCE	0.1 mM Lysozyme, 0.1 M Na^+ in 10 mM HCl	Ag|AgCl
Cell V:	Ag|AgCl	Saturated BTPPACl in 10 mM LiCl	10 mM BTPPATPBCl, in gelled 1,2-DCE	0.1 mM Lysozyme, 0.005 mM BSA in 10 mM HCl	Ag|AgCl

Differential pulse stripping voltammetry experiments were performed using the chronoamperometry (CA) technique as a pre-concentration step followed by

DPV detection. A pre-concentration potential of 0.85 V, was applied for 30, 60, 90, 120, 150, or 180 s.

Pre-concentration experiments with TPA^+ were performed using chronoamperometry in which a potential of 0.45 V was applied for 30, 60, or 90 s. The potential was applied 5 times, each time glass tube with organogel was placed in a different spot on the paper to prevent complete consumption of the transferred ions.

4.2.2.1 System with the organic phase gelled on the paper

Many attempts were made to obtain a low-cost and easy to use system. First experiments were performed with devices in which both phases were supported by paper. The Ag/AgCl mesh (1 cm x 0.5 cm) with the copper tape as an electrical contact was attached to a glass slide using insulating tape. Paper (1.5 cm x 2.5 cm) soaked with the aqueous solution was placed on the top of the mesh and then covered with the square Melinex membrane (3 cm x 4 cm) with a single, mechanically drilled 1 mM orifice. Paper with the NPOE organogel was put on the membrane and then covered with the glass slide with another Ag/AgCl mesh (1 cm x 0.5 cm). An additional small piece of paper (1 cm x 0.5 cm) soaked with the reference solution (saturated $BTPPA^+Cl^-$ in 10 mM LiCl) was placed between the mesh and the organogel paper. It was done to ensure the proper performance of the electrode. All measurements (CV and DPV) were done using the same parameters as described above for the electrochemical pen setup.

4.2.2.2 Atomic emission spectroscopy (AES)

Samples were prepared according to a standard protocol[40]. Briefly, 10 g of cellulose was ashed in an electric furnace at 575°C. Two sets of samples were prepared. In one case, paper was ashed after soaking in 3 L of deionoised water overnight to remove any loosely bound ions. Another sample was ashed directly. After ashing 5 ml of 6 M HCl was added and evaporated in a water bath (around

80 degrees) till dry. Next, another 5 ml of 6 M acid was added, and this solution was used for analysis which was done by dr Stanisław Kuś. Signals at 330.26 nm and 404.35 nm were analyzed for sodium, whereas 404.65 nm was used for potassium. The amount of sodium in the sample ashed directly was found to be 20 mg/l, and for the soaked paper 35 mg/l, with additional sodium probably coming from the container in which the paper was being soaked or from the air. The amount of potassium was below 5 mg/l for both samples.

4.2.3 Laser drilled membrane

Laser drilled Melinex membranes were prepared using a laser engraving system GCC Laser Pro C180II with 30 W metal tube Synrad CO_2 laser (USA). Circles of 0.1 mm drawn with hairline width, to be printed as a vector with Power set at 80% and Speed at 30%. Different sizes of pores, designed as lines of hairline width of different length (0.05 mm to 0.2 mm) or circles of different diameters (0.05 mm – 0.2) were tested however, the best results were obtained for the 0.1 circles, which resulted in 270 µm orifices with 530 µm center to center distance. Unfortunately, due to technical issues the size of these micropores is still not reproducible. For that reason, a laser-drilled Melinex membrane was used only for a few experiments.

4.2.4 Flow injection system

Simultaneous detection of protein and cation was performed in a flow injection system with 10 mM HCl as a background solution. A mixture (5 µl) containing 0.1 mM lysozyme and 0.1 M NaCl was injected at a distance of 2.5 cm from the place in which the organogel was in contact with the paper. The paper-based 2.5 x 30 mm channel with borders printed with wax was prepared using a Xerox Phaser printer. After printing the channel was heated on a hotplate to allow the wax to penetrate through the whole thickness of the paper sheet[41]. The inlet was submerged in the background electrolyte. The end of the channel was

equipped with a wicking pad that guaranteed continuous movement of the fluid. These experiments were performed using organogel with a laser-drilled membrane with 9 micropores. The same system configuration was used for the separation of 5 µl mixture of 0.1 mM lysozyme, and 0.005 mM BSA injected 2.5 cm from the detection point.

4.3 Results and discussion

4.3.1 Electrochemical characterization of the organogel/paper system

Similarly to the previously described systems, the paper has never been used before as liquid phase support in the polarizable ITIES with 2-electrode configuration. To the best of my knowledge, there are no reports in the literature presenting the combination of gelled organic phase in the pen-like form with paper platform serving as an aqueous phase reservoir. For that reason, I started with the electrochemical characterization of the proposed system. I performed cyclic voltammetry and differential pulse voltammetry measurements using model cations TEA^+ and TPA^+ (Cell I). As can be seen in Figure 4.2, both cations can be easily distinguished based on the peak potential. The shift between observed peaks is about 140 mV what is consistent with the literature data[42] and confirms the proper performance of the setup. However, the peak to peak separation is 150 mV and 170 mV for TPA^+ and TEA^+, respectively, so it is significantly higher than the expected 59 mV for a reversible reaction. Probably this might be caused by the dense gel structure hindering the diffusion since similar results were shown by other groups working in the field of ion-transfer across gelled organic interface[43–45] with the exception of studies on VISE by Bond[46,47]. Nevertheless, scan rate dependence studies show a linear correlation between the peak current and the square root of the potential sweep rate (Figure 4.3).

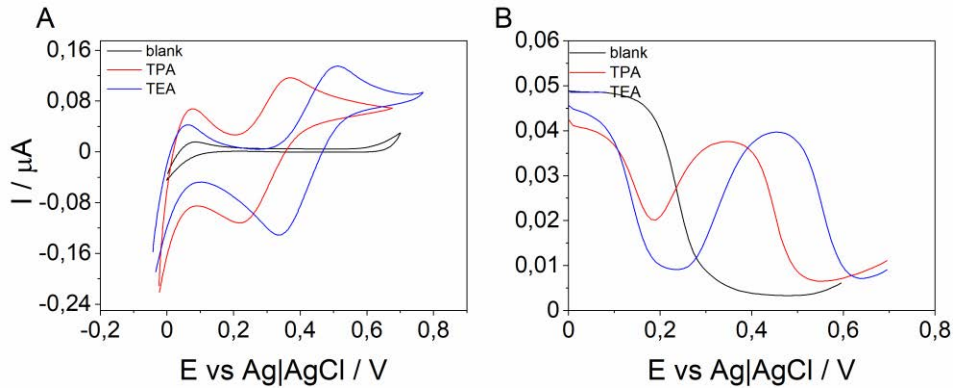

Figure 4.2 Cyclic voltammetry (A) and Differential Pulse Voltammetry (B) showing the transfer of quaternary ammonium cations TEA^+ and TPA^+ across the organogel/aqueous paper interface. The blank measurement was done only with the supporting electrolyte (LiCl) in the aqueous phase. IR compensation with 35 kOhm was applied to CVs.

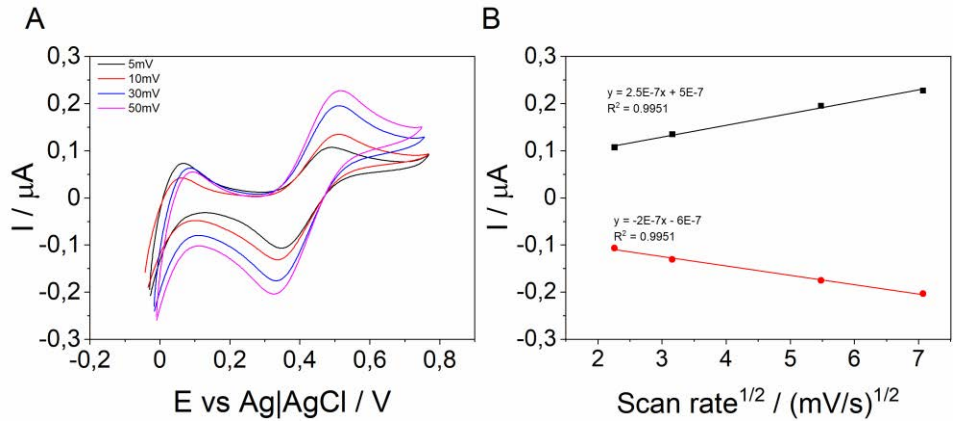

Figure 4.3 Cyclic voltammograms registered for TPA^+ transfer with different scan rates (A) and scan rate dependence plot prepared based on the obtained CVs (B). IR compensation: 35 kOhm.

A very important advantage of the system is the high reproducibility of the measured ion transfer currents (Figure 4.4). Reproducibility of results in terms of current is often a problematic issue in liquid/liquid experiments, however, it can be overcome by proper interface limitation and stabilization. Melinex membrane with a mechanically drilled orifice attached to the end of the glass tube provides a stable and well-defined interface area leading to the reproducible

electrochemical response. Moreover, the mechanical stability of the interface is additionally increased by the gelled organic phase and the paper platform.

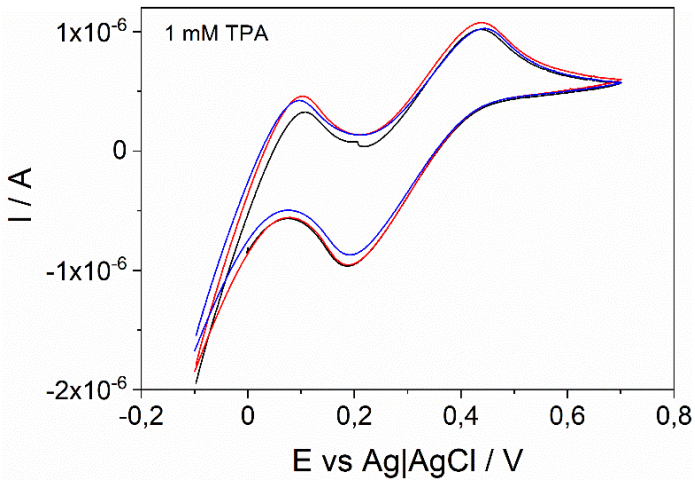

Figure 4.4 Comparison between cyclic voltammograms (second scans) for 1 mM TPA^+ transfer obtained in three separate systems. IR compensation was not applied.

4.3.2 Facilitated cation transfer

Transfer of ionic species facilitated by ionophores is one of the standard processes studied in ITIES-based systems. Therefore I performed such measurements using the electrochemical pen with organogel containing 1 mM DB18C6 (Cell II). To verify the proper performance of the setup, I investigated the reversible transfer of Na^+ from a bulk aqueous to the organic phase (Figure 4.5A) and compared it with the transfer from a paper supported aqueous phase (Figure 4.5B). In neither case, the transfer of Na^+ can be observed without ionophore added to the organic phase. The results from both systems are very similar, however, there is a noticeable difference in the CVs obtained for 0.01 mM Na^+. In the plot registered for the bulk aqueous phase, one can barely see the transfer peaks, while the paper-based setup results clearly indicate the transfer process.

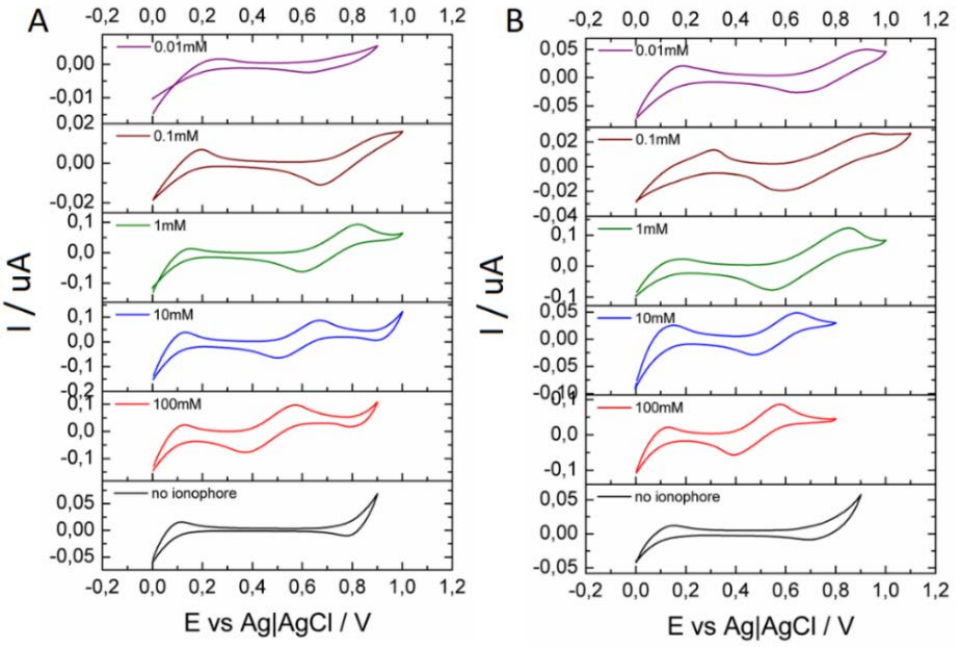

Figure 4.5. Transfer of Na^+ facilitated by ionophore DB18C6 measured in the system where organogel was immersed in the aqueous solution (A) or put in contact with paper soaked with the aqueous phase (B).

The higher sensitivity of the configuration with the paper platform is even more pronounced in the DPV plots. Contrary to the experiments in the beaker (Figure 4.6A), the transfer of 0.1 mM and 0.01 mM Na^+ across the paper/organogel interface is very well visible (Figure 4.6B). A decrease of the cation concentration in both systems results in the shift of the peak potential to more negative values, which is a typical behavior observed in potentiometric ISEs. Although the mid-peak potential E_{mid} depends linearly on the Na^+ concentration, the slope, in both cases, is higher than the expected 59 mV (Figure 4.7). A super-Nernstian response has been observed before in ion-transfer using 2-electrode configurations, however, this behaviour was left without comment or explanation by the authors [44,48].

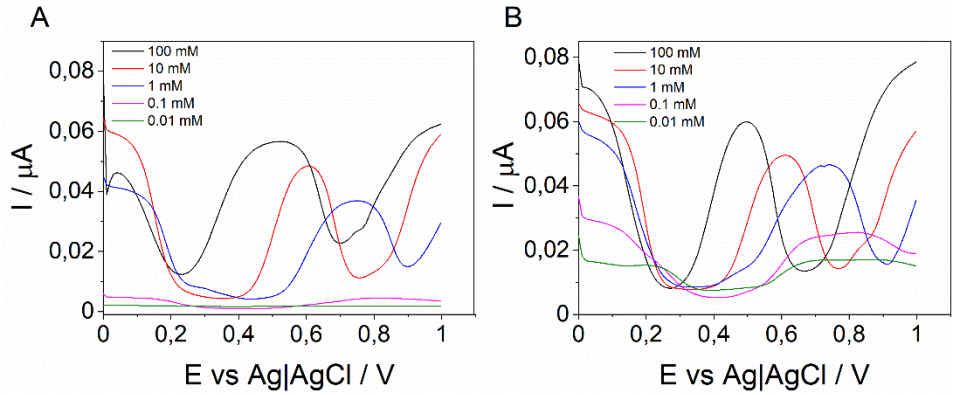

Figure 4.6 Comparison of DPV plots obtained for facilitated cation transfer in the organogel/beaker (A) and organogel/paper (B) configuration. Measurements were done for the same concentrations of $Na^{+,}$ as in the case of previously shown CVs.

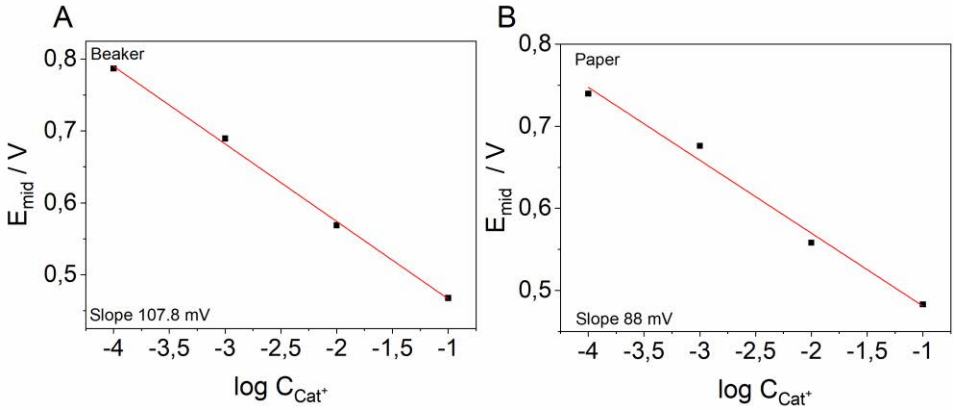

Figure 4.7 Correlation between mid-peak potential (extracted from CV curves) and concentration of Na, for experiments, performed using a gellified organic phase (A) in the bulk aqueous phase (B) on paper.

Since the non-Nerstian slope is observed regardless of how the aqueous solution is kept, it has to be related to the gelled organic phase. Finding the origin of this deviation is an intriguing challenge, but one that will have to be addressed in future studies.

4.3.3 Unsupported cation transfer

The presence of the supporting electrolyte is one of the essential factors responsible for the success of most electrochemical experiments. It guarantees high conductivity and minimizes the influence of migration effects[49]. However, in some cases, it is possible to perform electrochemical measurements without deliberately added electrolyte, e.g., analysis of seawater or brackish water samples, as these already contain high enough concentration of ions[50]. During the optimization of the electrochemical pen system, it turned out that it allows ion-transfer studies in the absence of added electrolyte. As shown in Figure 4.8, TEA^+ and TPA^+ transfer is clearly visible on the CVs, although both salts were dissolved in pure deionoised water. Of course, the overall high resistivity of the aqueous phase leads to a much larger value of ΔE_p (0.34 V) than for measurements with LiCl, but both cations can still be distinguished based on the peak potentials.

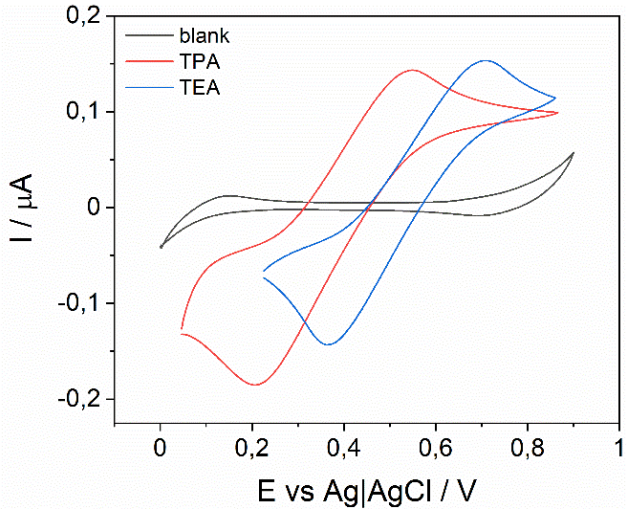

Figure 4.8 Cyclic voltammograms for of 1 mM TEA^+ and TPA^+ cations from aqueous solution without supporting electrolyte. Blank was measured in pure deionized water. IR compensation: 35 kOhm.

Interestingly, an increase of the current at the positive and negative end of the blank CV indicates that some ion-transfer processes are happening there. Moreover, both on the forward and backward scans, well-defined peaks are visible. Since the blank experiment was done using paper soaked only with deionized water, ionic species have to be present in the cellulose matrix. A comparison between DPV for the blank experiment with the previous results obtained for low Na^+ concentrations confirms this hypothesis (Figure 4.9). The plot registered in the deionized water has an identical double-peak shape as voltammograms obtained for 0.1 mM, 0.01 mM Na^+ transfer. For sure, this signal is not related to the organogel, because the DPV plot measured with an electrochemical pen immersed in the bulk aqueous phase does not exhibit this kind of electrochemical response.

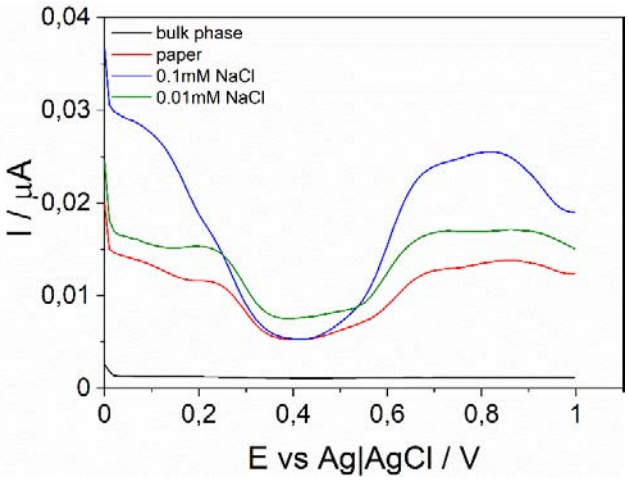

Figure 4.9 DPV plots obtained when organogel was in contact with the paper soaked in deionized water compared with the facilitated transfer of Na^+ cations.

Most likely, the paper structure contains a sufficient amount of charged groups to support the measurements. Paper is made from cellulose fibers, which possess carboxylic groups originating from cell wall constituents or introduced during the production process[51]. Some of those groups can be in a deprotonated

form with sodium or potassium as a counter ion. Since the ionophore DB18C6 is equally selective towards both mentioned ions, it is not possible to reliably state which of them is transferred based on the voltammograms. Therefore paper samples were analyzed using Atomic Emission Spectroscopy (AES). The obtained results confirmed the presence of Na^+ in the paper structure at the level of 0.01 mg/g of paper. The amount of sodium is low enough not to interfere in the detection of other species but high enough to provide sufficient conductivity of the aqueous phase.

This property of paper is extremely advantageous as it opens a new way for ion transfer measurement without the need for an additional electrolyte. It means that a sample can be simply spotted on a piece of paper and immediately analyzed.

4.3.4 Dip and pick pre-concentration

During optimization of the setup, I found another interesting feature of the electrochemical pen, namely, the possibility of accumulating the analyte in the gelled organic phase. When I performed measurements in 0.1 mM TPA^+ supported on a paper and then moved the same pen to a paper containing only LiCl, the signal of the cation transfer was still present on the CV (Figure 4.10). It means that some of the ions get trapped in the dense gelled organic phase while transferring across the aqueous/organogel interface. This phenomenon could be used as a pre-concentration approach similar to the stripping voltammetry commonly applied in liquid/liquid electrochemistry.

Cellulose matrix also can serve as a trap for the analytes enhancing the accumulation effect. Repeated spotting and drying of paper with a sample liquid is a well-known strategy in paper-based sensing to achieve lower detection limits[52]. However, I used a slightly different approach, utilizing the storage abilities of the gel, in which chronoamperometry was used to accumulate TPA cations in the

organogel (Cell I). After each pre-concentration step, the electrochemical pen was moved to the new spot to prevent the complete consumption of the analyte. The procedure was repeated five times, and the last CA measurement was followed by CV detection.

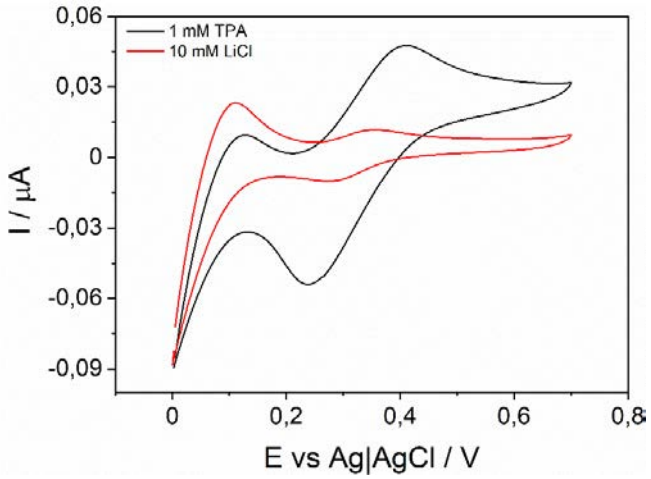

Figure 4.10 Comparison between CV made for paper soaked with 0.1 mM TPA^+ and for paper soaked with LiCl after measuring TPA^+ transfer. Gellified interface and both electrodes were rinsed with water between the experiments.

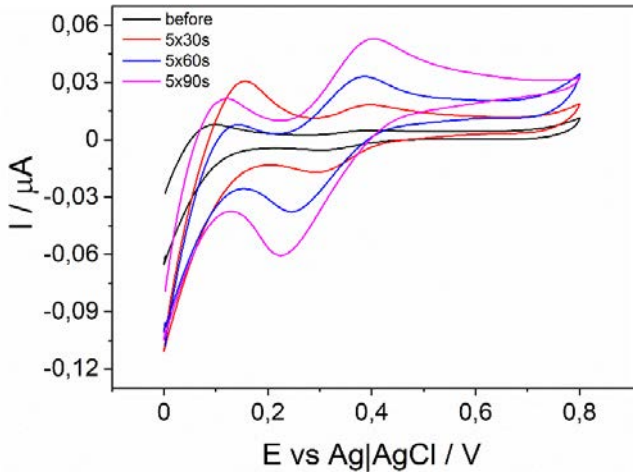

Figure 4.11 Comparison of CVs of TPA^+ transfer from 1 µM solution after chronoamperometry at 0.45 V with different accumulation times. The black CV is the control experiment without any pre-concentration.

The longer was the applied pre-concentration time, the more significant increase in the peak current related to 1 µM TPA^+ was observed (Figure 4.11). After 90s accumulation repeated for 5 spots the current grew by more than one order magnitude compared to the regular measurement. The obtained results show that the proposed "dip and pick" approach is a very interesting and efficient method of sample pre-concentration. It allows reaching low detection limits quickly and straightforwardly, without the need for time-consuming stripping or drying steps.

4.3.5 Pre-concentration of protein

The dip and pick approach described in the previous subchapter can be treated as a modification of the adsorptive stripping voltammetry (AdSV) analysis. The main difference comes from the voltammetric technique used for analyte detection, as in the latter, linear or differential pulse voltammetry is usually utilized, whereas in the dip and pick approach, cyclic voltammetry was applied. Moreover, pre-concentration potential is applied only once for a particular time, not a few times in different spots, like in the dip and pick method. Nevertheless, both techniques are somewhat similar, and therefore it should be possible to combine standard stripping analysis with the electrochemical pen. To verify that, I performed differential pulse stripping voltammetry experiments with lysozyme solution supported on the paper platform. It is one of the most well-known model proteins used for liquid/liquid electrochemistry. It was found by Scanlon et al.[53] that the behavior of the lysozyme at the ITIES can be described by a combination of complexation and adsorption/desorption processes. In the first step, the cationic form of lysozyme facilitates the transfer of organic anions by forming an anion-protein complex that adsorbs at the aqueous side of the interface. During the reverse scan, this complex desorbs from the interface and dissociates in the bulk aqueous phase. Peaks related to the adsorption (0.8 V) and desorption (0.55 V) processes can be observed on the CV recorded using the

electrochemical pen (Cell III) in the presence of 0.1 mM Lysozyme dissolved in HCl solution (Figure 4.12A).

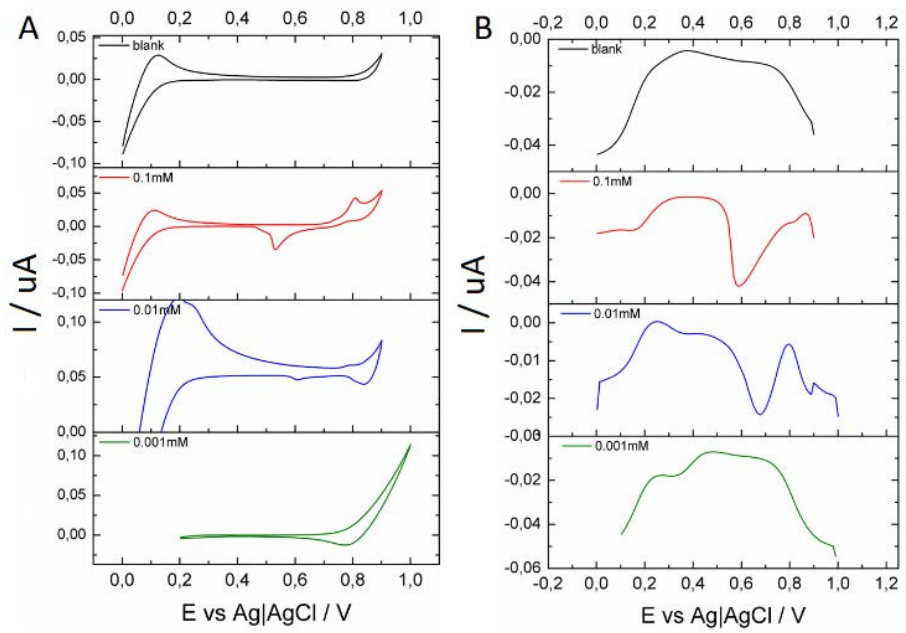

Figure 4.12 CV (A) and DPV (B) plots for adsorption/desorption of lysozyme at different concentrations measured in the organogel/paper system (pH 2). DPV was measured from 0.9 V to 0 V.

Moreover, a sharp, well-defined desorption signal (0.6 V) is also visible on the DPV plot registered for the same protein concentration (Figure 4.12B). However, for ten times lower protein concentration, CV is not informative anymore as the signal becomes barely visible, and for 0.001 mM lysozyme, it disappears completely. Therefore to test the effectiveness of the AdSV I performed measurements using 0.01 mM lysozyme and three lower concentrations: 0.005, 0.001, and 0.0001 mM (Figure 4.13). As a detection technique, I used DPV since it is more sensitive than linear sweep voltammetry. The adsorption potential, 0.85 V, I chose based on the CV for 0.1 mM concentration of lysozyme.

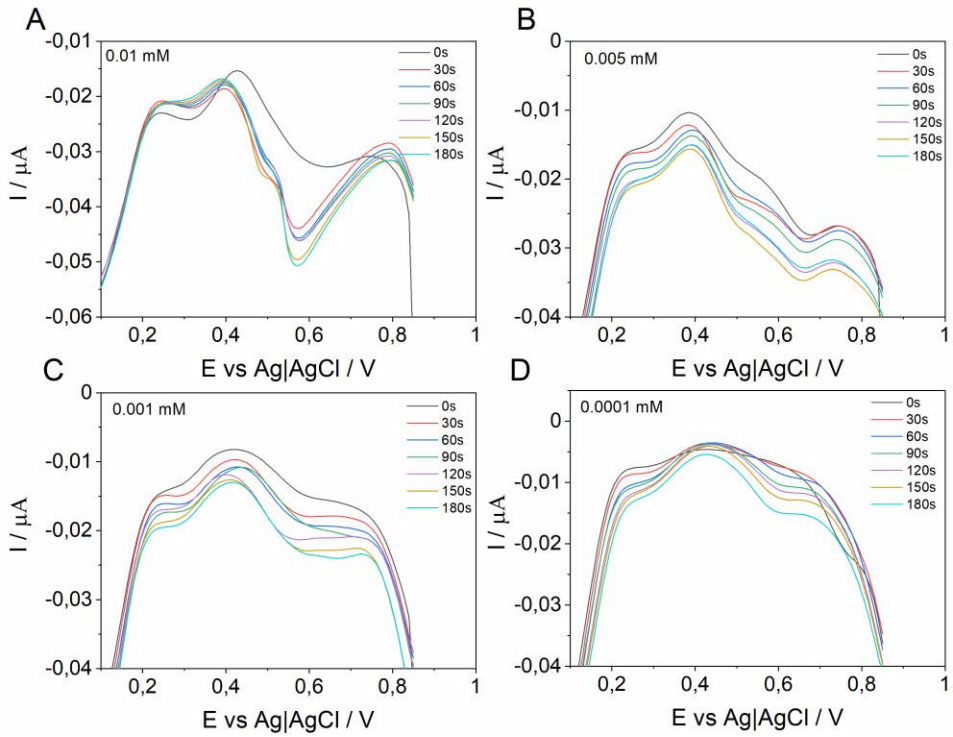

Figure 4.13 DPVs plots registered for 0.01 mM (A), 0.005 mM (B), 0.001 mM (C) and 0.0001 mM (D) lysozyme after application of pre-concentration potential 0.85 V for 30 s -180 s time range. 0 s represents the measurement performed before the application of the adsorptive potential.

As expected, for each lysozyme concentration, the peak current increased after applying the adsorptive potential (Figure 4.13). Moreover, the peak area integrated based on DPV plots also increases with time (Figure 4.14), confirming that the applied technique enables the pre-concentration of the protein at the organogel/paper interface. It is noteworthy that for 0,005 mM and 0,001 mM, lysozyme DPV exhibits a double-peak shape, which becomes more pronounced with increasing pre-concentration time. The presence of the additional peak might be related to the interaction of the protein with silver ions since the aqueous solution kept at the thin paper support is in very close contact with the Ag/AgCl electrode.

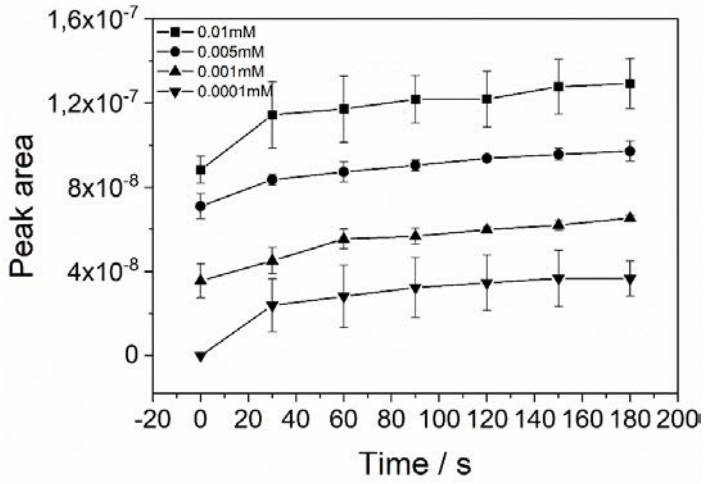

Figure 4.14 The relation between peak area (average value with standard deviation from 3 separate experiments), obtained by integrating DPSV peaks, and pre-concentration time.

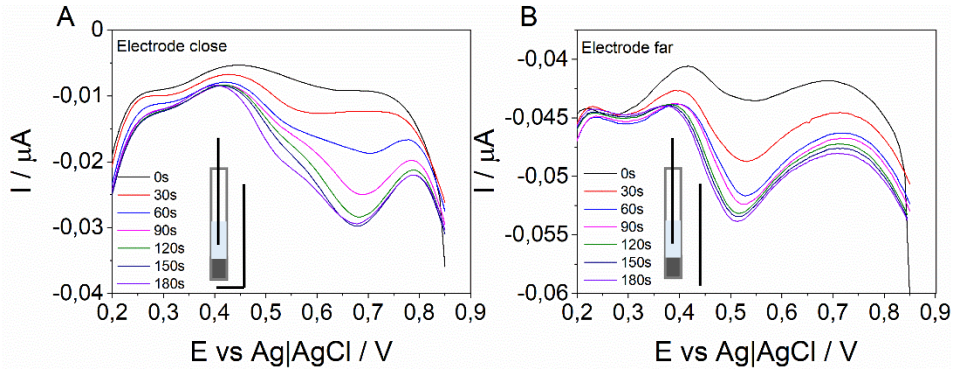

Figure 4.15 DPV plots registered after pre-concentration of 0.001 mM Lysozyme in the organogel/beaker system with Ag/AgCl electrode placed near (A) and far (B) from the organic/aqueous interface. The schematic representations of the electrodes configuration used in the experiments are presented as an inset on both plots.

Results obtained from experiments performed in an organogel/beaker system can serve as support for this proposed theory as there is a notable difference in electrochemical response depending on the distance between the interface and Ag/AgCl wire (Figure 4.15). When the aqueous Ag/AgCl electrode is close to the

interface obtained signal has a very similar shape to the one observed after pre-concentration of the lysozyme in a paper-based system.

In my opinion, this is a clear indication that protein molecules have to somehow interact with the electrode material what might lead to structural changes and affect the adsorption/desorption processes.

To further investigate this topic, I performed another experiment in which I measured the TPA^+ transfer before and after exposing Ag/AgCl electrodes to the lysozyme. First, I registered the CV of TPA^+ transfer, then I washed the Ag/AgCl from the aqueous side, exchanged the paper platform, and performed pre-concentration of lysozyme. After that, again, I washed the Ag/AgCl mesh, exchanged the paper, and repeat the TPA^+ transfer measurement. Each time I used fresh organogel to make sure that TPA^+ or lysozyme accumulated in the gel structure will not have an influence on the registered CV. As can be seen, after the exposure to the lysozyme, the signal of TPA^+ transfer from the organic to the aqueous phase changes significantly (Figure 4.16A). The peak shifts and current value decreases of almost half in comparison to the results obtained before the lysozyme pre-concentration. On the contrary, a signal of the transfer from the aqueous to the organic phase remains the same.

I performed an analogous experiment, but after the stripping analysis of lysozyme, I changed the Ag/AgCl wire from the organic phase for a fresh one. This time signal of the TPA transfer did not change much (Figure 4.16B). For me these results show that there is some kind of interaction between the protein and the reference electrode placed in the organic phase affecting its proper performance. However, due to the lack of literature data showing protein behavior at the organogel/paper interface or studies of the stability of the interface between

the organic phase and the reference solution, I cannot verify the validity of the proposed explanation or compare my results with others.

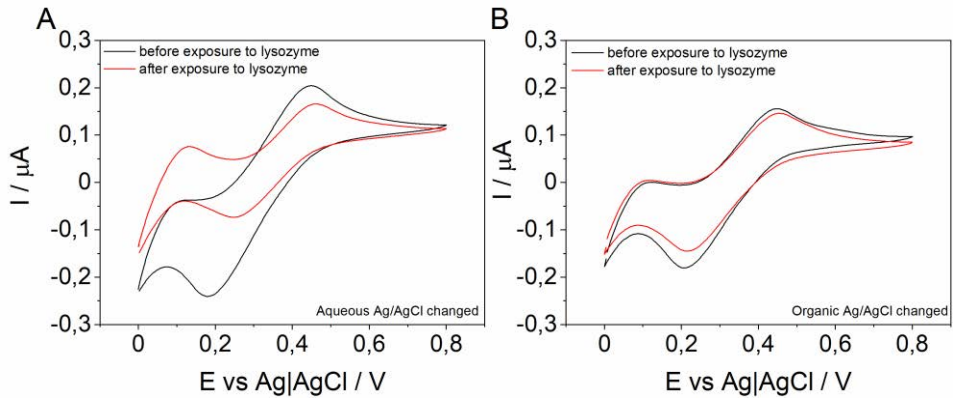

Figure 4.16 CV plots of TPA transfer registered before and after performing lysozyme pre-concentration in the system where Ag/AgCl electrode placed in aqueous (A) or organic (B) phase was changed between the experiments. Each of the experiments was performed using a freshly made electrochemical pen.

Nevertheless, the presented results confirm that the electrochemical pen can be combined with adsorptive stripping voltammetry to accumulate ions and thus enhance the analytical performance of the system.

4.3.6 Flow-injection measurements

Since ancient times, paper has been known as an excellent tool for the separation of liquid components[54]. The possibility to distinguish sample ingredients based on their interaction with the cellulose matrix led to the development of paper chromatography - probably one of the simplest and most well-known analytical techniques. It became a basis for a variety of paper-based detection systems such as lateral flow assays, colorimetric assays, or microfluidic paper-based devices. The latter often utilize electrochemical detection since electrodes can be easily integrated into the paper structure. Moreover, tuneable wicking properties and the possibility of paper patterning allow to precisely control the transport of liquids. Despite these unique capabilities, to the best of my

knowledge, paper has never been used before to separate sample components in the voltammetric ITIES systems. The only literature report I found describes the functionalization of filter paper with Fe^{3+} to selectively separate and detect Cl^- using an ion-selective electrode[55].

Therefore, I combined the electrochemical pen with a paper-wicking pad (Figure 4.17) to separate and then detect components of protein and protein-ion mixtures without the need of sample pre-treatment or application of sophisticated electrochemical techniques.

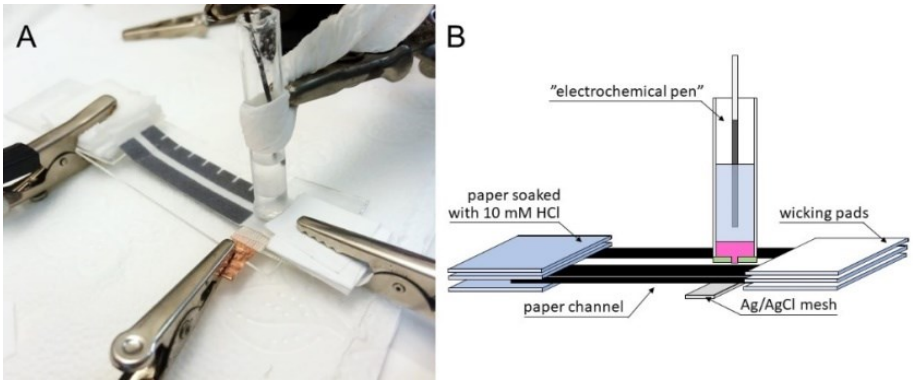

Figure 4.17 Picture (A) and scheme (B) of the flow-injection paper system used for the simultaneous detection of proteins and ions.

4.3.7 Characterization of the laser-drilled Melinex membrane

All the measurements described till now were done using area limited, however still macroscopic size, ITIES. The Melinex membrane with mechanically drilled orifice confines the phase boundary to a single 1 mm diameter circle. However, as explained in the introduction, the smaller liquid/liquid interface we are able to create, the higher sensitivity of the system. Therefore I wanted to check how a further decrease in the organogel/paper interface will influence the analytical performance of the electrochemical pen.

I started by testing a glass membrane with 200 µpore arrays kindly provided by prof. Arrigan. Unfortunately, it was too fragile and broke almost immediately when the pen was pressed against the paper. Therefore I decided to use an alternative and more mechanically resistant approach based on the Melinex membrane with laser-drilled µpores. Laser-drilled membranes were prepared by dr inż Emilia Witkowska Nery.

To verify the influence of size and number of pores in the membrane on the TEA^+ transfer across the organogel/paper interface, I performed a series of CV and DPV measurements (Figure 4.18). For these tests, I used membranes giving the most reproducible results, so arrays of 4 (2x2), 6 (3x2), and 9 (3x3) holes with 270 µm diameter.

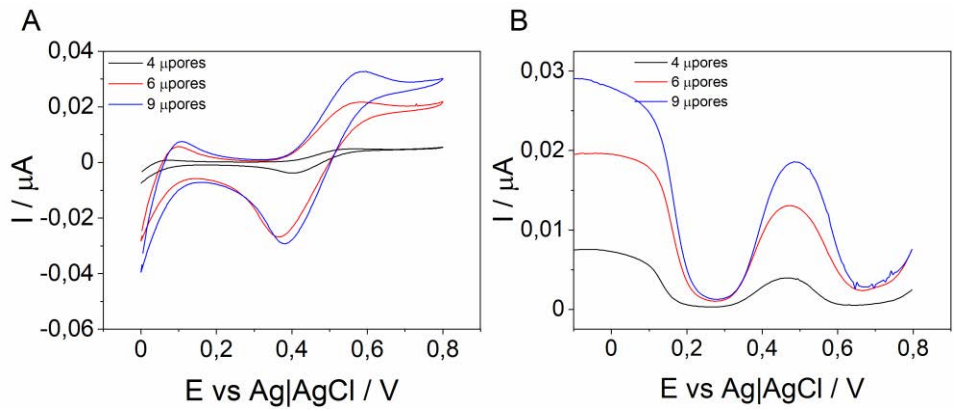

Figure 4.18. Cyclic voltammetry (A) and DPV (B) measurements for TEA^+ transfer across the laser-drilled Melinex membrane.

As expected, the current increases with the number of pores in the array and the highest value is obtained for 9 micropores. Interestingly, the shape of the CV indicates the presence of asymmetric diffusion zones, although micropores have similar sizes on both sides of the membrane (Figure 4.19). This can be explained by the fact that hydrophobic holes are filled with the organic gel, so the µITIES is formed at the pore orifice on the aqueous side. As a consequence, the transfer

of TEA^+ to the organic phase is controlled by the spherical diffusion, resulting in a steady-state limiting current. On the contrary, a clear peak present on the reverse scan is related to the TEA^+ transfer from the linear diffusion regime in the organic micropores[56]. The presented results show that the Melinex membrane can be a very good alternative to laser-ablated glass membranes, which are too brittle to be used in such a setup.

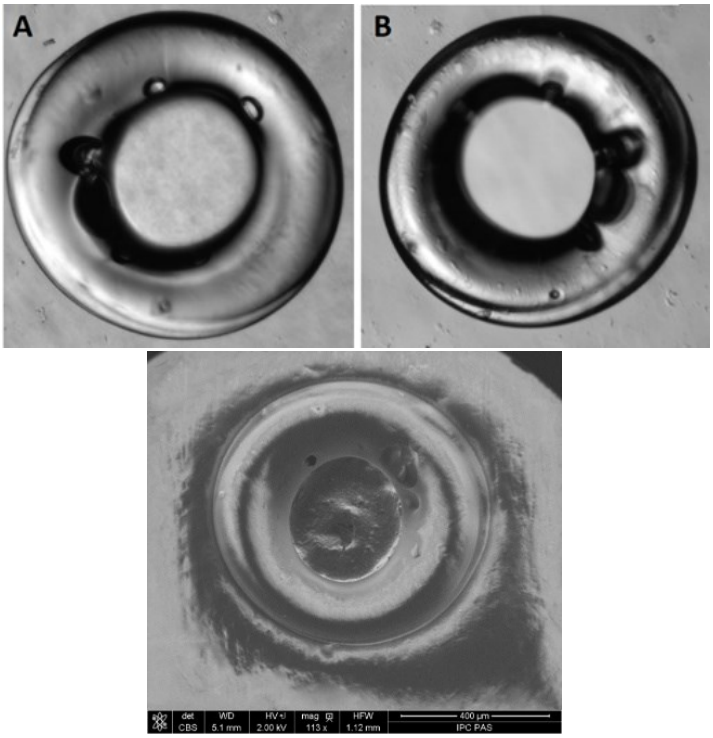

Figure 4.19 Optical microscope images of the laser-drilled Melinex membrane from its top (A) and bottom (B) side. SEM picture of the micropore (C), made with a Nova NanoSEM 450 scanning electron microscope.

Since the most pronounced increase of the ionic current was observed for membrane with 9 micropores, this one was chosen for the flow-injection experiments.

4.3.7.1 Simultaneous detection of proteins and inorganic cations

For the first experiments in the flow system, I chose the mixture of sodium cations (0.1 M) and lysozyme (0.1 mM). The decision was made based on the results

obtained under stationary conditions (aqueous phase supported on the paper without the wicking pad), which showed that the electrochemical pen can be used, to investigate both facilitated cation transfer and adsorption/desorption of lysozyme at the organogel/paper interface. I injected a 5 µl droplet of a cation-protein mixture into the paper channel, 2.5 cm away from the detection point-the place where organogel was in contact with the paper platform (Cell IV). The mixture was dissolved in HCl solution to ensure the presence of the cationic form of the lysozyme. 10 mM HCl was also used as a background electrolyte continuously flowing through the wicking pad during the measurement. To detect in which order and when analytes arrive at the interface, cyclic voltammetry was run through the whole time of the experiment. I expected that Na^+ would reach the detection point first because these small cations should be pulled along the flow with higher velocity than bigger lysozyme molecules. Exactly such a trend was observed on the CVs registered in the flow system (Figure 4.20).

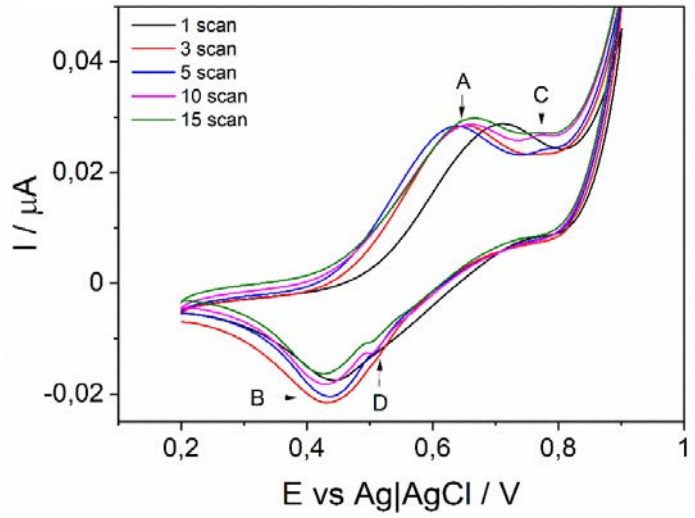

Figure 4.20 Cyclic voltammetry registered when 5µl of protein and NaCl solution was injected in the flow-injected organogel/paper system. Facilitated transfer of Na^+ from aqueous to organic phase (A) and backward (B), adsorption (C), and desorption of lysozyme at gel/liquid interface. Measurements were done using the Melinex membrane with 9 laser-drilled micropores.

In the first scan after the injection, only the transfer peak of H^+ (0.71 V) from the background electrolyte is visible. However, in the third scan, this peak shifts to the potential observed before for the sodium cation transfer (see Figure 4.5), meaning Na^+ arrived at the interface. After several scans, peaks related to the lysozyme adsorption (0.78 V) and desorption (0.5 V) appears. With continued scanning intensity of these signals decreases, but as the protein is getting trapped in the gel, I did not observe the complete disappearance of the peaks.

Although the flow system used here is very simple, obtained results prove it can be successfully applied for simultaneous separation and detection of protein and cation mixture using the ion-transfer technique.

4.3.7.2 Analysis of protein mixture

After the successful separation of inorganic cations and protein molecules, I moved to experiments with a more complicated sample, i.e., a mixture of two different proteins. In fact, paper chromatography is a well-known tool for the separation of proteins [57,58]. Thus the analysis of the protein mixture was a natural extension of the research described above. For that purpose, I choose model proteins, lysozyme, and bovine serum albumin (BSA), due to the significant difference in their molecular weights and well-known electrochemical behavior at the liquid/liquid interface[34]. Before starting the main experiment, I had to adjust the proper concentration ratio between both proteins to get a satisfactory electrochemical response. Too much BSA easily blocks the interface resulting in a high capacitive current observed on voltammograms (Figure 4.21).

As a final composition, I used 0.1 mM lysozyme and 0.005 mM BSA dissolved in 10 mM HCl. The analysis was done in the same paper-based system as previously, and again a 5 µl droplet of the sample was added 2.5 cm away from the detection point (Cell V).

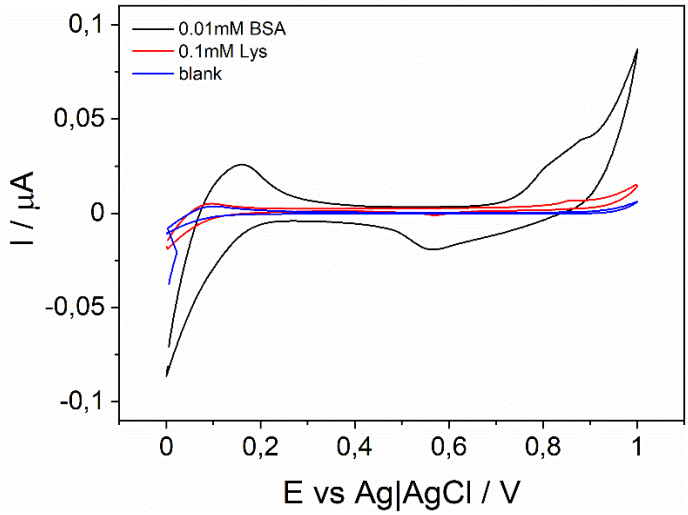

Figure 4.21 Comparison between CVs registered in the presence of 0.1 mM lysozyme and 0.01 mM BSA in the aqueous phase. Measurements were performed in two separate systems using the Melinex membrane with laser drilled 9 micropores.

This time lysozyme as a smaller molecule was expected to reach the interface as first, while the bigger BSA should be more retarded by the paper structure. Changes in the potential and current related to the adsorption/desorption processes can be seen on the cyclic voltammograms (Figure 4.22) registered during the experiments, however, their interpretation is not straightforward.

To simplify the analysis of the obtained data, I plotted the current changes at a certain forward (0.84 V) and backward (-0.56 V) potential as a function of time, creating an electrochemical chromatogram (Figure 4.23). As can be seen, both the forward and reverse currents reach local maxima twice, indicating the presence of two separate adsorption/desorption processes occurring at the interface.

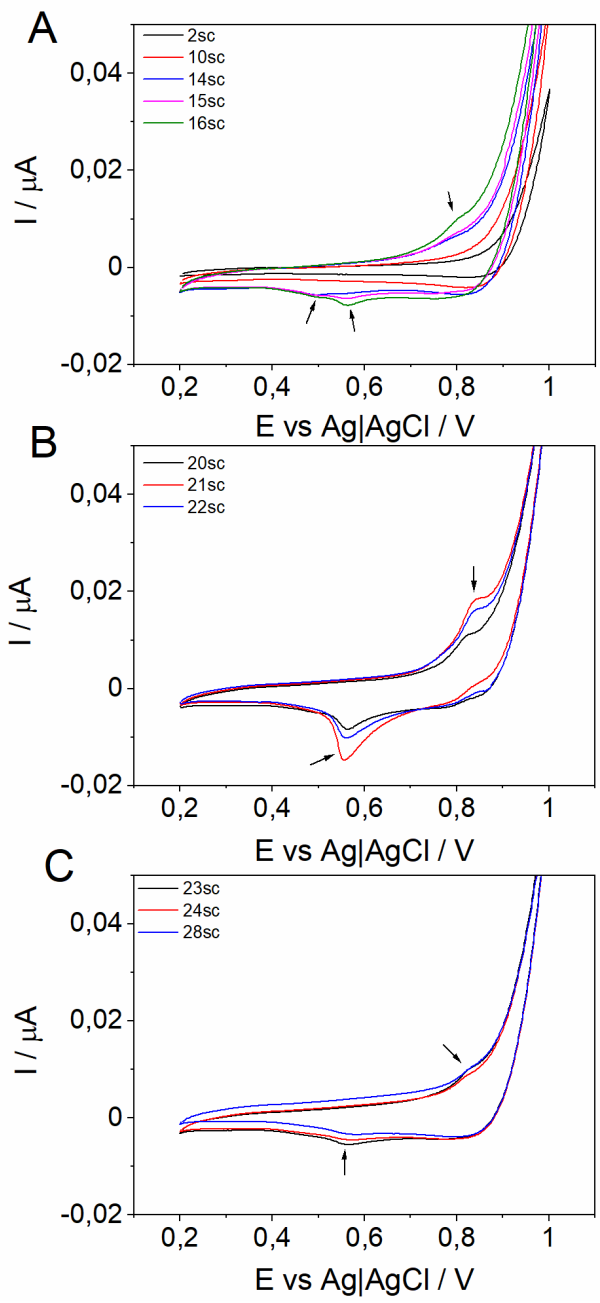

Figure 4.22 Cyclic voltammetry registered in the flow-injection organogel/paper system after adding 5 µl lysozyme and BSA solution. Arrows indicate adsorption and desorption peaks appearing with the increasing time of the experiment. Experiments were done using Melinex membrane with 9 laser-drilled micropores.

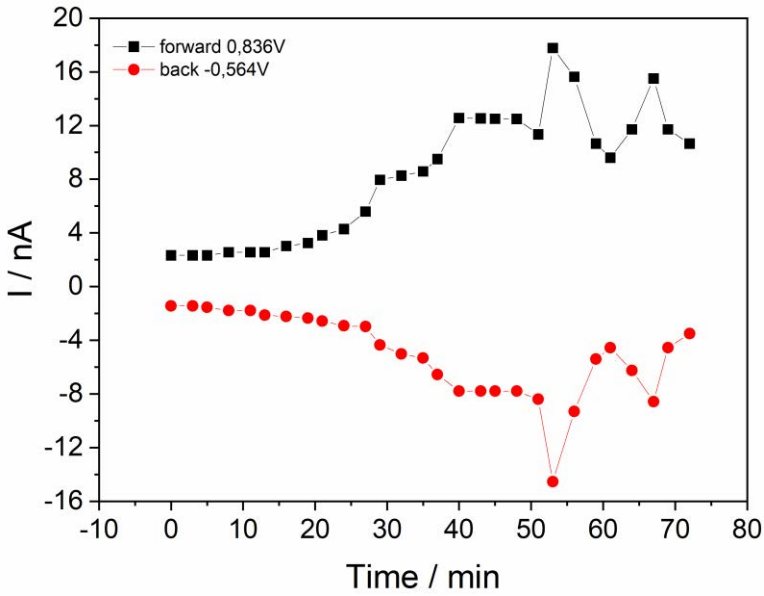

Figure 4.23 Electrochemical chromatogram - dependence between the current at potential 0.84 V, for the forward (black) and -0.56 V for the backward (red) sweeps as a function of time. Each time-step is a separate voltammetric cycle. Experiments were done using Melinex membrane with 9 micropores after the addition of 5 µl of lysozyme and BSA mixture.

The performed experiments confirm the applicability of the paper-based flow-injection system as a tool for protein separation. On the contrary, to classical paper chromatography, this modernized version allows for direct analysis of the samples without the need for protein staining. Consequently, it helps to overcome issues related to the optimization of chromatograms development for each analyzed mixture. Since this setup serves only as a proof-of-concept to further increase its separation efficiency, parameters such as length of the channel, flow rate, and ion-strength should be optimized. However, as the primary goal of my project was to design a novel, low-cost, and simple ion-transfer system and show that it can be utilized for simultaneous separation and analysis of protein mixtures, I did not perform its in-depth optimization.

4.4 An alternative approach – organic phase gelled on the paper support

The possibility of keeping the gelled organic phase in the form of a portable electrochemical pen already brings the ion-transfer technique a step closer to commercial applications. However, the possibility to support both liquid phases on flat elements would definitely simplify the device and make it even more suitable as a point-of-care device. Therefore, as a side project evolving from the electrochemical pen idea, I tested a system where the organogel was immobilized directly in a paper sheet (Figure 4.24). In that case, NPOE was used as an organic solvent because DCE is highly volatile and, when spotted on the paper, evaporated before the gel was created.

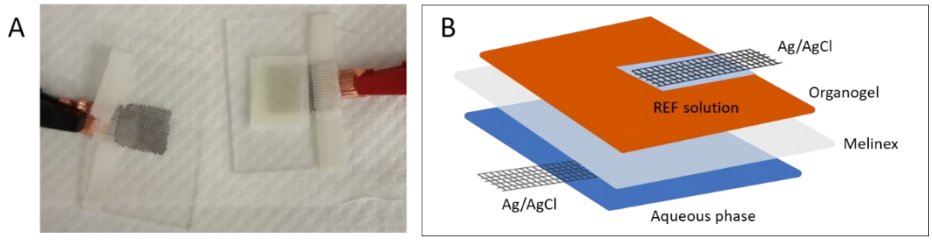

Figure 4.24 Picture (A) and schematic representation (B) of the system where both aqueous and organic phases are supported on the paper platform. Melinex membrane with mechanically drilled 1 mm orifice was placed between the papers. An additional piece of paper soaked with the reference solution was placed on the Ag/AgCl mesh.

4.4.1 Electrochemical characterization of the system

Following the same protocol as before, I performed basic ion-transfer experiments using model TEA^+ and TPA^+ cations. Both ions transfer reversibly across the paper/paper interface, and the difference in peak potentials allows to easily distinguish between them (Figure 4.25). It is noteworthy that although NPOE helps create a stable organogel on the paper, its high viscosity influences ions'

diffusion and makes the whole system more resistive (ΔE_p = 300 mV for TPA^+, ΔE_p = 270 mV TEA^+).

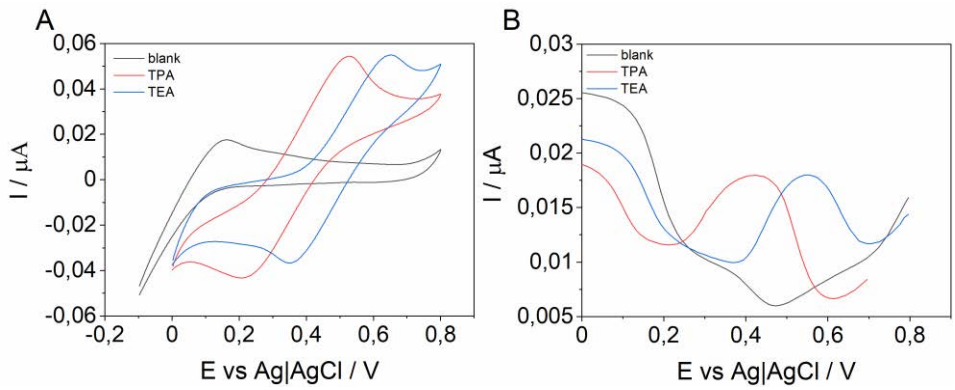

Figure 4.25 Cyclic voltammetry (A) and Differential Pulse Voltammetry (B) showing the transfer of quaternary ammonium cations TEA^+ and TPA^+ across the organogel paper/aqueous paper interface. The blank measurement was done only with the supporting electrolyte (LiCl) in the aqueous phase.

To overcome this issue, further optimization in terms of gel composition and proper geometry is needed. However, such studies are very laborious, preventing the project from being finished because of lack of time. Nevertheless, presented here, preliminary results can be treated as a proof-of-principle confirming the possibility of performing ion-transfer experiments in a fully flat ITIES system with both liquid phases immobilized in a paper platform.

4.5 Conclusions

Results described in this chapter present an exciting, low-cost, and easy to use alternative to the traditional 2-electrode ITIES systems. Instead of using a glass cell, the gelled organic phase is immobilized in the form of a pen-like device while the aqueous phase is supported on the paper platform. The competitive advantage of the presented system over existing ones is the fact that the electrochemical pen can be applied to samples supported on various surfaces without any sample pre-treatment. The proper performance of the electrochemical pen

was verified by performing simple and facilitated ion-transfer measurements. The research showed that the paper structure contains enough ions to provide conductivity sufficient for electrochemical measurements so that supporting electrolyte is not needed. This unique property of the cellulose matrix allows to simplify the analysis since the sample can be spotted directly on the paper platform without any pre-treatment. Moreover, the proposed system offers the possibility to perform pre-concentration voltammetry using a dip-and-pick approach. It also allows to investigate adsorption/desorption processes of the proteins at the organogel/paper interface as well as to detect them using adsorptive stripping voltammetry. Additionally, I used the ability of the cellulose matrix to transport fluids by capillary forces to create a flow-injection paper-based system. In this case, to increase the analytical sensitivity, the electrochemical pen was equipped with a laser-drilled membrane with a micropore array. The device proved its capability to simultaneously separate and detect protein-ion and protein-protein mixtures. To further boost the selectivity of the proposed system, various modified paper platforms can be investigated. The interface area can also be further decreased by using membranes with a higher number of micro- or nanopores.

The electrochemical pen concept opens a new, exciting way for ion-transfer analysis outside of the professional laboratories as it is simple, easy to handle, and allows sample analysis just by spotting on a paper or collecting by swabbing.

In basic proof-of-principle experiments, I also showed that the electrochemical pen idea could be even further simplified by gelling the organic phase directly on a piece of paper. The possibility to make a flat, even more miniaturized, disposable device with both liquid phases supported on low-cost paper platforms would definitely bring liquid/liquid electrochemistry a step closer to point-of-care applications.

4.6 References

[1] J. Koryta, *Electrochim. Acta* **1979**, *24*, 293–300.

[2] T. Osakai, Y. Yuguchi, E. Gohara, H. Katano, *Langmuir* **2010**, *26*, 11530–11537.

[3] G. Herzog, S. Flynn, C. Johnson, D. W. M. Arrigan, *Anal. Chem.* **2012**, *84*, 5693–5699.

[4] H. Sakae, Y. Toda, T. Yokoyama, *Electrochem. commun.* **2018**, *90*, 83–86.

[5] G. Herzog, *Analyst* **2015**, *140*, 3888–3896.

[6] R. A. W. Dryfe, *Phys. Chem. Chem. Phys.* **2006**, *8*, 1869–1883.

[7] H. Jänchenová, K. Štulík, V. Mareček, *J. Electroanal. Chem.* **2008**, *612*, 186–190.

[8] H. A. Santos, V. García-Morales, C. M. Pereira, *ChemPhysChem* **2010**, *11*, 28–41.

[9] H. Jänchenová, A. Lhotský, K. Štulík, V. Mareček, *J. Electroanal. Chem.* **2007**, *601*, 101–106.

[10] H. Jänchenová, K. Štulík, V. Mareček, *J. Electroanal. Chem.* **2007**, *604*, 109–114.

[11] L. Poltorak, A. Gamero-Quijano, G. Herzog, A. Walcarius, *Appl. Mater. Today* **2017**, *9*, 533–550.

[12] L. Poltorak, N. van der Meijden, S. Skrzypek, E. J. R. Sudhölter, M. de Puit, *Bioelectrochemistry* **2020**, *134*, 107529.

[13] S. Jeshycka, H. Y. Han, H. J. Lee, *Electrochim. Acta* **2017**, *245*, 211–218.

[14] S. Jeshycka, E. M. Kim, H. J. Lee, *Electrochim. Acta* **2018**, *282*, 964–972.

[15] R. Zazpe, C. Hibert, J. O'Brien, Y. H. Lanyon, D. W. M. Arrigan, *Lab Chip* **2007**, *7*, 1732–1737.

[16] S. Peulon, V. Guillou, M. L'Her, *J. Electroanal. Chem.* **2001**, *514*, 94–102.

[17] V. Sladkov, V. Guillou, S. Peulon, M. L'Her, *J. Electroanal. Chem.* **2004**, *573*, 129–138.

[18] S. Wilke, M. D. Osborne, H. H. Girault, *J. Electroanal. Chem.* **1997**, *436*, 53–64.

[19] S. Wilke, T. Zerihun, **1998**, *44*, 1–8.

[20] B. Hundhammer, T. Solomon, T. Zerihun, M. Abegaz, A. Bekele, M. Graichen, *J. Electroanal. Chem.* **1994**, *371*, 1–11.

[21] M. D. Scanlon, D. W. M. Arrigan, *Electroanalysis* **2011**, *23*, 1023–1028.

[22] G. Taylor, H. . Girault, *J. Electroanal. Chem.* **1986**, *208*.

[23] L. Poltorak, I. Eggink, M. Hoitink, E. J. R. Sudhölter, M. De Puit, *Anal. Chem.* **2018**, *90*, 7428–7433.
[24] Y. Wang, J. Velmurugan, M. V. Mirkin, P. J. Rodgers, J. Kim, S. Amemiya, *Anal. Chem.* **2010**, *82*, 77–83.
[25] Y. Shao, M. V. Mirkin, *J. Am. Chem. Soc.* **1997**, *119*, 8103–8104.
[26] Q. Li, S. Xie, Z. Liang, X. Meng, S. Liu, H. H. Girault, Y. Shao, *Angew. Chemie - Int. Ed.* **2009**, *48*, 8010–8013.
[27] K. Rudnicki, L. Poltorak, S. Skrzypek, E. J. R. Sudhölter, *Anal. Chim. Acta* **2019**, *1085*, 75–84.
[28] X. Huang, L. Xie, X. Lin, B. Su, *Anal. Chem.* **2017**, *89*, 945–951.
[29] N. T. Iwai, M. Kramaric, D. Crabbe, Y. Wei, R. Chen, M. Shen, *Anal. Chem.* **2018**, *90*, 3067–3072.
[30] M. L. Colombo, J. V. Sweedler, M. Shen, *Anal. Chem.* **2015**, *87*, 5095–5100.
[31] E. Alvarez De Eulate, L. Serls, D. W. M. Arrigan, *Anal. Bioanal. Chem.* **2013**, *405*, 3801–3806.
[32] S. O'Sullivan, E. Alvarez De Eulate, Y. H. Yuen, E. Helmerhorst, D. W. M. Arrigan, *Analyst* **2013**, *138*, 6192–6196.
[33] S. O'Sullivan, D. W. M. Arrigan, *Electrochim. Acta* **2012**, *77*, 71–76.
[34] S. O'Sullivan, E. Alvarez De Eulate, Y. H. Yuen, E. Helmerhorst, D. W. M. Arrigan, *Analyst* **2013**, *138*, 6192–6196.
[35] M. Sairi, D. W. M. Arrigan, *Talanta* **2015**, *132*, 205–214.
[36] C. J. Collins, C. Lyons, J. Strutwolf, D. W. M. Arrigan, *Talanta* **2010**, *80*, 1993–1998.
[37] L. Poltorak, K. Rudnicki, V. Kolivoška, T. Sebechlebská, P. Krzyczmonik, S. Skrzypek, *J. Hazard. Mater.* **2021**, *402*, DOI 10.1016/j.jhazmat.2020.123411.
[38] H. J. Lee, P. D. Beattie, B. J. Seddon, M. D. Osborne, H. H. Girault, *J. Electroanal. Chem.* **1997**, *440*, 73–82.
[39] M. D. Scanlon, G. Herzog, D. W. M. Arrigan, *Anal. Chem.* **2008**, *80*, 5743–5749.
[40] In *Anal. Methods At. Absorpt. Spectrosc.*, The Perkin-Elmer Corporation, **1996**, p. 293.
[41] E. Carrilho, A. W. Martinez, G. M. Whitesides, *Anal. Chem.* **2009**, *81*, 7091–7095.
[42] B. d'Epenoux, P. Seta, G. Amblard, C. Gavach, *J. Electroanal. Chem.* **1979**, *99*, 77–84.

[43] D. Scanlon, D. W. M. Arrigan, *Phys. Chem. Chem. Phys.* **2010**, *12*, 10040–10047.
[44] F. S. Diba, H. J. Lee, *J. Electroanal. Chem.* **2016**, *769*, 5–10.
[45] S. N. Faisal, C. M. Pereira, S. Rho, H. J. Lee, *Phys. Chem. Chem. Phys.* **2010**, *12*, 15184–15189.
[46] A. R. Harris, J. Zhang, R. W. Cattrall, A. M. Bond, *Anal. Methods* **2013**, *5*, 3840–3852.
[47] J. Zhang, A. R. Harris, R. W. Cattrall, A. M. Bond, *Anal. Chem.* **2010**, *82*, 1624–1633.
[48] M. D. Scanlon, J. Strutwolf, D. W. M. Arrigan, *Phys. Chem. Chem. Phys.* **2010**, *12*, 10040–10047.
[49] A. J. Bard, L. R. Faulkner, *Electrochemical Methods: Fundamentals and Applications*, Wiley, **2000**.
[50] J. B. Cooper, A. M. Bond, *J. Electroanal. Chem.* **1991**, *315*, 143–160.
[51] H. W. Maurer, *Starch in the Paper Industry*, Elsevier Inc., **2009**.
[52] A. Apilux, W. Siangproh, N. Praphairaksit, O. Chailapakul, *Talanta* **2012**, *97*, 388–394.
[53] M. D. Scanlon, E. Jennings, D. W. M. Arrigan, *Phys. Chem. Chem. Phys.* **2009**, *11*, 2272–2280.
[54] P. the Elder, *Natural History*, **79AD**.
[55] J. Bobacka, *Sensors Actuators B. Chem.* **2016**, DOI 10.1016/j.snb.2016.11.128.
[56] A. Berduque, R. Zazpe, D. W. M. Arrigan, *Anal. Chim. Acta* **2008**, *611*, 156–162.
[57] Y. Kobatake, A. Irimajiri, N. Matsumoto, *Biophys. J.* **1970**, *10*, 728–744.
[58] A. Meniga, N. Muić, *Anal. Biochem.* **1960**, *1*, 502–510.

5 Conclusion

The main focus of this thesis was to develop novel, simple, and easy-to-use systems that can serve as an alternative to classical setups to study the transfer of ions across the interface between two immiscible liquids. The traditional 3- and 4-electrode systems suffer from mechanical instability of the interface and, related to that, problems with reproducibility of the measured ion currents, a limited number of organic solvents that can be used for creating liquid/liquid interfaces, and difficulties in practical handling. The latter one is especially problematic as it keeps the ion-transfer technique strictly bound to specialized laboratories, although it is an excellent tool for label-free detection of various ionized species and could be utilized by scientists from different fields or implemented for point-of-care applications.

This thesis presented how to overcome the mentioned issues and create simple, user-friendly devices for ion-transfer studies based on low cost and abundant materials such as paper or pencil lead.

In the first two chapters, I described alternative versions of the droplet-based three-phase electrode system. To simplify the setup and provide a mechanically stable interface, I used paper as organic and aqueous phase reservoirs. This system was applied to investigate anion transfer across the aqueous/NOP interface driven by the electrochemical oxidation of decamethylferrocene dissolved in the organic phase. Moreover, using both experiments and computer simulations, we confirmed that the simultaneous transfer of two anions is possible only when the concentration of anions is at least a few times lower than the concentration of the redox probe. Importantly, to the best of my knowledge, the presented paper-based setup is the first device for ion-transfer studies utilizing paper to support the liquid phases.

The second alternative three-phase electrode system was made to investigate the facilitated cation transfer triggered by the reduction of fullerene C_{60} dissolved in dichlorobenzene. It was the first time that C_{60} was used as a redox probe for such studies. The liquid/liquid interface was stabilized thanks to the utilization of a glass vial for organic phase made from a Pasteur pipet together with a pencil graphite electrode passing through the phase boundary. Successful experiments performed in the presence of three potassium ionophores, DB18C6, valinomycin, and ionophore III, proved that this system could be a very good tool for comparing ionophores. It allows for fast and reliable evaluation of the ionophores' selectivity coefficients without immobilizing them in the membrane, thus eliminating the influence of membrane components on the obtained results.

The third system described here is a novel approach to the ion-transfer measurements using a polarizable liquid/liquid interface. The device was called an electrochemical pen because the organic phase was gelled in the glass tube with an attached Melinex membrane looking similar to a pen. Gellification of the organic phase and limited interface area helped stabilize the phase boundary and significantly improved current reproducibility. Importantly, thanks to the pen-like form, the device is portable and can be applied for the analysis of samples supported on various types of surfaces. Experiments presented in this thesis were performed by pressing the electrochemical pen against the paper platform soaked with the aqueous phase. The performance of the systems was verified by performing standard experiments such as simple and facilitated cation transfer as well as investigation of protein adsorption/desorption processes using stripping voltammetry. The interesting observation made during the research is that the paper structure contains enough ions to provide conductivity sufficient for electrochemical measurements so that supporting electrolyte is not needed. Moreover, I propose that a dip-and-pick approach can be used as a voltammetric

pre-concentration technique for samples spotted on the paper platform. In the next step of the research, the electrochemical pen was combined with paper chromatography to create a flow-injection paper-based system for simultaneous separation and detection of protein-ion and protein-protein mixtures. In this case, to increase the analytical sensitivity, the electrochemical pen was equipped with the Melinex membrane with a laser-drilled micropore array. Additionally, the third chapter contains basic proof-of-principle experiments done using a flat paper-based system where the organic phase was gelled directly on a piece of paper.

In conclusion, three novel systems presented in this thesis simplify the way in which ion-transfer experiments can be performed. Each of them makes it possible to obtain a mechanically stable liquid/liquid interface, helps minimize the sample volume used for analysis, and most importantly, is simple and easy to handle. I have shown that paper is an excellent material for the development of ion-transfer systems due to many advantages such as:

- ability to support both organic and aqueous phase;
- stabilization of the liquid/liquid interface;
- possibility to analyze the sample by spotting or collecting by swabbing;
- sufficient conductivity provided by sodium cations present in the cellulose matrix;
- transport of fluids by capillary forces;
- separation of analytes based on their interaction with cellulose matrix;

I believe that the results presented here open a new, exciting way for ion-transfer analysis outside professional laboratories using simple and easy to handle systems and can serve as a basis for the future development of disposable, low-cost sensing tools.

6 Future outlook

Results presented in this thesis can be expanded as separate substantial research projects. Each of the systems described herein shows a new simpler way of performing ion-transfer measurements but also brings questions about the mechanism of the transfer process and many ideas for the development of other low-costs and easy-to-handle devices.

One such interesting topic for future research is further development of the paper-based 3-electrode system to analyze water samples. As was shown, the double-ion transfer mechanism depends on the concentration ratio between the redox probe and the anion of interest. Therefore it would be worth testing whether a change of the redox probe concentration would influence the separation of signals related to the simultaneous transfer of two or maybe even three anions. Also, more advanced chemometric tools could be applied to analyze and classify the samples more efficiently. A disposable, low-cost paper-based device would for sure be a handy tool for fast and simple water quality assessment.

Another interesting topic from a basic research point of view is the explanation of the non-Nernstian behavior observed for the sodium transfer in the setup with the graphite lead as a working electrode. Since fullerene C_{60} has never before been used as a redox probe for facilitated cation transfer, there are no studies concerning its interaction with the ionophores, cations or complexes of both. It is highly probable that fullerene anions influence the stoichiometry of the ion-ionophore complex resulting in distortion of the transfer mechanism. More extensive experimental work combined with theoretical simulations could help to verify this hypothesis and explain the exact mechanism of the ion-transfer process in the presence of fullerene molecules.

A similar issue was observed in the electrochemical pen system, where the slope of the concentration dependence for the sodium transfer was far from the expected 59 mV/decade. However, in this case, the deviation is probably caused by the dense gel structure affecting the diffusion of transferred species. Since the organogel/aqueous interface is a relatively new approach to liquid/liquid studies, there are many questions to be answered. In my opinion, it is essential to understand the processes happening at the phase boundary between the organic solvent and the aqueous reference solution. In the literature, this interface is usually described as non-polarizable, however, results presented in the third chapter of this thesis clearly show that there has to be some ion exchange process happening at that interface. Moreover, the distance between the interface and the Ag/AgCl electrode also seems to play an important role in the transfer mechanism since the measured signal was significantly changing with the electrode's position. These are very intriguing observations definitely requiring further studies and finding the proper explanation.

Another project that could be realized in the future is developing a paper-based system with a gelled organic phase. The preliminary results presented in this thesis confirm the possibility of performing ion-transfer experiments in the system where the organic phase is gelled directly on the paper platform. However, even a simpler version could be made by placing paper sheets soaked with aqueous and gelled organic phase in a side-by-side configuration. The interface area could be limited with perforation or membrane, or platforms could be connected by a narrow bridge cut from the paper. The most tricky part might be the creation of a well-defined phase boundary, preventing evaporation of the aqueous solution, and finding the proper composition and thickness of the gel. Nevertheless, these are technical issues that can be solved during the optimization process. One can imagine that the more advanced version contains inkjet-printed electrodes, so the whole device would be just a small piece of paper.

Such a system would be perfect for point-of-care applications with great commercial potential.

In conclusion, I truly believe that liquid/liquid electrochemistry and especially ion-transfer can become a well-known analytical technique familiar and applied by scientists from different fields of science, not only by a few specialized research groups. This technique has a huge potential to be a basis for various sensing tools also in commercial versions. I hope that the novel setups presented here will bring ion-transfer at least a small step closer to that goal and make the experiments with liquid/liquid interfaces easier and more user-friendly.

Institute of Physical Chemistry
Polish Academy of Sciences

Kasprzaka 44/52
01-224 Warsaw, Poland

www.ichf.edu.pl